

# MASTERTHESIS

On Covalent Immobilisation of Indicators in Optical Oxygen Sensors

*Lukas Hutter*

Institute of Analytical Chemistry and Food Chemistry  
University of Technology, Graz



Supervisor: Univ.-Prof. Dipl.-Chem. Dr.rer.nat. Ingo Klimant

Graz, May 2012



---

## Abstract

In this thesis synthetic strategies towards the covalent immobilisation of PtTPTBP (Pt(II)-*meso*-tetraphenyltetrabenzoporphyrin) as indicator dye in a polystyrene-matrix are developed and examined in the context of optical chemical sensors. The strategies rely on modification of the indicator dye to yield products carrying aryl-bromide residues and subsequent modification by means of Suzuki coupling. Two distinct approaches are examined: Grafting of the indicator dye to a modified polystyrene-polymer carrying bronc acid residues by means of Suzuki coupling and the preparation of a co-polymerisable indicator dye by functionalising it with styrene groups, realised employing Suzuki coupling, and its subsequent polymerisation. Sensors are prepared from functionalised polymers using materials from both approaches and characterised with respect to their use in optical oxygen sensing.

The produced sensor polymers show all the desirable characteristics realised in comparable sensor polymers based on physically entrapped indicator dyes, yet are commonly characterised by a higher degree of linearity in intensity-based Stern-Volmer plots, higher sensitivity and slightly higher quantum yield. Furthermore, covalent linking is expected to further improve sensor performance over time by preventing problems connected to dye mobility such as leeching and aggregation of the dye.

The developed sensor polymers constitute an improvement over established systems and are thus expected to be of high relevance in practical applications. Furthermore, the developed strategy offers a new way of modifying benzoporphyrins in many other ways such as the preparation of cross-linked polymer nano-particles, metal-organic frameworks and dye-bio-conjugation, which is expected to be of high relevance in fields such as sensor applications, the study of biological systems as well as OLED-technology and photodynamic therapy.

---

## Kurzfassung

Diese Arbeit beschäftigt sich mit der Entwicklung und Untersuchung von Synthesestrategien zur kovalenten Immobilisierung von PtTPTBP (Pt(II)-*meso*-tetraphenyltetrabenzoporphyrin) Indikator-Farbstoffen in Polystyrene-Matrices im Kontext Optischer Sauerstoffsensoren. Diese Strategien beruhen auf der Modifikation des Indikatorfarbstoffs um Produkte die über Aryl-Bromid-Gruppen verfügen zu erhalten und deren anschließende Funktionalisierung mittels Suzuki-Kupplung. Zwei unterschiedliche Ansätze wurden untersucht: Binden des Indikatorfarbstoffs an ein Arylboronsäure-modifiziertes Polystyrene-Polymer mittels Suzuki-Kupplung, sowie die Herstellung eines copolymersierbaren Indikatorfarbstoffes durch Funktionalisierung mit Styrene-Gruppen durch Suzuki-Kupplung und dessen anschließende Copolymerisation. Diese so hergestellten funktionalisierten Polymere wurden zur Herstellung von Sensoren verwendet, welche hinsichtlich ihrer Eigenschaften in Hinblick auf Sensor-Anwendungen untersucht wurden.

Die hergestellten Sensorpolymere zeigen alle wünschenswerten Charakteristika von vergleichbaren Sensorsystemen, welche auf rein physikalischer Immobilisierung des Indikatorfarbstoffs beruhen, zeigen jedoch generell auch einen höheren Grad an Linearität in Intensitäts-basierten Stern-Volmer-Plots, höhere Sensitivität und geringfügig höhere Quantenausbeuten. Darüberhinaus wird eine weitere, längerfristige Verbesserung der Sensor-Eigenschaften, durch die Minimierung von Problemen die mit der Mobilität des Indikatorfarbstoffs in Verbindung stehen, wie das Auswaschen und die Aggregation des Indikatorfarbstoffs, erwartet.

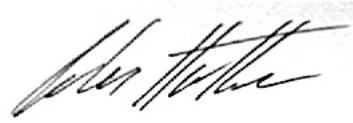
Die entwickelten Sensormaterialien stellen somit eine Verbesserung gegenüber vergleichbaren, etablierten Sensorsystemen dar, eine Entwicklung von potentieller Relevanz für praktische Sensoranwendungen. Zusätzlich stellen die entwickelten Strategien eine vielversprechende Möglichkeit zur Modifikation von Indikatorfarbstoffen auf vielfältigste Weise dar. Als mögliche Strategie zur Herstellung von quer-vernetzten Polymernanopartikeln, Metal-Organic-Frameworks und zur Indikatorfarbstoff-Biokonjugation besteht eine Relevanz sowohl für die Sensor-Technologie und die Untersuchung biologischer Systeme, als auch für Anwendungsfelder wie OLED-Technologien und Photodynamische Therapie.

---

## Statutory Declaration

I declare that I have authored this thesis independently, that I have not used other than the declared sources / resources, and that I have explicitly marked all material which has been quoted either literally or by content from the used sources.

9 May, 2012  
Date



Signature

---

## Danksagung

*Es sind Ideen, die das Denkbare mit dem Tatsächlichen verbinden.*

Der Vorgang des Um- oder vielmehr Übersetzens von Ideen, verlangt nach Kreativität - um Brücken zu schlagen- und kritischem Denken - um darüber zu navigieren. Das Durchleben dieses Spannungsfeldes ist die wohl tiefgreifendste Erfahrung die ich im Laufe der Monate, die zur Verfassung dieser Arbeit geführt haben, machen durfte. An dieser Stelle soll all jenen gedankt werden, ohne deren Beitrag dies nicht möglich gewesen wäre:

Ingo - Ohne die Gabe, deinen scheinbar unerschöpflichen Schatz an Ideen zu teilen, deiner Fähigkeit mich, mit oftmals auch unbequemen Fragen, dazu anzuhalten, den richtigen Weg zu finden und deine Größzügigkeit wäre diese Erfahrung nie möglich gewesen.

Sergey - Du beweist jeden Tag, was es heißt leidenschaftlich an etwas zu arbeiten und Wissen zu teilen. Du bist ein großartiger Lehrer, guter Freund und vielleicht auch der pessimistischste Optimist den ich kenne.

Klaus - In deinem Tatendrang, deiner Kompetenz, deiner Begeisterung, deiner Fähigkeit zu motivieren, soziale Netze zu spinnen und zu stärken bist du mir ein großes Vorbild. Ich kann mich glücklich schätzen, als dein erster Diplomand, als Freund und Kollege, viel mit dir gelernt zu haben.

Diese Danksagung wäre schlichtweg unvollständig, würde ich mich nicht bei der gesamten Arbeitsgruppe, gar dem ganzen Institut bedanken. - Für das unvergleichliche Arbeitsklima, die Mittagessen, die gemeinsamen Pausen, die fachliche und bürokratische Unterstützung und die menschliche Wärme, die allesamt dazu beigetragen haben, dass meine Zeit am Institut nicht nur lehrreich, sondern auch schön war.

Meinen Eltern gebührt Dank für ihre Unterstützung und Liebe. Bei meinen Geschwistern, meiner gesamten Familie und all meinen Freunden möchte ich mich dafür bedanken, dass sie mir ein Umfeld bereitet haben, in dem ich mich entfalten und wachsen konnte.

Ohne euch wäre ich nicht jener, der ich bin.

Ich kann mich glücklich schätzen, dass es euch gibt!

Lukas Hutter

Graz, May 2012

---

# Contents

<b>1</b>	<b>Introduction</b>	<b>1</b>
<b>2</b>	<b>Theoretical Background</b>	<b>2</b>
2.1	Luminescence . . . . .	2
2.1.1	Absorption . . . . .	2
2.1.2	Franck-Condon-Principle . . . . .	3
2.1.3	Internal Conversion . . . . .	4
2.1.4	Inter-System Crossing . . . . .	4
2.1.5	Fluorescence . . . . .	5
2.1.6	Phosphorescence . . . . .	5
2.1.7	Delayed Fluorescence . . . . .	6
2.1.8	Lifetime . . . . .	6
2.1.9	Luminescence Quantum Yield . . . . .	7
2.1.10	Quenching . . . . .	7
2.1.11	Stern-Volmer-Kinetics . . . . .	8
2.1.12	The Two-Site Model . . . . .	9
2.2	Optical Oxygen Sensors . . . . .	10
2.2.1	Basic Concepts in Chemical Sensors . . . . .	10
2.2.2	Optical Chemical Sensors . . . . .	10
2.2.3	Optical Oxygen Sensors . . . . .	12
2.2.4	Application Areas . . . . .	13
2.2.5	Oxygen Indicators . . . . .	13
2.2.6	Parameters Determining Sensitivity . . . . .	14
2.2.7	Analytical Criteria and Key Considerations . . . . .	15
2.2.8	Sensor Matrices . . . . .	16
2.3	Immobilisation . . . . .	17
2.3.1	Bio-Conjugation-Inspired Techniques . . . . .	17
2.3.2	Click-chemistry . . . . .	19
2.3.3	Further Considerations . . . . .	20
2.4	Suzuki Coupling . . . . .	21
2.4.1	Mechanism . . . . .	22
2.4.2	Organoboranes . . . . .	23
2.4.3	Catalysts . . . . .	23
2.4.4	Conditions . . . . .	24
<b>3</b>	<b>Materials and Methods</b>	<b>25</b>
3.1	Chemicals Used . . . . .	25
3.2	Sensor Preparation . . . . .	26
3.2.1	Sensor Films . . . . .	26
3.2.2	Fibre Based Sensors . . . . .	26

3.3	Photophysical Characterisation . . . . .	27
3.3.1	Absorbtion Spectra . . . . .	27
3.3.2	Determination of Extinction Coefficients . . . . .	27
3.3.3	Determination of Quantum Yields . . . . .	27
3.3.4	Sensor Calibration . . . . .	28
3.3.5	Photostability Experiments . . . . .	30
3.4	Polymer Characterisation . . . . .	31
3.4.1	Gel Permeation Chromatography . . . . .	31
3.4.2	Elemental Analysis . . . . .	31
3.5	Structural Analysis . . . . .	31
3.5.1	MALDI-MS . . . . .	31
<b>4</b>	<b>Experimental Section</b>	<b>33</b>
4.1	Synthetic Strategy . . . . .	33
4.1.1	Strategic Considerations: Dye Synthesis . . . . .	33
4.1.2	Strategic Considerations: Choice and Position of The Functional Group . . . . .	33
4.1.3	Strategic Considerations: The Coupling Approach . . . . .	34
4.2	Dye Synthesis . . . . .	35
4.2.1	PtTPTBPBr <sub>4</sub> . . . . .	36
4.2.2	PtTPTBPBr . . . . .	39
4.3	Polymer Synthesis . . . . .	41
4.3.1	Synthesis of Styrene-Vinylbenzeneboronic acid-Copolymers . . . . .	41
4.4	Suzuki Coupling . . . . .	43
4.4.1	Polymer Modification . . . . .	43
4.4.2	Dye Modification . . . . .	45
<b>5</b>	<b>Results and Discussion</b>	<b>47</b>
5.1	Polymer Characterisation . . . . .	47
5.1.1	Boronic acid-residue-Loading . . . . .	47
5.1.2	Molecular Weight Distribution . . . . .	47
5.2	Dye Characterisation . . . . .	49
5.2.1	Photophysical Properties . . . . .	49
5.2.2	Chemical Analysis . . . . .	50
5.3	Covalent Coupling . . . . .	52
5.3.1	The Effect of Suzuki Coupling on the Polymer's Molecular Weight Distribution . . . . .	52
5.3.2	Coupling efficiency . . . . .	53
5.3.3	Comparison and Discussion of the Synthetic Approaches . . . . .	53
5.4	Sensor Characterisation . . . . .	55
5.4.1	Sensor films - Photo-physical Characterisation . . . . .	55
5.4.2	Calibration Curves . . . . .	60
5.4.3	Sensor Response . . . . .	64
5.4.4	Photostability . . . . .	65
<b>6</b>	<b>Outlook and Conclusions</b>	<b>67</b>
<b>7</b>	<b>References</b>	<b>68</b>



---

<b>8</b>	<b>List of Figures</b>	<b>71</b>
<b>9</b>	<b>List of Tables</b>	<b>73</b>
<b>10</b>	<b>Appendix</b>	<b>75</b>
10.1	Failed Experiments . . . . .	76
10.1.1	PtTPTBP-NH <sub>2</sub> . . . . .	76



---

# 1 Introduction

Oxygen is a substance central to life. It constitutes 21 % of the air we breathe and almost all living organisms, even anaerobic, require oxygen to a certain extent. To illustrate this statement: Roughly  $9.5 \cdot 10^6$  kg of oxygen are being produced per second on a global scale by means of photosynthesis, whereas  $7.3 \cdot 10^6$  kg of oxygen are consumed by respiration every second.

The discovery of oxygen in the 18<sup>th</sup> century, which is attributed both to Joseph Priestley and Carl Wilhelm Scheele, and the subsequent re-shaping of the theoretical framework surrounding it, formulated by Antoine Lavoisier, marked a milestone in the coming of age of chemistry as a science[1].

Due to its essential role in chemistry and biology, oxygen is an analyte of utmost importance. Knowing the concentration of oxygen does not only prove crucial in a broad variety of technological processes and aspects of everyday-life, it also helps us to elucidate the complex behaviour of biological and ecological systems. In this context, the field of optical oxygen sensors provides analytical tools characterised by a high degree of flexibility and robustness, which can be tailored to meet the requirements set by even complicated analytical problems.

In this thesis, a technical aspect of optical oxygen sensors, the possibility of covalent immobilisation of luminescent oxygen indicators, is examined. The purpose of the following introductory pages is to provide the reader with the concepts necessary for understanding the technicalities involved, as well as to shed light on the context of this work.

## 2 Theoretical Background

### 2.1 Luminescence

Luminescence is a process of **emission of photons** i.e. electromagnetic radiation, which occurs **due to the relaxation of an electronic system** from an electronically excited state. A molecule exhibiting luminescence is referred to as "**luminophore**". Excitation from electronic ground states to excited states can happen in a variety of ways, most notably by means of absorption of electromagnetic radiation.

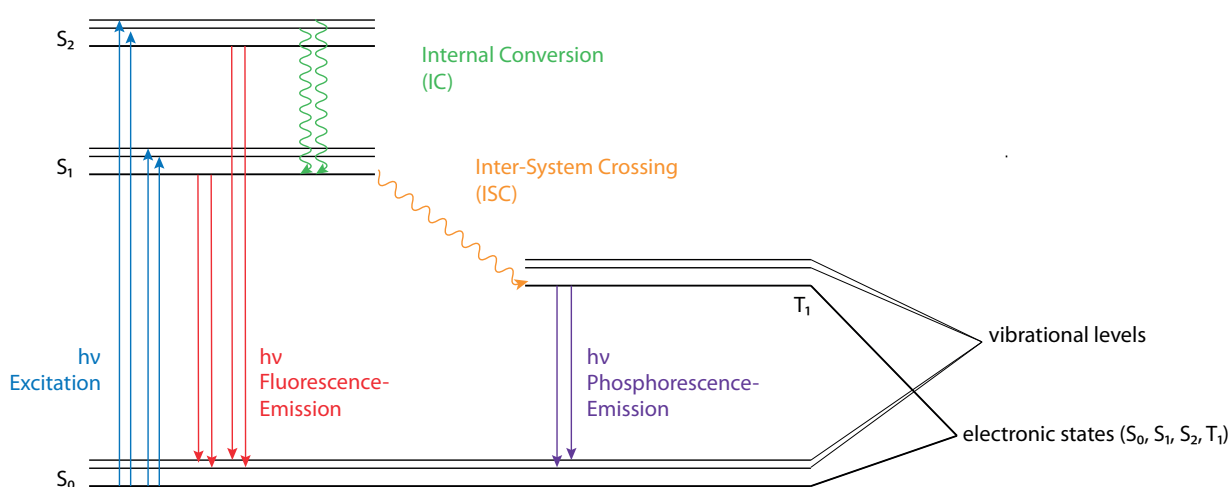


**Figure 2.1:** A Jablonski diagram illustrating the photo-physical processes connected to luminescence phenomena.

#### 2.1.1 Absorption

Absorption of light and scattering processes are the two fundamental forms of interaction between light and matter. In the case of absorption, an **electronic transition** is caused in a molecule upon **taking up the discrete energy of a photon** from the UV-visible range of the electromagnetic spectrum. [2, pp. 20-24]

In other words: the absorption of photons causes electrons to be promoted from a **ground state** to an energetically higher lying, unoccupied state - the **excited state**. The energetic difference between ground state and

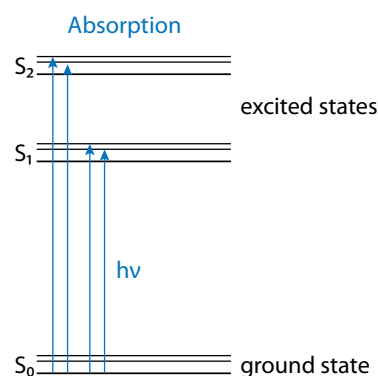


**Figure 2.2:** A Jablonski diagram illustrating the process of absorption.

the excited state corresponds to the energy of the photon.

The major selection rule for absorption transitions is concerned with the spin multiplicity of the states between which the transition occurs:

**Transitions are allowed if the spin multiplicity remains unchanged.**

Thus singlet-singlet-transitions ( $S \rightarrow S$ -transitions) and triplet-triplet-transitions ( $T \rightarrow T$ -transitions) are allowed, whereas  $S \rightarrow T$ -transitions and  $T \rightarrow S$ -transitions are quantum-mechanically forbidden.[2, p. 30]

Processes of absorption or emission of a photon occur at a time-scale of femto-seconds ( $10^{-15}$ s). However, once in an excited state molecules remain in the excited state for a time ranging from picoseconds ( $10^{-12}$ s) to microseconds ( $10^{-6}$ s), depending on the type of molecule, the type of excited state and the medium, before undergoing further photo-physical processes.[2, pp. 30-31]

### 2.1.2 Franck-Condon-Principle

According to the Born-Oppenheimer approximation, electronic processes take place at a much more faster time-scale than the nuclei's movements.

Consequently processes of the domain of nucleic movement, such as molecular vibrations, do not play a role when considering electronic processes. Thus electronic excitation typically occurs without a change in the positions of the nuclei respective to each other.

However electronic excitation, i.e. an altered electronic structure generally leads to an altered potential area describing equilibrium conformation of the molecule. (see Figure 2.3) To rephrase: The molecule's conformation at vibrational equilibrium at the electronic ground state generally does not correspond to the molecules conformation at vibrational equilibrium in an excited state.

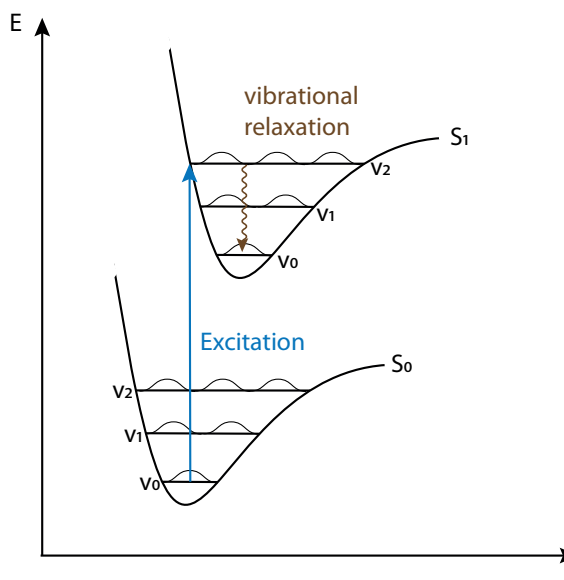


**Figure 2.3:** A schematic illustration of the Franck-Condon Principle, depicting electronic states and their associated vibrational states as a Morse-Function.

Based on an equivalent line of reasoning, the Franck-Condon-Principle states that **electronic excitation typically happens from a vibrational ground state in the electronic ground state to an excited vibrational state in the excited electronic state.**

Electronic excitation is, however, quickly followed by a process of non-radiative vibrational relaxation to the vibrational ground state. [2, pp. 30-32]

### 2.1.3 Internal Conversion

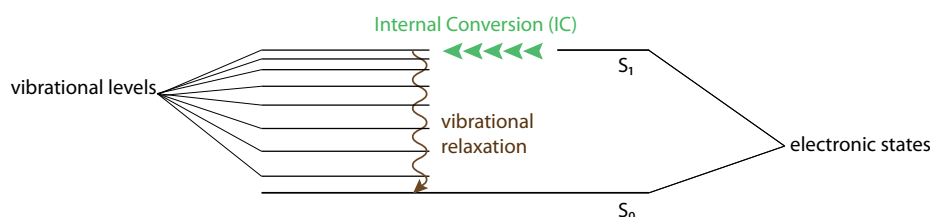


**Figure 2.4:** Internal Conversion illustrated using a Jablonski Diagram.

Internal Conversion (IC) is a process of **non-radiative transition between a vibrational ground state and an excited vibrational state of a lower lying electronic state**, which is usually followed by vibrational relaxation to the corresponding vibrational ground state.

The characteristic time-scale for internal conversion lies between 10 ps ( $10^{-11}$  s) and 1 ns ( $10^{-9}$  s), whereas the following vibrational relaxation occurs ten times faster.[2, p. 37]

### 2.1.4 Inter-System Crossing

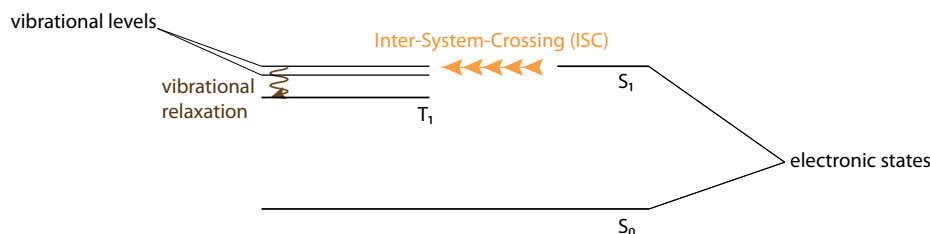


**Figure 2.5:** The processes involved in Inter-System Crossing illustrated in a Jablonski Diagram.

Inter-System-Crossing (ISC) is a process of **non-radiative transition between two vibrational states of equal energy but different spin multiplicity**, which is commonly followed by vibrational relaxation to the respective vibrational ground state.

Transitions which involve a change in spin multiplicity are quantum-mechanically forbidden.

Provided the electronic system exhibits strong spin-orbit coupling, the probability for transitions involving states characterised by different spin multiplicity can be increased.

Spin-orbit coupling, the coupling of the orbital magnetic moment ( $m_l$ ) and the spin magnetic moment ( $m_s$ ) varies with the fourth power of the atomic number, thus can be increased

due to the presence of heavy atoms.

Compared to Internal Conversion, the process of Inter-System-Crossing is about ten times slower, occurring at a time-scale of typically 100 ps ( $10^{-10}$  s) to 10 ps ( $10^{-11}$  s). [2, pp. 38-41]

### 2.1.5 Fluorescence

Fluorescence is a process of **spontaneous emission of photons that accompany the transition between two singlet states (radiative relaxation)**, generally  $S_1 \rightarrow S_0$ .

Due to energy losses caused by vibrational relaxation following excitation the fluorescence

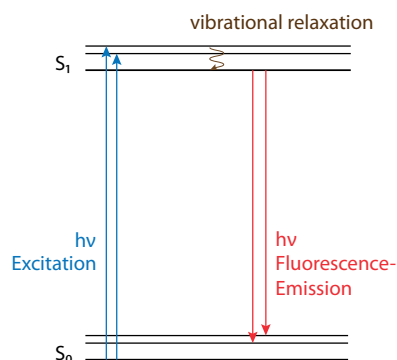


**Figure 2.6:** A Jablonski diagram illustrating the basic photo-physical processes involved in fluorescence.

emission spectra are in general shifted towards the longer wavelength (lower energy) domains of the electromagnetic spectrum.

Absorption and emission spectra partially overlap under laboratory conditions, which is attributable to the fact that under room temperature a considerable fraction of luminophores resides in excited vibrational level corresponding to the electronic ground state. [2, pp. 37-38]

### 2.1.6 Phosphorescence

Phosphorescence, a process of radiative relaxation, is the **emission of photons that accompanies the transition from the excited triplet-state  $T_1$  to the singlet ground-state  $S_0$** .

The **precondition** for phosphorescence to occur is **ISC**.

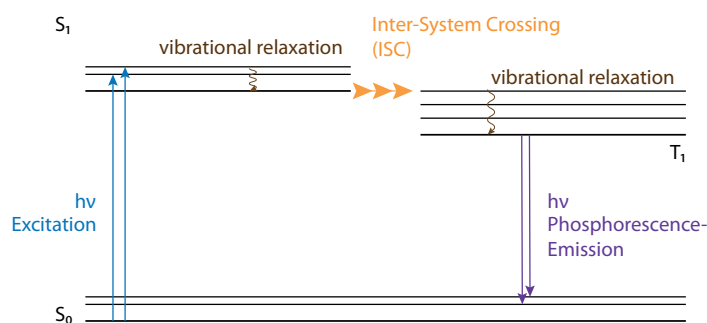


**Figure 2.7:** A Jablonski diagram illustrating the basic photo-physical processes involved in phosphorescence.

Both processes are quantum-mechanically forbidden and rely on strong spin-orbit coupling of the electronic system. Additionally, phosphorescence competes with both ISC and vibrational de-excitation. Both processes are favoured at high temperatures and in solution. As a consequence, phosphorescence is favoured under conditions which limit the possibility and probability of collisions such as a rigid medium and low temperatures.

Generally,  $T_1$  levels lie energetically lower than  $S_1$  levels. Thus, compared to the a substance's fluorescence spectrum its phosphorescence spectrum would be shifted even more towards the longer wavelength end of the electromagnetic spectrum. [2, p.41]

### 2.1.7 Delayed Fluorescence

Similarly to phosphorescence, delayed fluorescence requires a  $S_1 \rightarrow T_1$  transition. Instead of direct relaxation via phosphorescence, however, the system undergoes a second, highly temperature-dependent reverse inter-system-crossing step back to  $S_1$ , before the radiatively relaxing from  $S_1$  to  $S_0$  via fluorescence.

This process results in the luminophore showing an emission spectrum which is identical to its

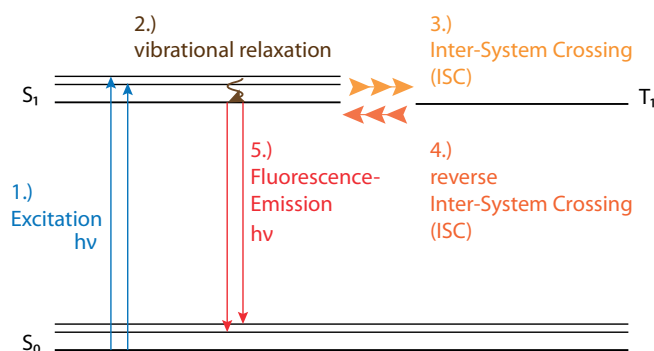


**Figure 2.8:** A Jablonski diagram illustrating the basic processes involved in delayed fluorescence.

fluorescence spectrum whilst being characterised by a longer, i.e. delayed decay time. The process of delayed fluorescence is highly temperature dependent, since the reverse inter-system-crossing step is favoured at higher temperatures and only occurs between  $T_1$ -states and  $S_1$ -states of similar energy. [2, p.41]

### 2.1.8 Lifetime

Radiative de-excitation processes are characterised by typical lifetimes, which arise from the fact that spontaneous emission of radiation in the course of de-excitation does not occur immediately. A molecule would typically remain in the excited state ( $S_1$ ,  $T_1$ ,...) before undergoing de-excitation processes. The process of de-excitation after pulsed excitation can be described using simple first-order kinetics:

$$-\frac{d[A^*]}{dt} = k[A^*] \quad (2.1)$$



$[A^*]$ ... concentration of species A in excited state  $S_1$

Here  $k$  denotes the rate constant for all possible de-activation processes for a given electronic state, which is further specified by:

$$k = \Sigma(k_{\text{deactivation}}) = k_{\text{radiative}} + k_{\text{non-radiative}} \quad (2.2)$$

Solving equation 2.1 by separation of variables and integration from  $t = 0$  to  $t$  and  $[A^*]_{t=0} = [A^*]_0$  to  $[A^*]$  yields:

$$[A^*] = [A^*]_0 * e^{-kt} \quad (2.3)$$

Rate constants for first-order reaction have the unit of  $[s^{-1}]$  thus the inverse of a first-order rate constant is an entity of time characteristic for the reaction. In the case of luminescence  $\tau$  is referred to as the lifetime of the excited state of interest.

$$\tau = 1/k \quad (2.4)$$

Combining equations 2.3 and 2.4 we obtain:

$$[A^*] = [A^*]_0 * e^{-t/\tau} \quad (2.5)$$

From rearranging the above equation and setting  $t = \tau$ , we obtain:

$$\frac{[A^*]}{[A^*]_0} = e^{-1} \approx 0.368 \quad (2.6)$$

Thus the lifetime  $\tau$  can be interpreted as the time-frame within which relaxation occurs for 63% of the excited molecules.

Characteristic lifetimes for excited singlet states range from tens of picoseconds to hundreds of nanoseconds ( $10^{-11}$  s -  $10^{-7}$  s). Excited triplet states are generally characterised by longer lifetimes in the range of microseconds to even seconds ( $10^{-6}$  s -  $10^0$  s). [2, pp.42-46]

### 2.1.9 Luminescence Quantum Yield

Based on the kinetic line of reasoning outlined in the section on lifetime, the quantum yield of a luminophore can be formulated as follows:

$$\Phi = \frac{k_{\text{radiative}}}{k_{\text{radiative}} + k_{\text{non-radiative}}} = k_r \tau \quad (2.7)$$

Thus the radiative quantum yield is defined as the **fraction of excited state molecules that return to the ground state by emission of radiation**. [2, pp. 46-48]

### 2.1.10 Quenching

Up to now the discussion of de-excitation-phenomena has been limited to merely intra-molecular processes. **Intermolecular de-excitation-processes** are collectively referred to as "quenching", in which an excited molecule  $A^*$  interacts with another molecule Q.

This bimolecular process involves a variety of possible processes, which ultimately lead to de-excitation of the excited molecule, such as: collision with a heavy atom or paramagnetic species, energy transfer, electron transfer, proton transfer or formation of an "excimer" or "exciplex".

On a more general level, quenching may occur in several ways, most importantly static and dynamic quenching.

**Static quenching** refers to a situation of luminophore and quencher being in close spatial proximity to one another (often referred to as effective quenching shell), which formally reduces the concentration of active luminophore able to exhibit luminescence. This results in decreased luminescence intensity while leaving the luminescence lifetime unaffected.

**Dynamic quenching** on the other hand refers to the case of diffusion-dependent interaction between excited luminophore and quencher, which results in decreased fluorescence intensity and decreased luminescence decay time. [2, pp. 72-77]

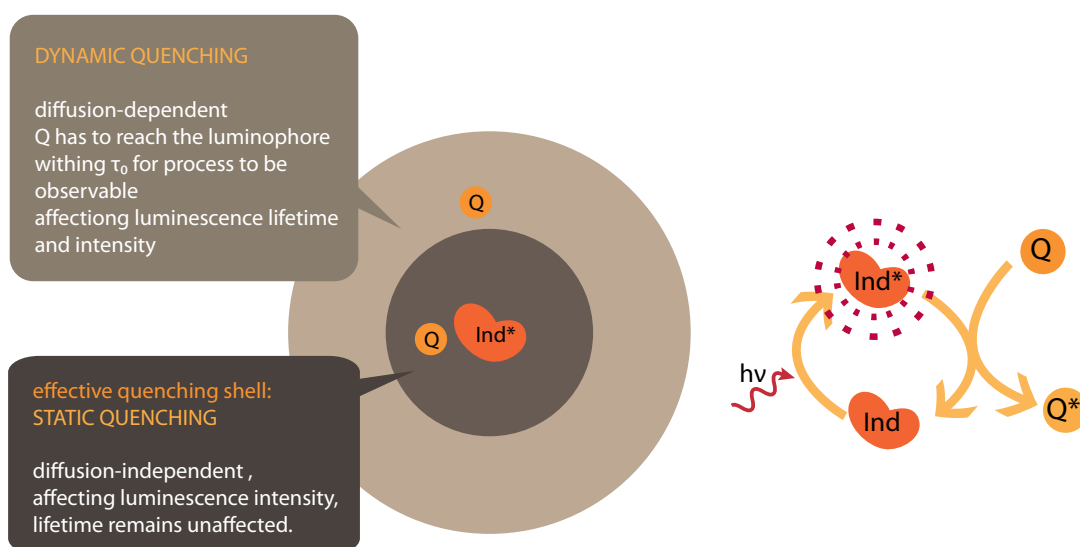


**Figure 2.9:** This picture illustrates the difference between static and dynamic quenching and depicts a quenching cycle.

### 2.1.11 Stern-Volmer-Kinetics

The discussion of quenching as a bimolecular process requires the use of appropriate kinetic models. In this respect, the Stern-Volmer model represents a basic and widely used tool:

$$\frac{I_0}{I} = \frac{\tau_0}{\tau} = 1 + k_Q\tau_0[Q] = 1 + K_{SV}[Q] \quad (2.8)$$

$I_0$  ...luminescence *intensity* in the absence of the quencher

$\tau_0$ ...luminescence *lifetime* in the absence of the quencher.

The above equation, the so-called Stern-Volmer relation, describes a **linear relationship** between the ratios  $\frac{I_0}{I}$  or  $\frac{\tau_0}{\tau}$  and the **concentration of the quencher**, with  $K_{SV}$  representing the slope of the graph.  $K_{SV}$ , the **Stern-Volmer constant** is equal to the product of the bimolecular quenching constant  $k_Q$  and the luminescence lifetime in the absence of the quencher,  $\tau_0$ .

The Stern-Volmer model is simple and of great practical use, however deviations from linear behaviour may occur due to a variety of reasons such as *transient effects*, *time-dependency of the quenching "constant"* or *saturation effects*. [2, pp. 77-79]

### 2.1.12 The Two-Site Model

If quenching is to be studied in a system involving a **complex matrix** such as a polymer film, Stern-Volmer-plots frequently show a downward curvature. The deviation from ideal Stern-Volmer behaviour arises due to **micro-heterogeneities** in the matrix, which lead to the formation of multiple quenching domains.

Based on this concept of micro-heterogeneities, the **Two-Site Model** postulates the existence of **two distinct quenching domains**, each characterised by their own degree of quenchability.

$$\frac{I_0}{I} = \frac{1}{\frac{f_1}{1+K_{SV1}[Q]} + \frac{1-f_1}{1+K_{SV2}[Q]}} \quad (2.9)$$

$f_0$ ... factor determining the influence of one domain on the observed lifetime  
 $K_{SV1}, K_{SV2}$ ... Stern-Volmer constant of the individual quenching domain

Despite a considerable amount of simplification involved in this model, postulating merely two distinct quenching domains, it provides good correlation for Stern-Volmer plots of luminophores in polymer matrices. [3]

In the **Simplified Two-Site Model**, a further simplification is established by setting one of the two Stern-Volmer constants to zero. This is equivalent to modelling a system which is characterised by two distinct luminophore environments: one domain where quenching can occur, whereas in the other quenching is not possible.

## 2.2 Optical Oxygen Sensors

### 2.2.1 Basic Concepts in Chemical Sensors

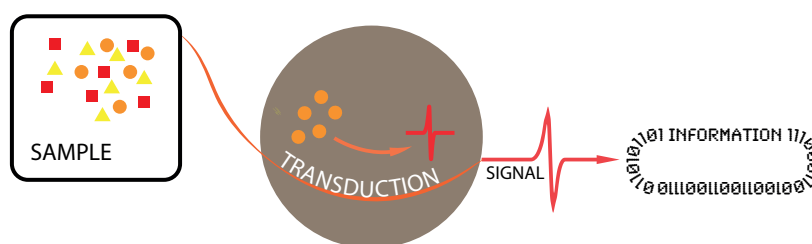


**Figure 2.10:** An illustration of the basic steps involved in chemical sensors.

"Chemical Sensors are miniaturised devices that can deliver real-time and on-line information on the presence of specific compounds or ions (**analytes**) in even complex samples" [4] and represent both accurate and flexible analytical tools for the investigation of a variety of chemical species of interest in a broad range of applications.

The field of chemical sensors encompasses a tantamount of different chemical and physical interactions which are harnessed in order to gather information about a variety of analytes. Moreover, a series of different sensor layouts are employed to provide both specificity and ease of use in fields of application as diverse as clinical diagnostics, environmental field studies and process monitoring.

Consequently, several levels of classification have to be stressed in order to appropriately describe a chemical sensor. A very general way of classifying chemical sensors looks at the method employed in **signal transduction**: One of the key issues in the realisation of chemical sensors, signal transduction is a process of relating the information of interest, in general the concentration of a chemical species, to a signal which is distinct, easily detectable as well as robust and processable.

Among chemical sensors we find systems involving electrochemical signal transduction, also known as "**Electrodes**", and systems involving optical signal transduction, which are also known as "**optodes**" or "**Optrodes**", to be most common. Other effects harnessed for signal transduction are employed in **mass-sensitive sensors** and **thermometric sensors**. Electrochemical sensors are further classified based on their means of transduction (amperometric, potentiometric, conductivity-based and capacitive). It lies beyond the scope of this introduction to further elucidate the principles involved in electrical chemical sensors, however, a more detailed discussion of the principles and concepts involved in optical chemical sensors shall be provided.

### 2.2.2 Optical Chemical Sensors

The most basic level of classification of optical chemical sensors is based on the relationship between the analyte and signal transduction: If signal transduction is based on optical properties of the analyte itself, the sensor is classified as **intrinsic**. If the sensor relies on an interaction between analyte and an indicator, a molecule not present in the sample, it is classified as **extrinsic**.

In the latter, the indicator dye acts as a transducer. It possesses photo-physical properties such as characteristic absorbance or luminescence, which gets reversibly altered in a manner which is detectable and depends on the concentration of the analyte, by chemically or physically interacting with the analyte. Common interactions between analyte and dye are processes such as dynamic luminescence quenching, electron-transfer mechanisms or protonation/deprotonation reactions.

A general sensing scheme for an extrinsic optical chemical sensor consists of an **indicator dye** immobilised in a **polymer matrix** and a suitable **detector and readout unit**.

The purpose of the polymer matrix is, among others, to keep the dye's concentration constant

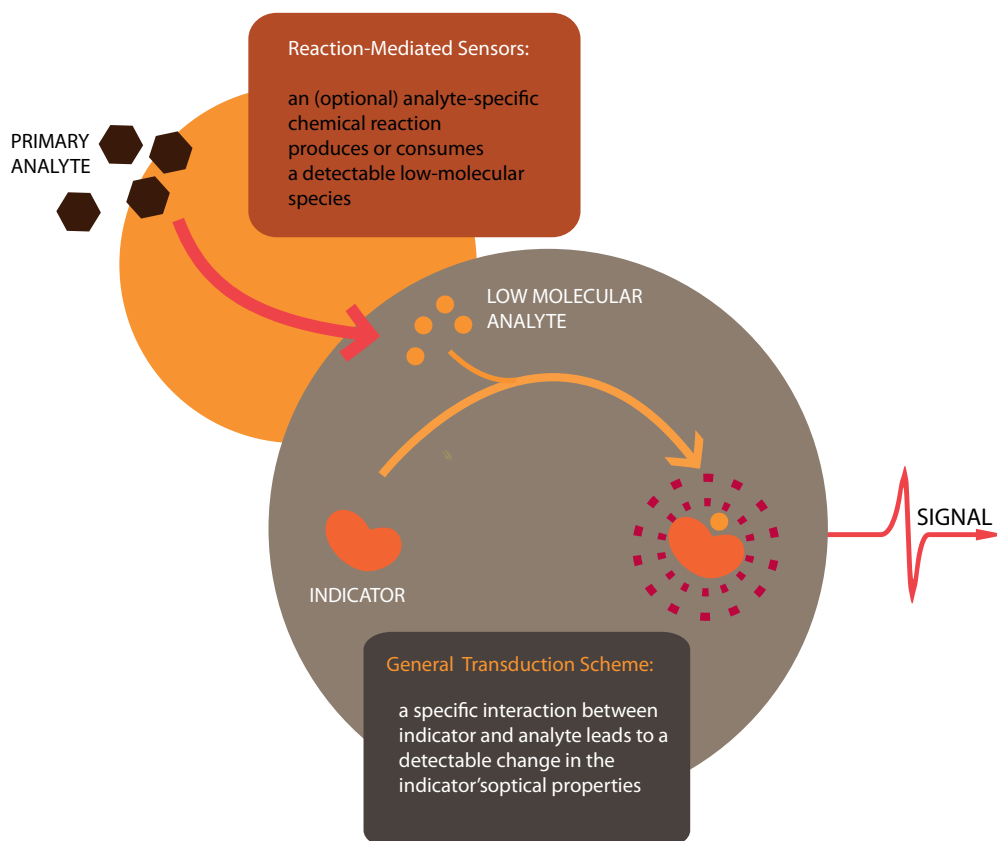


**Figure 2.11:** A figure illustrating the general principle of transduction in optical chemical sensors.

by means of immobilisation and to provide a level of specificity by acting as a barrier for the undesired components of the sample matrix.

In some cases, due to the lack of reliable systems based on direct interaction between the analyte and the indicator an auxiliary element is added to the sensing scheme. In so-called **reaction mediated sensors** a highly analyte-specific reaction, often involving enzymes, is coupled with the detection of a chemical species that gets consumed or is produced in the course of this reaction and is capable of directly interacting with the indicator.

Chemical sensors in general do not include separation steps, as commonly found in mod-

ern instrumental analytics. The sensor's specificity, i.e. its ability to recognize only the analyte of interest in even complex samples is established by means of molecular recognition elements within the matrix, specific interactions between the analyte and the indicator or specific reactions in the case of reaction mediated sensors. Biomolecules such as enzymes, DNA or antibodies offer a high degree of specificity and flexibility with regards to possible analytes and are easily accessible. Consequently, such biomolecules are frequently incorporated into optical sensor systems. By convention, these sensors are referred to as **biosensors**.<sup>[5]</sup>

Optical chemical sensors exist for a variety of analytes ranging from gaseous analytes such as oxygen ( $pO_2$ ), carbon dioxide ( $pCO_2$ ) or ammonia ( $pNH_3$ ) to  $pH$ -sensors, sensors for *glucose* and sensors for *ionic species*, and are based on a variety of optical phenomena such as *absorption*, *refractivity* or *luminescence*.

Apart from classification which can be drawn based on the **classes or types of analytes** and the **optical principle** used in signal transduction, a third way to classify optical chemical sensors looks at the **optical layout**. Depending on the individual application, sensor platforms are commonly based on *sensor films*, *fibre sensors* (waveguides), *capillary sensors* or *sensor arrays*.

### Luminescence-based Chemical Sensors

Luminescence-based chemical sensors represent a prominent group among optical chemical sensors. This situation is attributable to the high intrinsic sensitivity <sup>[4]</sup> of luminescence based transduction systems, the availability of a large variety of indicator dyes offering the possibility to choose excitation and emission spectra with regard to their suitability in the sensor's context of application.

#### 2.2.3 Optical Oxygen Sensors

Optical oxygen sensors typically consist of an **organic dye immobilised in an oxygen permeable polymer matrix**. The fundamental principle of **transduction** is based on the luminescence of the indicator being quenched upon collision with molecular oxygen, resulting in the formation of singlet oxygen as well as a decrease in luminescence lifetimes and intensities. <sup>[6]</sup> The process of **collisional quenching** is diffusion-limited and can be described by the models discussed in the section on quenching. In the case of oxygen acting as a quencher, equations 2.8 and 2.9 transform to:

$$\frac{I_0}{I} = 1 + K_{SV}pO_2 \quad (2.10)$$

and

$$\frac{I_0}{I} = \frac{\tau_0}{\tau} = \frac{1}{\frac{f_{01}}{1+K_{SV1}pO_2} + \frac{1-f_{01}}{1+K_{SV2}pO_2}} \quad (2.11)$$

respectively, with  $pO_2$  representing the oxygen partial pressure.

Optical oxygen sensors generally show cross-sensitivity to temperature which is attributable to thermal quenching of the luminophore and to the fact, that the gas permeability of polymers usually increases with temperature, due to the temperature-dependency of diffusion processes. To overcome this drawback, systems allowing the simultaneous measurement of temperature via luminescent probes have been developed.<sup>[7]</sup>

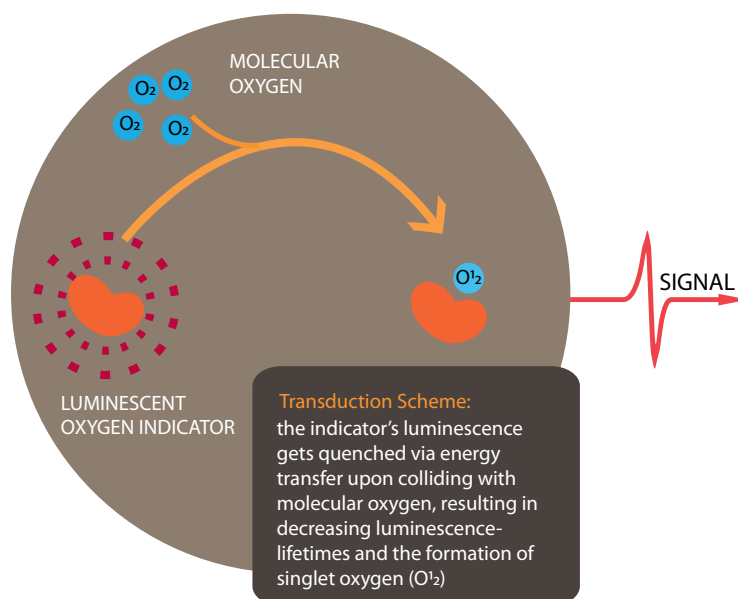


**Figure 2.12:** A figure illustrating the general principle of transduction in optical oxygen sensors.

### 2.2.4 Application Areas

Apart from the use of oxygen sensors in fields such as environmental and marine science and biotechnology, oxygen serves as a key low-molecular-weight analyte in a variety of enzyme-based reaction-mediated chemical sensors, such as glucose sensors[5], due to its important role in many enzymatic processes. In many application areas it has become of interest to expand the sensor layout towards systems consisting of dispersed entities taking care of the signal transduction, such as sensor nano- or micro-particles [8], which in some cases even harbour magnetic properties to allow easy separation and spatial orientation [9]. Furthermore, bio-conjugated oxygen indicators represent a powerful tool in the study of cellular function[10].

### 2.2.5 Oxygen Indicators

The most common classes of oxygen indicator dyes are **Pt(II) and Pd(II) complexes with porphyrins and their derivatives** as ligands [11], [12],[13], **cyclometalated Ir(III) and Pt(II) complexes** and **Ru(II) polypyridyl complexes**. Historically, fluorescent, polyaromatic hydrocarbons are of importance. However, they are characterised by short lifetimes and are consequently less sensitive towards oxygen, when compared to modern indicator dyes.

Among the metalloporphyrinoids, Pd(II) complexes usually exhibit longer phosphorescence lifetimes than their Pt(II) counterparts and are thus suitable for use in trace oxygen sensors. Metalloporphyrinoids offer a great degree of versatility regarding their spectral properties, with classical complexes such as Pt(II)-octaethylporphyrin absorbing UV-light and visible light in the green region and  $\pi$ -extended porphyrins, such as Pt(II)-tetraphenyltetrabenzoporphyrin absorbing blue and red light and even emitting in the NIR range of the electromagnetic spectrum. The latter indicator is especially well suitable for applications in highly scattering media and *in vivo* measurements. [8] **Figure 2.13** gives examples of the main classes of oxygen indicator

dyes and **table 2.1** gives an overview of important oxygen indicators and their key spectral and photo-physical properties.

**Table 2.1:** An overview of common luminescence-based oxygen indicators

Indicator	$\lambda_{\max}^{\text{abs}}$ [nm]	$\epsilon$ * [M <sup>-1</sup> *cm <sup>-1</sup> ]	$10^{-3} \lambda_{\max}^{\text{em}}$ [nm]	$\phi$	$\tau_0$ [ $\mu$ s]	Ref.
Ru(dpp) <sub>3</sub>	463	28.6	618	0.37	6.4	
Ir(Cn) <sub>2</sub> (acac)444, 472		86.8, 92.8	563	0.54	11.3	[14]
PtOEP	380, 535	220, 46.1	646	0.41	90	[15]
PtTPTBP	430, 564, 614	205, 16, 136	770	0.51	47	[12], [16]
PdTPTBP	444, 578, 628	416, 21, 173	800	0.21	286	[12], [17]

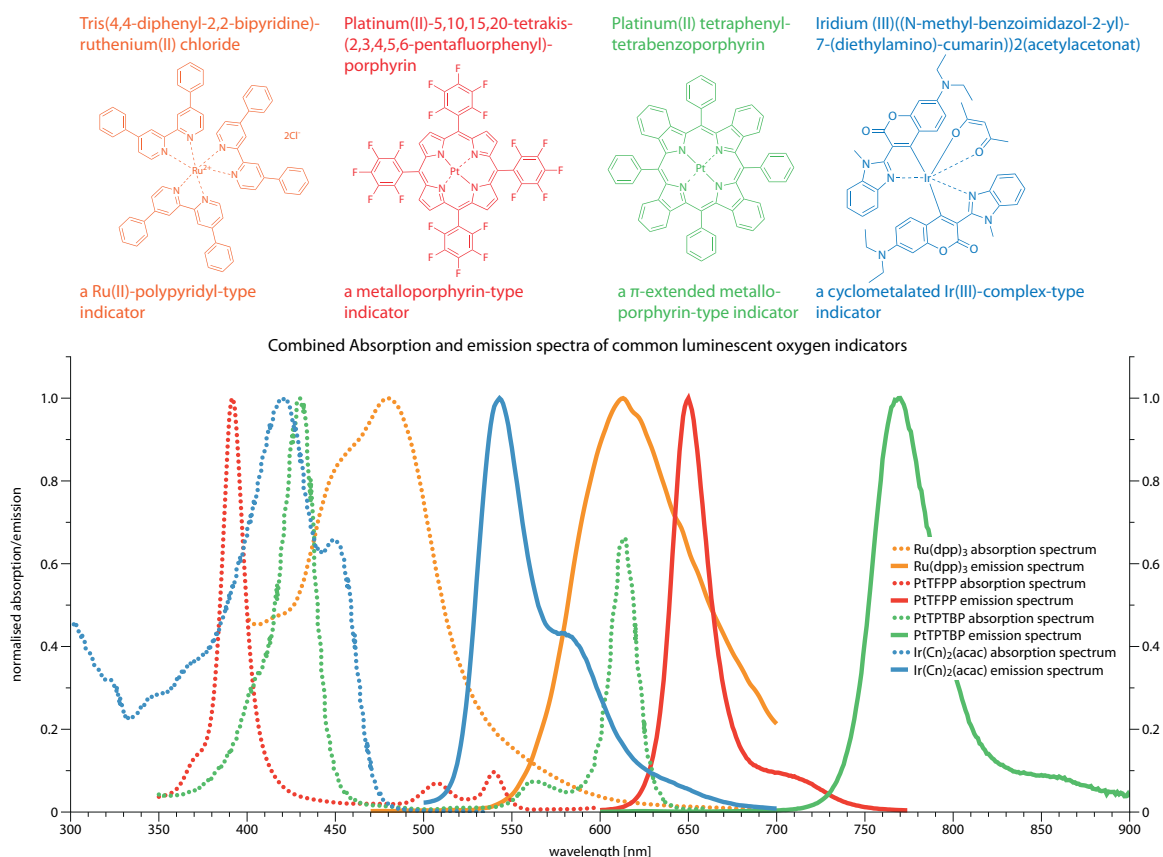


**Figure 2.13:** This figure illustrates examples of common oxygen indicator classes. The combined absorption-emission spectra illustrate the range of possible excitation and emission wavelengths possible, depending on the indicator. (*Spectral data obtained from <http://www.fluorophores.tugraz.at/>*)

## 2.2.6 Parameters Determining Sensitivity

The sensitivity of an optical oxygen generally is a function of two parameters:



- **Luminescence Lifetime**

The luminescence lifetime represents the timeframe in which quenching can occur. A longer lifetime results in a higher Stern-Volmer-Constant, which corresponds to the slope of the curve in the Stern-Volmer plot. Thus, with longer lifetimes the response to small changes in oxygen concentration at trace levels becomes more pronounced.

- **Oxygen Permeability of the Matrix**

The better the oxygen permeability of the matrix, the better the response to small changes in oxygen concentration at trace levels.

### 2.2.7 Analytical Criteria and Key Considerations

A sensor device not only serves fundamental scientific interests, but should fulfil a series of criteria relevant for its practical use.[18] The key considerations relevant for chemical sensors in the context of their application shall be outlined and briefly discussed below.

- **Signal to Noise Ratio**

It is desirable for a chemical sensor to be characterised by a high ratio of analyte-specific signal to inherent unspecific signal (noise).

- **Optical Response**

The change in the optical signal generated in signal transduction should be well pronounced. In optical oxygen sensors the change in signal is represented by a change in luminescence lifetime and luminescence signal intensity. The strength of the optical response is reflected in Stern-Volmer plots, with the slope of the curve, for linear Stern-Volme plots the  $K_{SV}$ -value, corresponding to the sensor's sensitivity.

- **Referencing of the Signal**

It should be possible to easily reference the signal, without the necessity to incorporate complicated additional apparatus or procedures. Optical oxygen sensor systems are commonly realised employing lifetime measurements, which can be considered as reference-free.

- **Mathematical Modelling of the Optical Response**

A fairly simple mathematical relation should underpin the change in the optical signal brought about by the interaction between analyte and indicator, making the data obtained easy to process and interpret by non-experts.

In the case of optical oxygen sensors, the models describing the sensors optical response are Stern-Volmer-Kinetics or the Two-Site Model, which represent mathematical models which are fairly easy to interpret.

- **Material Adherence**

The sensor material should properly adhere to the supporting material to provide flexibility and robustness with respect to the sensor's use.

- **Photostability**

Photophysical processes involve excited-state molecules, which exhibit altered chemical properties when compared to their ground states. Generally, molecules in excited state act as better bases and acids, and possess an altered redox-potential. Hence, indicators used in optical sensors are exposed to a potentially harmful chemical environment, which

can ultimately lead to the inactivation of indicators as functional component in signal transduction. A change in the concentration of indicator molecules results in an altered optical response and can lead to errors with regard to the interpretation of the data obtained during use. Consequently, it is desirable to design indicators in such manner, as to increase their stability under prolonged exposition to light, i.e. photo-stability.

- **Compatibility with Common Semiconductor-Based Optical Components**

It has become a necessity to design indicators used in optical sensors in such manner, as to provide compatibility with common semiconductor-based optical elements such as photo-diodes used for excitation of luminescence-indicators. The use of semiconductor-based optical components has a series of advantages such as lower cost, higher robustness and a greater potential for further miniaturisation.

- **Costs**

The design of optical sensors is highly application-driven, as such, the issue of cost is not negligible.

- **Toxicity**

Many sensors are designed for applications in biological systems, biotechnology, food processing or for diagnostic purposes. Hence, it is vital for sensor systems to be non-toxic. The most commonly used optical oxygen indicators are poorly soluble in water and employed in very low concentrations, hence reducing the likelihood of toxic effects.

- **Shelf-Life**

A sensor should be designed in such manner, as to reduce potential performance loss over periods of storage.

- **Leaching, Deterioration**

Indicators used in optical chemical sensors are commonly physically entrapped in the polymeric support, or get covalently immobilised in the polymer matrix. Despite the fact, that a polymer can be considered as a fairly rigid matrix, the indicator is still moderately mobile in the matrix which can lead to phenomena such as leaching, i.e. the indicator being washed out over time, or indicator aggregation in the matrix, which can lead to processes such as self quenching. In both cases, the optical response of the sensor gets altered and can ultimately result in errors in the interpretation of the measurement data obtained. Covalently linking the indicator to the polymer matrix can alleviate this problem by suppressing the indicators mobility, and is as such desirable.

### 2.2.8 Sensor Matrices

A large variety of oxygen-permeable matrices are used in optical oxygen sensors. Among the less oxygen permeable matrices are **polystyrene based polymers, polysulfones and polymethacrylates**, whereas **silicone based polymers, ethylcellulose, ormosils and fluoropolymers** represent highly oxygen permeable matrices. [6]

## 2.3 Immobilisation

As already outlined above, the leaching of the dye is a key problem in the field of optical chemical sensors. In the most simple set-up, immobilisation of the indicator is realised by physically entrapping the indicator dye in the polymer matrix. In the case of sensors for the detection of hydrophilic analytes such as protons (pH) and ions, the use of covalent immobilisation techniques is almost mandatory [18], since such systems commonly involve hydrophilic indicators in hydrophilic polymer matrices and aqueous medium and are as such highly prone to exhibit leaching. Despite the fact, that covalent immobilisation is not yet common in oxygen sensors, it is highly desirable, since it potentially increases sensor performance with respect to sensor-stability and shelf life.

A basic approach towards covalent immobilisation of indicator dyes is based on the dye carrying a monomeric residue that allows for the **co-polymerisation of the indicator dye** in the matrix of choice without compromising the dyes photophysical properties. If this approach is not an option a broad set of reactions allows for the indicator dye to be grafted to the matrix. In principle any reaction resulting in the formation of a covalent bond may be regarded as a potential starting point for a covalent immobilisation approach, yet practical considerations regarding the yield of the reaction, the formation of possible by-products and the reaction conditions applied constrain the set of possible reactions.

### 2.3.1 Bio-Conjugation-Inspired Techniques

The chemistry involved in the covalent immobilisation of proteins (bio-conjugation) offers a **broad variety of well-established techniques**, which employ **inexpensive chemicals**, are characterised by a **high degree of reproducibility, flexibility, good yields at mild reaction conditions** and allow the indicator to be grafted to a **broad variety of matrices**. These techniques mainly rely on functional groups common to all proteins, such as carboxylic acid residues, amines or thiol-groups and are a source of well-tried conjugation-techniques to the field of chemical sensors.

#### Immobilisation based on Amines and Carboxylic Acids

Activated carboxylic acids readily undergo reactions with amines, a fact that is exploited in the EDC/NHS-coupling-method.

Apart from their use in this potential approach, amines readily react with thio-isocyanates to yield thiourea. Thioisocyanates can be prepared by reacting amines with thiophosgen, however the approach involves the use of a highly toxic reactant. Figure 2.14 provides a scheme illustrating thiophosgen based coupling.

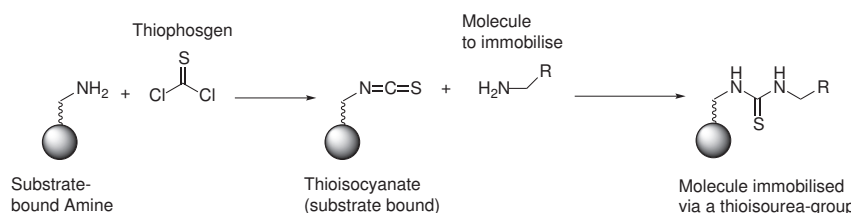


**Figure 2.14:** A reaction scheme illustrating thiophosgen-based coupling

### NHS/EDC-coupling

NHS/EDC coupling is a well established bio-conjugation technique. A carboxylic acid gets activated upon reaction with an activation-reagent such as *1-Ethyl-3-(3-dimethylamino-propyl)carbodiimid* (**EDC**) and subsequently reacts with *N-Hydroxysuccinimid* (**NHS**) or a derivative to form a **NHS-ester**, which represents an activated carboxylic acid and readily reacts with amino-groups. [19]

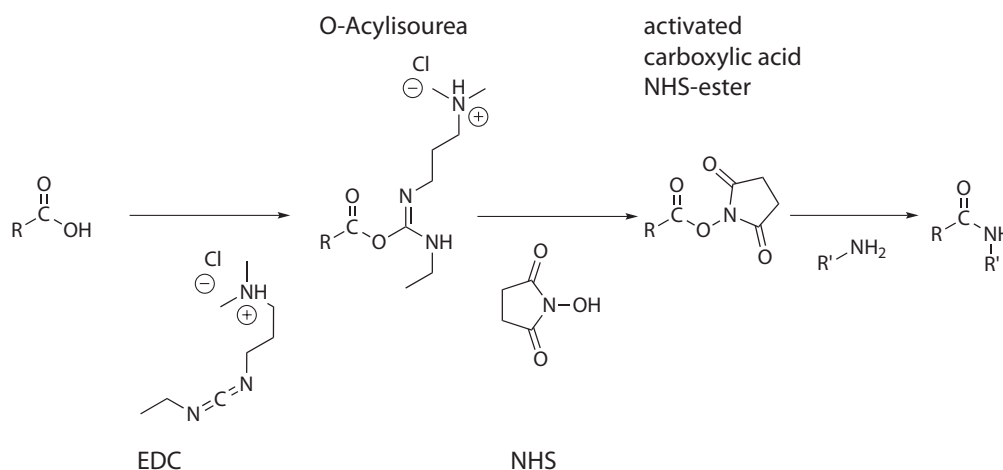


**Figure 2.15:** An overview of the steps involved in EDC/NHS-conjugation.

### Immobilisation based on vicinal diols

The presence of vicinal diols in substrates such as sugars and their derivatives can be exploited in a variety of immobilisation approaches. Reaction of the vicinal diol with ethyl chloroformate or cyanogen bromide yields reactive cyclic carbamates or imido-carbamates, respectively. Upon reaction with the amino-group of the molecule to be immobilised N-substituted carbamates or isourea derivatives are formed.

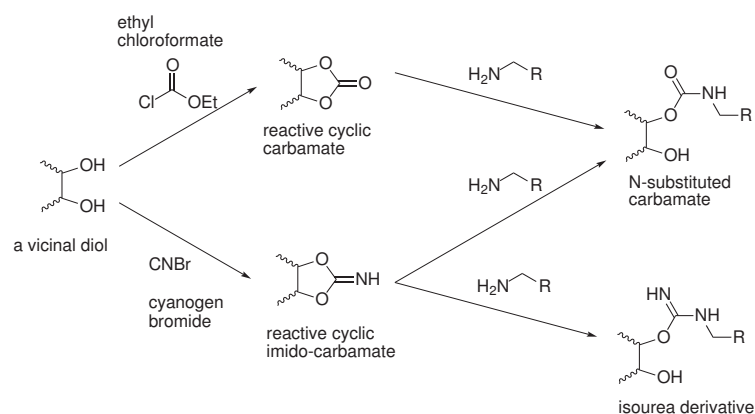


**Figure 2.16:** A reaction scheme depicting immobilisation based on vicinal diols.

## 2.3.2 Click-chemistry

By definition, click chemistry reactions are characterised by **high yields**, a **high degree of modularity**, **wide scopes**, **simple reaction conditions**, **inoffensive byproducts**, **simple product isolation** and can be performed with **moderately cheap and readily available starting materials**. [20] As such they qualify as simple and flexible approach towards the immobilisation of indicator dyes, particularly in cases when functional groups such as carboxylic acids are not accessible for chemical modification. A series of different reactions fall under the label of "click-chemistry". Figure 2.17 gives a graphical overview of the most prominent reactions.

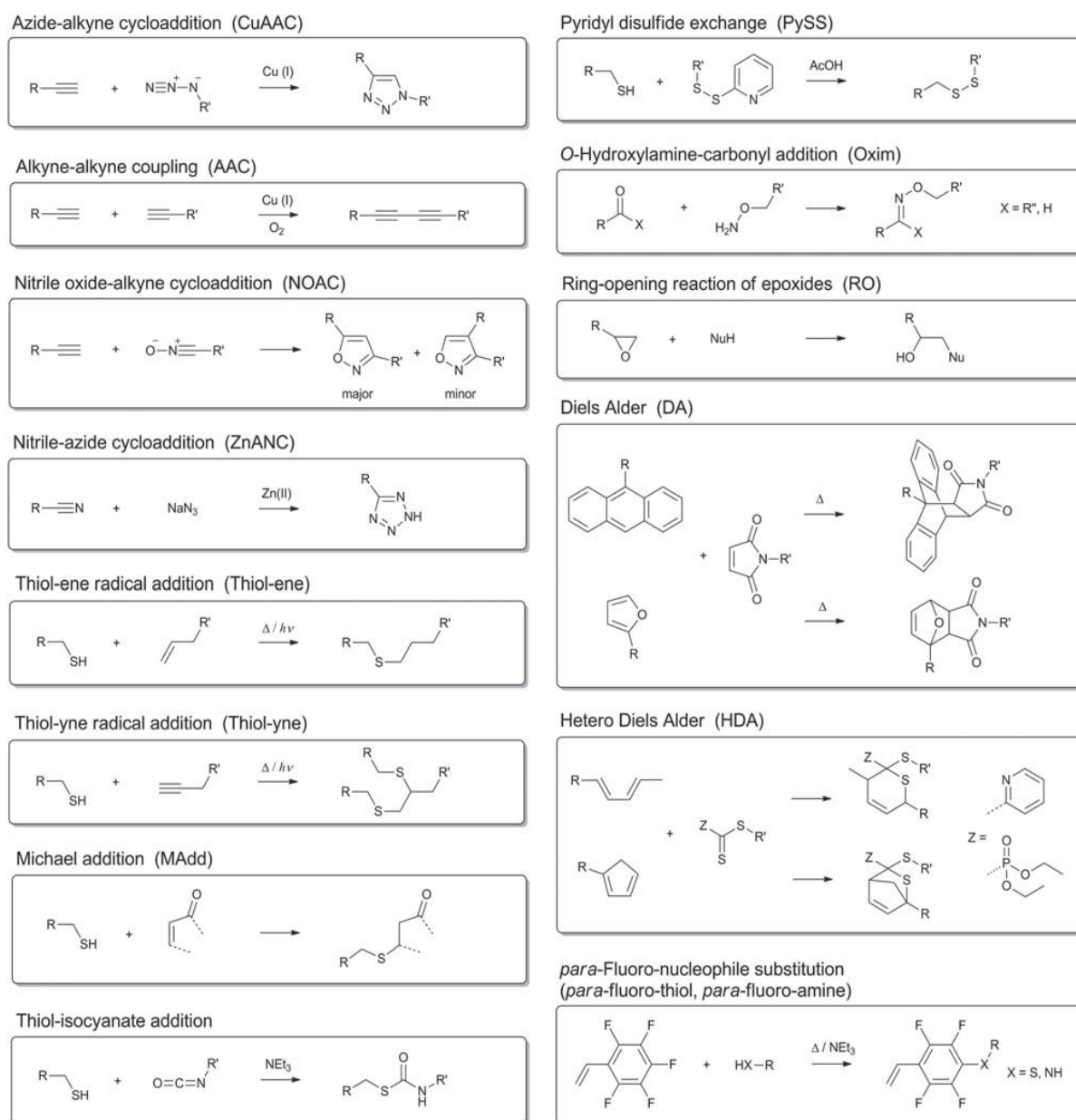


**Figure 2.17:** An overview of the various types of reactions generally classified as click-chemistry reactions. [21]

### 2.3.3 Further Considerations

Based on the set of reactions outlined above, schemes for the immobilisation of a variety of molecules on a variety of substrates may be conceived. By modifying silica surfaces with silyl reagents such as amino- or thiopropyltriethoxysilane, the surface of glass or silica particles is made accessible to simple covalent immobilisation by means of thiol-based click chemistry techniques or EDC/NHS-coupling.

Many immobilisation techniques require substrates carrying functional groups characterised by a minimum degree of reactivity (carboxylic acids, amines, thiols, boronic acids). The presence of such entities, however, may restrict the choice of synthetic procedures applicable to an indicator dye. The use of transition-metal-catalysed cross-coupling reactions, such as the Suzuki-coupling, offers the possibility to prepare indicators carrying halides, which can be considered as moderately unreactive groups, and their subsequent post-synthetic modification to yield immobilised products or products carrying functional groups which facilitate immobilisation by means of established techniques. The application of Suzuki-coupling in this approach is investigated in this thesis.

## 2.4 Suzuki Coupling

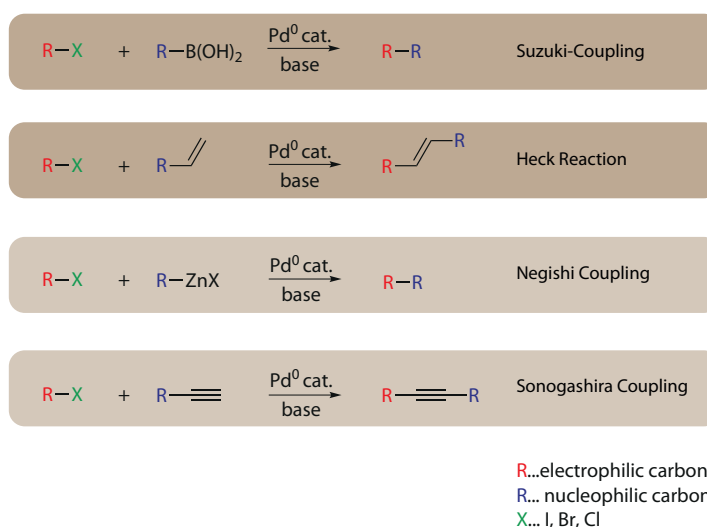


**Figure 2.18:** Overview of the most common Pd(0) catalysed cross-coupling reactions.

Transition-metal catalysed cross-coupling reactions offer reliable ways towards C-C-bond formation in organic synthesis. They generally involve the coupling of an electrophilic organic species with a nucleophilic organic species in a series of transition-metal mediated steps resulting in the formation of a C-C-bond. Such transition-metal catalysed reactions offer a series of advantages over reactions of comparable scope, which qualify them for being put to use in the last steps of multi-step total syntheses [22]:

- Ready availability of reactants
- Mild reaction conditions, non-toxic reactants, environmentally benign reaction conditions.
- High yields
- Water stability
- Easy use of the reaction under both aqueous and heterogeneous conditions
- High functional-group tolerance, regio- and stereospecificity
- Insignificant effect of steric hindrance
- Possibility of one-pot syntheses

Early transition-metal catalysed cross-coupling reactions established coupling between organometallic "Grignard" reagents acting as nucleophiles and organohalides serving as electrophiles and made use of Nickel-based catalysts.[23] From the mid-1970s onwards the field of transition-metal catalyzed cross-coupling reactions has been receiving increasing attention leading to the development of a series of named reactions, which nowadays belong to the standard toolkit of the synthetic chemist. A development, which in 2010 culminated with three pioneers of the field, Akira Suzuki, Ei-ichi Negishi and Richard F. Heck, being awarded the Nobel Prize in Chemistry.

Among the many named reactions in the field of transition-metal catalyzed cross-coupling reactions, the Suzuki-Coupling, the Sonogashira-Coupling, the Negishi-Coupling and the Heck reaction are most prominent.

These coupling reactions all typically employ a **Pd(0) catalyst**, a **base** and an **organyl-halide**, however they differ in terms of the nucleophilic species involved. Figure 2.18 provides a schematic overview of these four common cross-coupling reactions.

### 2.4.1 Mechanism

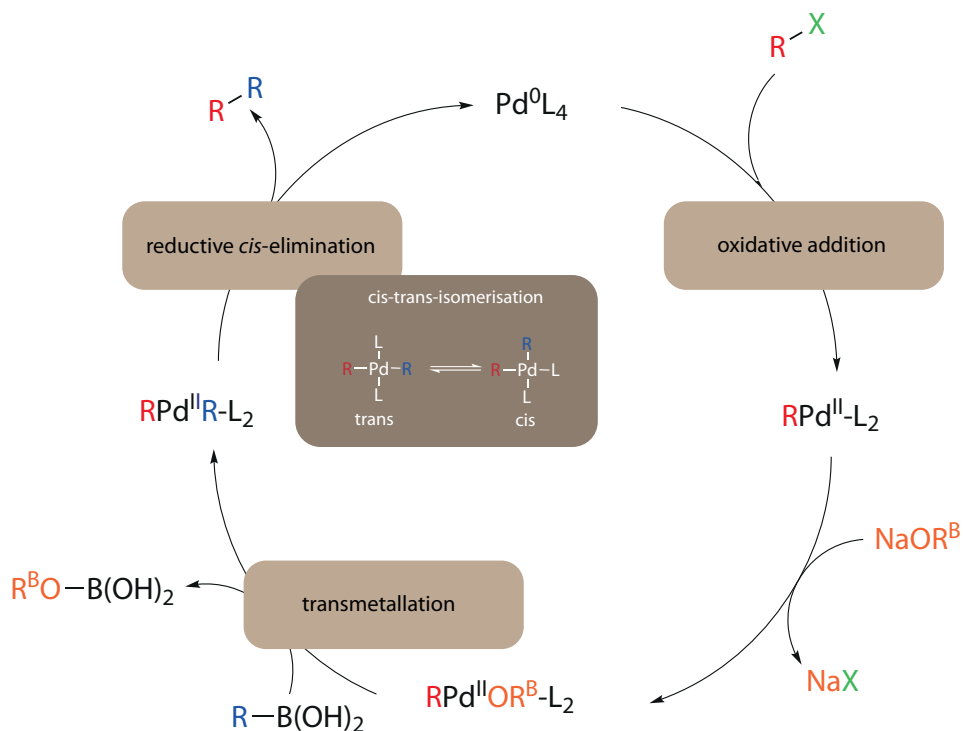
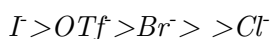


**Figure 2.19:** An overview of the reaction steps involved in the catalytic cycle of the Suzuki reaction.

Suzuki-coupling employs **organoboronic acids as nucleophilic reactants**. The catalytic cycle comprises three distinct steps:

#### 1. Oxidative Addition

Pd(0) inserts into the R-X-bond of the nucleophilic organo-halide, resulting in its oxidation to Pd(II). The reactivity of the leaving group decreases according to:



Soft nucleophiles (X) are favoured as leaving groups, because they are more likely to participate in oxidative addition.[24]

Oxidative addition initially results in the formation of a *cis*-complex, which rapidly isomerises into a *trans*-complex.[25]

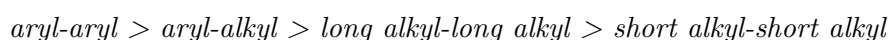


## 2. Transmetallation

A thermodynamically favourable exchange step resulting in the formation of a salt and the exchange of the leaving group with the anionic component of the base is followed by the actual transmetallation step. The exact role of the base in the transmetallation step is not known, yet it is necessary for transmetallation to occur since organoboron-compounds are highly covalent in character and do not undergo transmetallation in the absence of a base. The formation of quaternary boron-"ate" complexes upon reaction with the base is often invoked in this respect.[26]

## 3. Reductive Elimination

A reductive elimination step yields the coupling product via a four-membered transition state. Precondition for reductive elimination to occur is the formation of the *cis*-complex with regard to the coupling-substrates. The rate of the reductive elimination step is dependent on the coupling-substrates[27]:



### 2.4.2 Organoboranes

Common substrates for Suzuki coupling reactions include organoboronic acids, organoboronic esters and tertiary organoboranes. ( $sp^2$ )C-B compounds such as arylboronic acids readily react under regular conditions. ( $sp^3$ )C-B compounds require the use of special electron-rich ligands.[28]

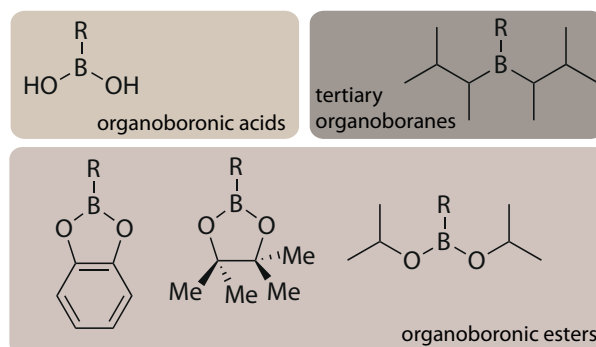


**Figure 2.20:** Some examples of commonly used organoboranes.

### 2.4.3 Catalysts

The most commonly used catalytic system employed in Suzuki coupling reactions is  $\text{Pd}(\text{PPh}_3)_4$ , which is commercially available. Other approaches involve the *in situ* formation of Pd(0) catalyst via reduction of a Pd(II)-precursor compound in the presence of phosphine-ligands. By means of in-situ preparation of the catalyst a large variety of ligands are accessible. **Bulky, electron-rich ligands** are characterised by a **higher reactivity** and allow the use of inactive substrates such as arylchlorides and ( $sp^3$ )C-B-species. Most ligands employed are stable in the presence of water, but require handling under inert atmosphere due to their sensitivity towards oxidation [29],[30].

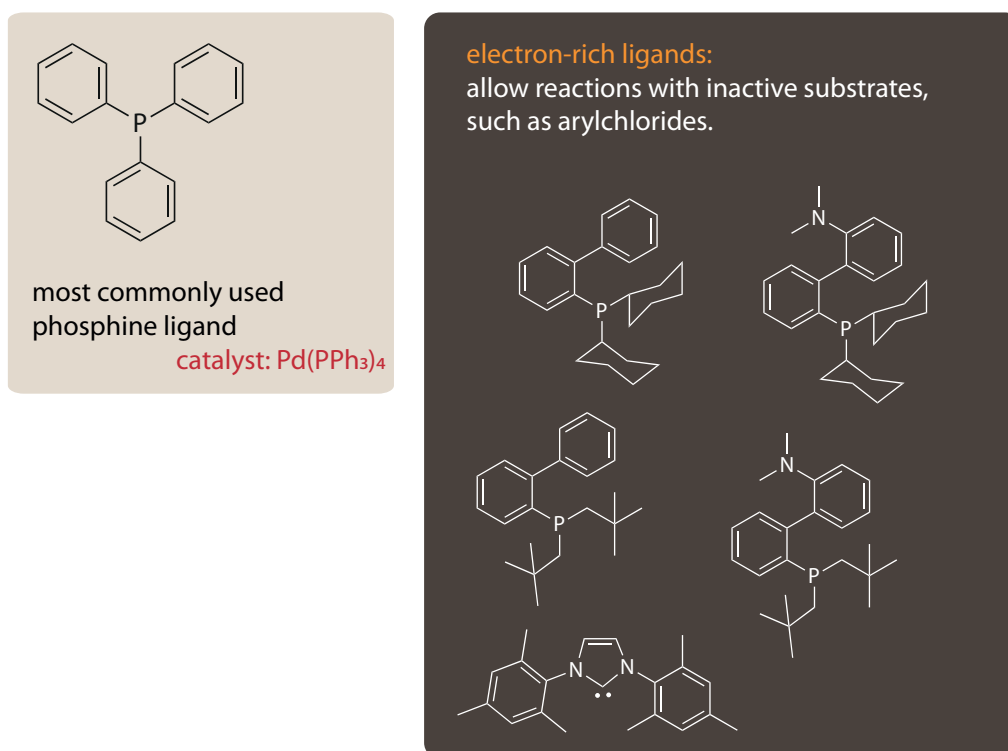


Figure 2.21: Some examples of commonly used ligands.

#### 2.4.4 Conditions

Suzuki coupling reactions are commonly conducted in a **biphasic mixture of organic solvent and aqueous phase**, but can also be conducted purely in water. Many common organic solvents can be used. Key considerations regarding the choice of solvent are solubility of substrates, catalysts and ligands, as well as reaction work-up.

Common bases employed in Suzuki reactions are **alkali-alkoholates** and **alkali-carbonates**. Reaction times and temperatures are highly dependent on the system of substrates, bases and ligands employed and are subject to variations. [31], [32]

---

## 3 Materials and Methods

### 3.1 Chemicals Used

**Table 3.1:** A list of chemicals used

Substance	purchased from	CAS-Number
Dichloromethane	Acros	75-09-2
Chloroform	Roth	67-66-3
Toluene	Roth	108-88-3
Tetrahydrofuran	Roth	109-99-9
Acetone	Roth	67-64-1
Ethanol	Australco AT	64-17-5
1,3,5-Trimethylbenzene	Merck	108-67-8
Styrene	Fluka	100-43-5
4-Vinylbenzeneboronic acid	abcr	2156-04-0
Polystyrene	Acros	9003-53-6
Aza-isobutyronitrile	Acros	78-67-1
Phenylacetic acid	Aldrich	103-82-2
4-Aminophenylacetic acid	abcr	1197-55-3
4-Bromophenylacetic acid	abcr	1878-68-8
Phthalimide	Aldrich	85-41-6
1,2-Dicyanobenzene	Aldrich	91-15-6
4-Vinylbenzeneboronic acid	abcr	2156-04-9
Pentafluorophenylboronic acid	abcr	1582-24-7
Potassium Carbonate	Aldrich	584-08-7
Caesium Carbonate	Aldrich	534-17-8
Potassium-tert-butoxid	Aldrich	865-47-4
Tetrakis(triphenylphosphin)palladium	abcr	14221-01-3
Benzonitrile	Aldrich	100-47-0
Platiniium chloride	abcr	10025-67-7
Methanesulfonic acid	Aldrich	75-75-2
Aluminium oxide	Acros	1344-28-1

## 3.2 Sensor Preparation

The sensors prepared and characterised in the course of this thesis consist of a Pt(II)-meso-tetraphenyltetraenzoporphyrin-based dye covalently bound or physically entrapped in a polymer matrix coated onto a substrate. Two types of sensor layouts were employed: Sensor films and films and fibre based sensors.

### 3.2.1 Sensor Films

Sensor films of defined thickness were prepared by knife coating cocktails of comparable viscosity onto Mylar®-films using a 25  $\mu\text{m}$  spaced *Gardner 1MIL WET FILM* coating knife. Cocktails typically contained 1 *wt%* of polymer dissolved in chloroform (HPLC-grade). Unless otherwise stated, sensor cocktails contained 1 *wt%* of dye with respect to the amount of polymer employed. The dye content of the sensor-films prepared from the covalently-functionalised sensor polymers varied according to the degree of functionalisation. After casting, the sensor films were carefully dried for 24 h at 70 °C to ensure complete removal of solvent before characterisation.

### 3.2.2 Fibre Based Sensors

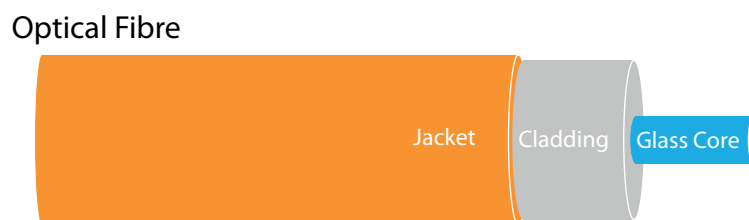


**Figure 3.1:** A schematic illustration of an optical fibre.

Figure 3.1 depicts the basic components of optical fibres. Fibre-based sensors were obtained following the protocol outlined below:

1. Jacket and cladding were removed using appropriate de-cladding tools set at 200  $\mu\text{m}$ , thus removing a majority of the cladding but leaving a very thin layer of cladding on the fibre.
2. The glass core surrounded by a thin layer of residual cladding was broken perpendicular to the fibre axis to obtain a flat surface.
3. The residual cladding was removed by burning it off.
4. The fibre tip was washed with ethanol.
5. By carefully dipping the fibre tip into a sensor cocktail, composed as described in the section on sensor films, the flat surface at the tip of the fibre was coated.
6. The coated fibres were left to dry at 70 °C conditions for one day before being characterised.

### 3.3 Photophysical Characterisation

#### 3.3.1 Absorbtion Spectra

Absorption spectra were recorded between 800 nm and 350 nm on a "Varian Cary 50 Conc" UV-Vis Spectrometer set at fast scan rate using baseline correction and an adequate blank sample.

Unless otherwise stated, dyes were dissolved in Dichloromethane an measured in *Hellma 100-QS 10mm precision cuvettes* or *Hellma 101-OS 10mm precision cuvettes*.

#### 3.3.2 Determination of Extinction Coefficients

Extinction coefficients were determined by measuring absorption spectra of solutions containing a defined amount of dye in a defined volume of Dichloromethane.

$$E = \epsilon \cdot c \cdot d \quad (3.1)$$

$\epsilon$  ... molar extinction coefficient [ $L \cdot mol^{-1} \cdot cm^{-1}$ ]

$c$  ... concentration of the absorbing species [ $mol \cdot L^{-1}$ ]

$d$  ... lenth of the optical pathway in through the absorbing sample [cm]

Extinction coeffecients for Soret-band-absorption of Benzoporphyrins in Dichloromethane range around  $250\,000 L \cdot mol^{-1} \cdot cm^{-1}$ . According to Beer's Law (eqn. 3.1), solutions of benzoporphyrins in Dichloromethane exhibit an absorption of about 0.5 at the Soret-band maximum, provided a value of 1 cm for  $d$  and a concentration of  $2 \cdot 10^{-6} M$ . Taking the benzoporphyrin's molar mass into consideration, the mass necessary for obtaining such solutions was calculated for a sample volume of 1 L.

Three samples were prepared by weighing the appropriate amount of dye using an *AND Model ER182A analytical balance*, carefully dissolving it in Dichloromethane in an 50 mL volumetric flask and subsequent dilution by a factor of 20 using piston-driven air replacement pipettes by Eppendorf.

An absorption spectrum was recorded for each sample and the absorbance at the Soret-band maximum was determined using the spectrometer-software. Extinction coefficients were determined by applying Beer's law and taking into account the solution's concentration calculated from the actual mass weighed. Similarly, when the extinction coefficient was known, Beer's Law was applied to determine the dye-concentration in solutions.

#### 3.3.3 Determination of Quantum Yields

##### Reference Method - Solutions of Dyes

Due to constraints in the experimental set-up, a reference method had to be applied in order to determine quantum yields for dyes in solution. The reference method entails the comparison of the integrated emission spectra of the dye and a suitable reference. PtTPTBPF<sub>4</sub> was chosen as a suitable reference due to close similarity to the dyes synthesized in terms of chemical and photo-physical properties.

Solutions characterised by a maximum absorbance smaller than 0.01 were prepared by dissolving an appropriate amount of dye in toluene. The solutions were transferred into *Hellma screw-cap fluorescence cuvettes* sealed with both a Teflon, and a Silicon-rubber septum. The samples were

de-oxygenated by bubbling argon through the solutions for 25 min. The degree of de-oxygenation was checked on by a quick frequency-domain measurement determining the dye's luminescence lifetime using a *Presens mini-lock-in device*.

$$S_{\text{corr}} = S \cdot (1 - 10^{A_{\text{ex}}}) \quad (3.2)$$

S ... value obtained from the integration of the emission spectrum

$S_{\text{corr}}$  ... corrected value for S

$A_{\text{ex}}$  ... absorbance at the excitation wavelength

Corrected emission spectra upon excitation at 615 nm were measured at a *HORIBA Jobin Yvon Fluorolog-3* using the system's built-in photo-multiplier sensitivity correction. The spectra were integrated and the obtained value corrected for the solution's absorbance according to eqn. 3.2. The quantum yield relative to the reference dye was obtained by dividing  $S_{\text{corr, sample}}$  by  $S_{\text{corr, reference}}$ . By multiplying the obtained relative value with the absolute quantum yield of the reference obtained from literature.

### Absolute Method - Sensor Films

The quantum yield in sensor films could be determined using an absolute approach, employing an *integrating sphere-based set-up at the HORIBA Jobin Yvon Fluorolog-3*. In this approach, a circular piece of sensor film of a defined diameter of 1.27 cm is placed into an integrating-sphere, which is a spherical, hollow optical component. The cavity of the integrating sphere is covered with an diffuse, reflective coating and an indirect excitation spectrum as well as an emission spectrum is recorded.[33]

The sphere was de-oxygenated for 40 s after any manipulation of the set-up.

The film's absorbance was determined by measuring the emission signals across the excitation wavelength: The luminophores were excited at 620 nm, the emission profile was scanned between 590 nm and 650 nm. The excitatory monochromator-slits were set at 3 nm and the emission-monochromator-slits were set at 7 nm. A neutral density filter characterised by 5% transmission was placed in front of the detector in order to protect the detector from too high light intensities. The film's emission spectra were recorded between 710 nm and 950 nm using the same excitation- and monochromator-settings, yet dispensing of the neutral density filter.

All spectra recorded were corrected using the built-in photo-multiplier sensitivity correction. The quantum yields were calculated using the quantum yield calculator provided by the HORIBA Jobin Yvon Fluorolog-3-system's software. The indirect absorbance spectra were integrated between 610 nm and 630 nm, the emission spectra were integrated between 710 nm and 950 nm. The calculation was conducted using the system's Ulbricht-sphere correction settings, an area balance factor of 20 accounting for the neutral density filter used in the indirect excitation spectrum. The Mylar®-film's intrinsic optical properties were accounted for, by conducting blank measurements using a plain Mylar®-film and considering the blanks correctively in the automated quantum yield calculation.

#### 3.3.4 Sensor Calibration

Sensor calibration curves were determined by performing frequency-domain measurements of luminescence lifetimes at defined oxygen partial pressures.

Frequency domain measurements entail the excitation of the luminophore by means of modulated light. The luminophore's excited state lifetime gives rise to a detectable shift between

excitation and emission phases (Fig. 3.2).

In the case of luminophores exhibiting mono-exponential decay, the phaseshift  $\phi$  can range

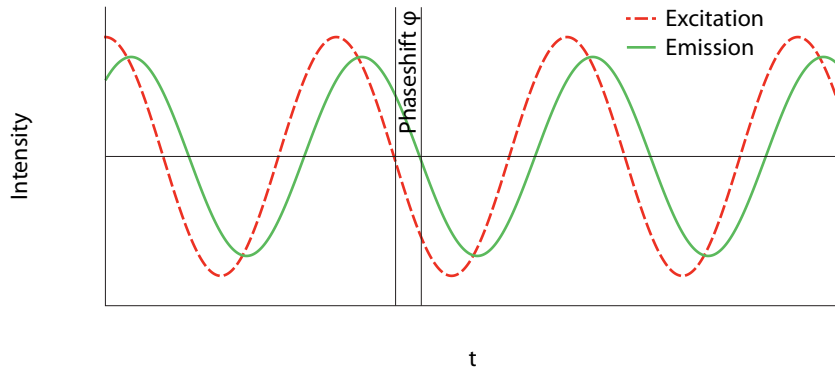


**Figure 3.2:** A plot of modulated excitation and emission intensities as a function of time, illustrating the phaseshift.

from  $0^\circ$  to  $90^\circ$  and is related to the luminescence lifetime according to eqn. 3.3.

$$\tan\phi = \omega\tau \quad (3.3)$$

$$\begin{aligned} \phi & \dots \text{ phaseshift [rad]} \\ \omega & \dots \text{ circular modulation frequency [rad} \cdot \text{s}^{-1}] \\ \tau & \dots \text{ luminescence lifetime} \end{aligned}$$

Modulation frequencies are usually given as  $f[\text{Hz}]$  rather than as circular modulation frequencies. Using eqn. 3.4 and upon rearranging, eqn. 3.3 transforms into eqn. 3.5:

$$\omega = 2\pi \cdot f \quad (3.4)$$

$$\tau = \frac{\tan\phi}{2\pi \cdot f} \quad (3.5)$$

### Data Acquisition

Excitation light was generated using a 435 nm LED obtained from *Roithner, Austria* and filtered through a *BG12* filter obtained from *Schott, Germany*. The excitation light was sinusoidally modulated at a frequency of 5000 Hz and guided to the sensor film using a bifurcated fibre bundle. Through the same fibre bundle, the emitted light was guided to a *photomultiplier unit (H5701-02)* obtained from *Hamamatsu, Japan*. The emission light was filtered through an *RG9* filter obtained from *Schott, Germany*. Phase shifts were measured using a *Stanford Research Systems Model SR830 DSP lock-in amplifier*.

### Gas Mixing, Sensor Mounting Temperature Control

A range of different oxygen partial pressures was established using a custom-built gas-mixing device based on mass-flow controllers, by mixing nitrogen, compressed air and oxygen.

The sensor was mounted into a custom-built sample holder, providing connectors to the gas-mixing device, and a *HAAKE DC50/ThermoHAAKE K10 thermostat* to establish a constant temperature of 25 °C.

### **Assessment of the Sensor Response**

Sensor response time was assessed employing the experimental set-up outlined above, yet using continuous irradiation and a faster sampling rate. The gas mixing was set to change between nitrogen and air saturation every 30 s over a time of 10 min.

### **3.3.5 Photostability Experiments**

The photo-stability of the indicator-dyes was assessed based on the following experiment: Optical fibres of 200  $\mu\text{m}$  in diameter were coated with a sensor cocktail as described in the section on sensor preparation. These fibre sensors were exposed to intense irradiation using a *PyroScience Firesting* set at 100 % LED-intensity, a photo-diode amplification factor of 80, a sampling rate of 1 Hz and 100ms of measurement time. Phase shifts were recorded every 1000 s under nitrogen, using 10 % LED-intensity, and an amplification factor of 200. The signal drift was assessed over time.



## 3.4 Polymer Characterisation

### 3.4.1 Gel Permeation Chromatography

Gel permeation chromatography experiments and analyses of polymers synthesised in this thesis were performed by Mrs. Josefine Hobisch at the Institute for Chemistry and Technology of Materials, Graz University of Technology, giving average molecular weights as well as polydispersity indices.

The following setup was used:

*Merck Hitachi L6000 pump*, separation columns from *Polymer Standards Service* (8 mm\*300 mm, STV 5  $\mu\text{m}$  grade size; pore size: 106  $\text{\AA}$ , 104  $\text{\AA}$  and 103  $\text{\AA}$ ), an *Optilab DSP Interferometric Refractometer (Wyatt Technology)* refractive index detector. Polystyrene standards from Polymer Standard Service were used for calibration. All SEC runs were performed with THF as the eluent.

### 3.4.2 Elemental Analysis

Elemental analyses, determining boron- and platinum-content of polymers synthesised and modified in this thesis were performed by Ing. Herbert Motter at the Institute for Analytical Chemistry and Food Chemistry, Graz University of Technology, by ICP-OES after microwave assisted digestion.

## 3.5 Structural Analysis

### 3.5.1 MALDI-MS

Maldi-MS experiments and structural analyses were performed by Dr. Robert Saf's group at the Institute for Chemistry and Technology of Materials, Graz University of Technology.

Mass spectrometry was performed on a *Micromass TofSpec 2E Time-of-Flight Mass Spectrometer*. The instrument is equipped with a nitrogen laser (337 nm wavelength, operated at a frequency of 5 Hz), and a time lag focusing unit. Ion generation was established by irradiation just above the threshold laser power. Positive ion spectra were recorded in reflectron mode applying an accelerating voltage of 20 kV and externally calibrated with a suitable mixture of poly(ethyleneglycol)s (PEG). The spectra of 100–150 shots were averaged to improve the signal-to-noise ratio. Analysis of data was done with MassLynx-Software V3.5 (Micromass/Waters, Manchester, UK). Samples were dissolved in THF (0.1  $\text{mgmL}^{-1}$ ), dithranol was used as matrix (10  $\text{mgmL}^{-1}$  in THF), respectively. The solutions were mixed in the cap of a microtube in the ratio of 1  $\mu\text{L}$ :10  $\mu\text{L}$ . Then, 0.5  $\mu\text{L}$  of the resulting mixture were deposited on a stainless-steel sample plate and allowed to dry under air.



---

## 4 Experimental Section

### 4.1 Synthetic Strategy

The aim of this thesis being covalent immobilisation of Pt(II) meso-tetraphenyltetrabenzoporphyrin-based oxygen indicators, the development of a chemically and economically reasonable synthetic strategy constituted a key challenge in the early stages of this thesis.

#### 4.1.1 Strategic Considerations: Dye Synthesis

In terms of strategies towards the synthesis of benzoporphyrins, methods commonly employed are a multi-step synthesis often referred to as *Lindsey-Condensation*[34] and template-directed syntheses[11], in which, given the proper conditions, porphyrin structures self-assemble around a metal-ion template.

Lindsey-Condensations commonly yield the desired product in high purity and employ mild conditions, thus allowing for the introduction of diverse functional groups, as desirable with regards to covalent immobilisation. Due to the high number of intermediate steps and subsequent column-chromatography clean-up steps, however, a strategy employing Lindsey-Condensation for the synthesis of a functionalised indicator dye was deemed to be unreasonable.

Template-directed syntheses, on the other hand, commonly do not involve more than three intermediate steps, and thus represent a rather quick alternative. Due to the fact, that such syntheses commonly require rather high temperatures, they are characterised by low yields and complex product-mixtures. Moreover, possibilities regarding the introduction of functional groups are restricted, since most functional groups, such as those desirable for click-chemistry-coupling or EDC/NHS conjugation, would non-specifically react under the conditions applied. Despite the low yields expected and the restriction to stable functional groups commonly considered to be unreactive, an approach based on a template-directed synthesis of the benzoporphyrin dye appeared to be more feasible:

Firstly, this approach would provide a certain degree of flexibility regarding the testing of a variety of coupling-approaches and functional groups, due to its aspect of not being excessively time-consuming.

Secondly, a template-directed approach, due to being relatively inexpensive in terms of the substrates employed and the amount of work necessary, appears to be more consistent with one of the key-criteria, which apply for optical sensors, namely their inexpensiveness.

#### 4.1.2 Strategic Considerations: Choice and Position of The Functional Group

In order to avoid dramatical changes to the photophysical properties of the benzoporphyrin dyes, the functional groups would have to be introduced in such a manner, as to minimize their influence on the benzoporphyrin's electronic system. Consequently, the *para*-position of

the *meso*-phenyl ring, which is freely rotatable and thus only weakly influences  $\pi$ -system, was chosen as target-position for the introduction of functional groups. A series of preliminary tests were conducted in order to assess the options regarding the introduction of functional groups to the benzoporphyrin structure by using adequate, functional-group carrying substrates in the template-directed synthesis. Molecules carrying carboxylic acid- or hydroxy-residues were deemed unsuitable for template synthesis due to their high reactivity under the conditions employed. Hence, small scale template syntheses (see section 4.2.1) were conducted for the most promising functionalised phenylacetic acids (p-aminophenylacetic acid, p-methylphenylacetic acid and p-bromophenylacetic) and product formation was assessed based on TLC and absorption spectra.

#### 4.1.3 Strategic Considerations: The Coupling Approach

Halogen-substituents were shown to only have a slight influence on the overall yield of the template-directed synthesis whilst being stable under the conditions applied. Furthermore, they would provide the functional basis necessary for transition-metal catalysed coupling approaches such as Suzuki-coupling reaction. Hence, it was decided to develop a synthetic protocol for the synthesis of bromo-substituted Pt(II)-benzoporphyrin and further follow a synthetic route employing well-established and widely used Suzuki-coupling between the bromo-modified dye and a polymer carrying phenyl-boronic acid residues to establish covalent immobilisation. In this respect the use of a bromo-phenyl-carrying dye as a substrate represents a reasonable middle ground between iodo-phenyl substrates, which react more readily under Suzuki-conditions, yet are expected to be less stable in the template-directed synthesis, and chloro-phenyl substrates, which are less-active substrates in the Suzuki-reaction, yet are expected to be more stable in the template-directed synthesis.

## 4.2 Dye Synthesis

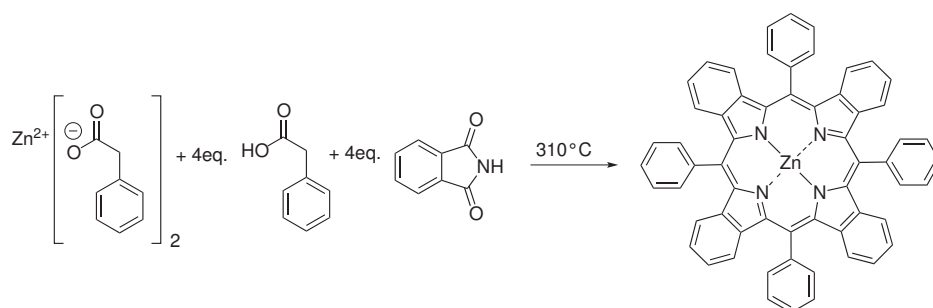


**Figure 4.1:** a reaction scheme for the template-directed synthesis of ZnTPTBP as published in [11]

Figure 4.1 offers a reaction scheme for the template-directed synthesis of *ZnTPTBP*. The reaction is carried out under nitrogen and solvent-free conditions. At a temperature of 310°C all components exist as melts, the mixture is stirred to ensure mixing of all the components, and left to react for 90 min. Upon cooling, the melts are dissolved in *dichloromethane*, resulting in a dark green solution. Clean-up of the product mixture is established by repeated precipitation from a mixture of ethanol and water and subsequent centrifugation. In order to remove the water-insoluble by-products, the centrifugate is cleaned by means of column chromatography on aluminium oxide employing a mixture of *dichloromethane* and *toluene* as eluent.

Figure 4.2 illustrates a modified template-directed synthesis of ZnTPTBP, developed, but not

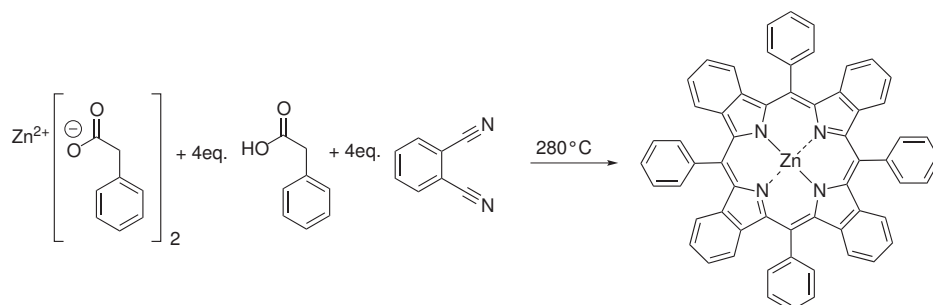


**Figure 4.2:** a reaction scheme for a modified template-directed synthesis of ZnTPTBP, [*Borisov unpublished results*]

yet published by S.M.Borisov. By using *dicyanobenzene* instead of *phthalimide*, the reaction occurs more readily at lower temperatures and after shorter reaction times. In terms of product clean-up, this modified approach is in line with the classical protocol. Due to the milder conditions employed, this modified template-directed synthesis served as a starting point for the development of a synthetic protocol for the synthesis of tetra- and mono-bromo-substituted PtTPTBP.

After successful synthesis of the benzoporphyrin-structure, the central metal has to be substituted in order to obtain *PtTPTBP* from *ZnTPTBP*. This is realised by *de-metalation* of the complex in *methanesulfonic acid* and *platination* using an appropriate Pt-precursor complex.

4.2.1 PtTPTBPBr<sub>4</sub>

Tetra-bromo substituted PtTPTBP (*PtTPTBPBr<sub>4</sub>*) was chosen as a model compound to further study covalent immobilisation of benzoporphyrins. It was prepared by substituting *phenylacetic acid* ("PhAcOH") and "Zn(PhAcO)<sub>2</sub>" with *4-bromophenylacetic acid* ("4-BrPhAcOH") and "Zn(4-BrPhAcO)<sub>2</sub>", respectively.

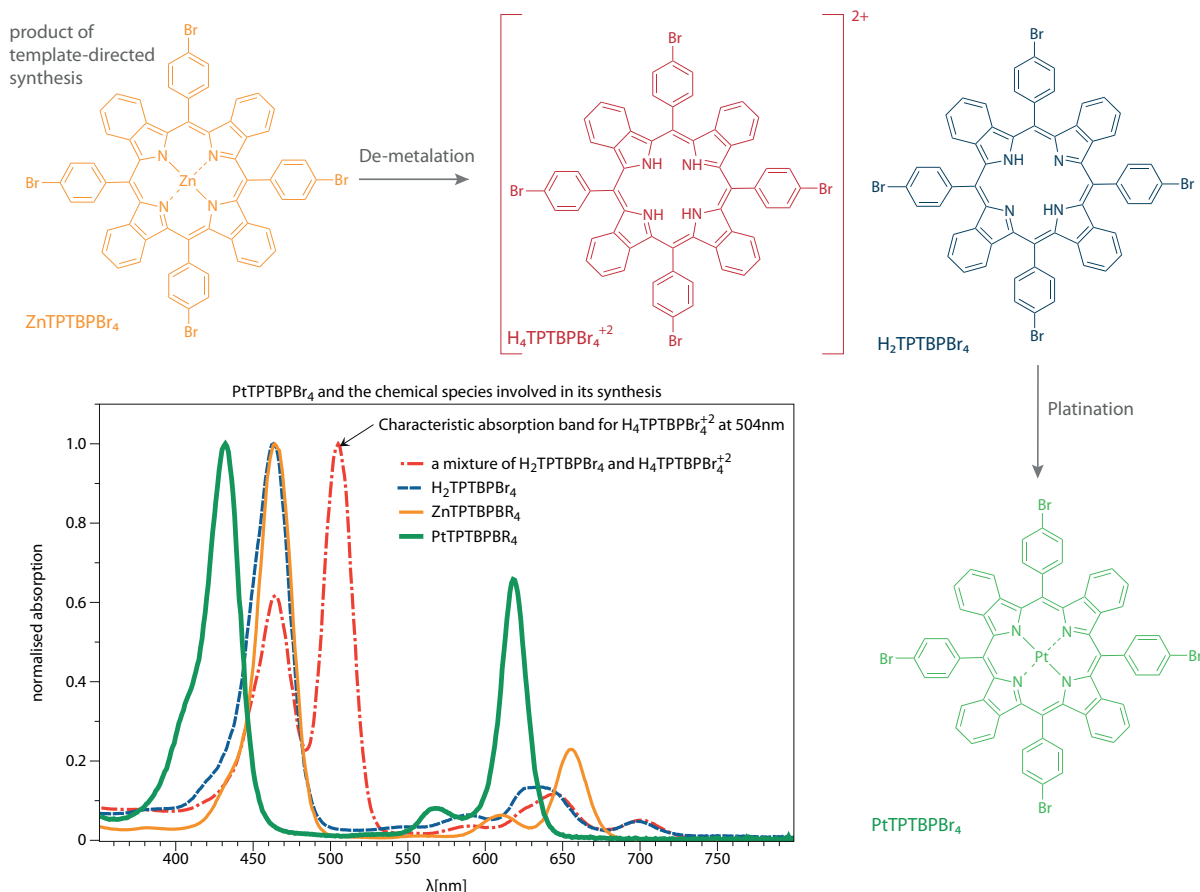


**Figure 4.3:** A schematic illustration of the steps and species involved in porphyrin synthesis. Each key-species possesses a characteristic absorption spectrum, which enables the use of simple spectrophotometry as analytical tool in reaction control.

## Template Condensation

One equivalent of "Zn(4-BrPhAcO)<sub>2</sub>" [493.46], four equivalents of *dicyanobenzene* [128.13] and eight equivalents of "4-BrPhAcOH" [215.04] were weighed, mixed and homogenised using a mortar. The solid mixture was split into equal portions of roughly 700 mg, placed into a 2.5 mL Supelco@vials and compressed. A suitable magnetic stirring bar was placed atop, the vials were de-oxygenated by gently blowing Argon into the vial for 2 min each. The vials were sealed with a metal screw cap and placed into a pre-heated aluminium heating block at 140 °C. The mixtures were heated to a temperature of 280 °C and left to react for 40 min while stirring. The vials were removed from the heating block and left to cool. Upon cooling the melt in each vial was dissolved in acetone.

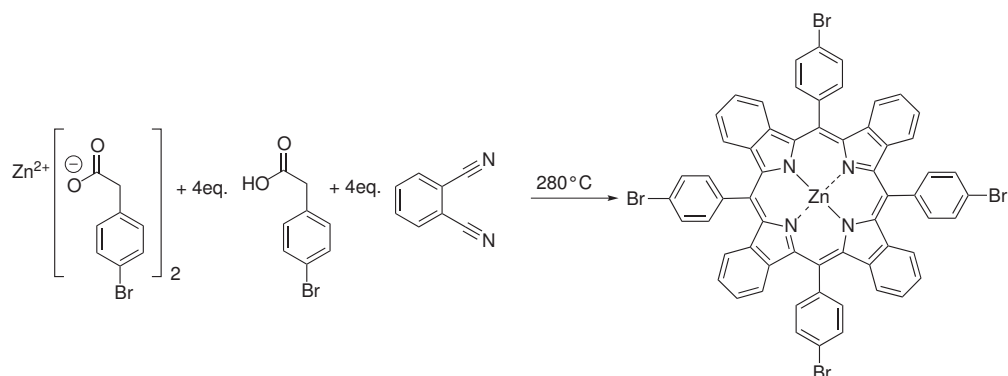


**Figure 4.4:** A reaction scheme for the template-directed synthesis of ZnTPTBPBr<sub>4</sub>

#### CLEAN-UP:

Absorption spectra were recorded and thin-layer chromatography was conducted using Alox-TLC-plates and a mixture of 60% *dichloromethane* and 40% *hexane* to assess product formation. The unified solutions of raw product were precipitated from an equal volume of ethanol with 10% saturated brine added. The suspension was centrifuged, the solution discarded. The precipitate was redissolved in *dichloromethane*. This process was repeated three times. After each step absorption spectra were recorded.

The precipitate was redissolved and dried onto aluminium oxide to facilitate column chromatography. The raw product dried onto aluminium oxide was placed atop a chromatography column, packed with aluminium oxide in *hexane* and covered with sea sand. The product was eluted after purple, red and yellow fractions by gradually increasing the polarity from *hexane* to a mixture of *dichloromethane* (90%) and *etrahydrofuran* (10%). Absorption spectra were recorded to identify the fractions containing product. The product containing fractions were unified. The solvent was removed and the residual solvent dried in the oven at 70 °C. The solid was redissolved in *dichloromethane* and precipitated from a four-fold volume of *hexane*. The solid was filtered off and dried in the oven over night, yielding a dark-blue solid.

#### CLEAN-UP:

The product was characterised using MALDI-TOF-MS, thin layer chromatography and absorption spectra.

#### De-metallation

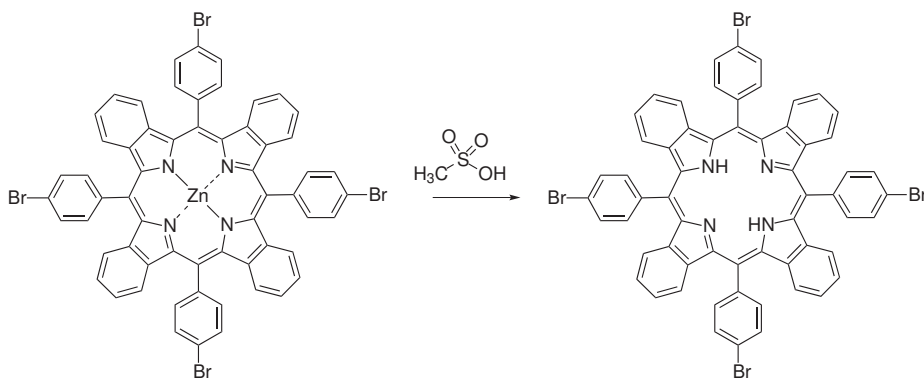


**Figure 4.5:** A reaction scheme for the demetallation of ZnTPTBPBr<sub>4</sub>

De-metalation was established by dissolving one equivalent of " $ZnTPTBPBr_4$ " [1193.95] in a small volume of acetone and adding 25 equivalents of *methanesulfonic acid* [96.11] to the green solution, resulting in the formation of a green to red product after 15 min of stirring at 25 °C.

#### CLEAN-UP:

The product, a green to brown coloured solid was precipitated by adding water to the solution. Upon centrifugation of the suspension and removal of the solvent, the precipitate was redissolved in acetone. The product was again precipitated by adding water, resulting in the formation of a green precipitate and the clearing of the solution. Absorption spectra were recorded after every washing step. The washing had to be repeated thrice, until the cationic species  $H_4TPTBPBr_4^{+2}$  (characteristic absorption band at 504 nm in *dichloromethane*) had been completely neutralised.

Upon neutralisation the product was once more precipitated, centrifuged and placed in the oven to dry, yielding 369 mg of solid, dry  $H_2TPTBPBr_4$  (characteristic symmetric triplet of absorption bands, centered around 630 nm in *dichloromethane*).

#### Platination

One equivalent of " $H_2TPTBPBr_4$ " [1130.55] was placed into a single-neck flask and dissolved in a small volume *trimethylbenzene*. The resulting solution was heated to 170 °C. Two equivalents of  $Pt(C_6H_5CN)_2Cl_2$  [472.24] were pre-dissolved in a small volume of *trimethylbenzene*, preheated and added to the solution containing  $H_2TPTBPBr_4$ . The resulting solution was left to react at 170 °C while stirring using a magnetic stirring bar. The progress of the reaction was monitored by measuring absorption spectra every 10 min. Due to the observed formation of the protonated ligand " $H_4TPTBPBr_4^{+2}$ ", additional 0.5eq. of  $Pt(C_6H_5CN)_2Cl_2$  [472.24] were added.

#### CLEAN-UP:

Upon completion of the reaction, which is observable the solvent was removed and the raw product was cleaned by means of column chromatography. (aluminium oxide in *hexane*, elution with a mixture of *hexane* (40%) and *dichloromethane* (60%).

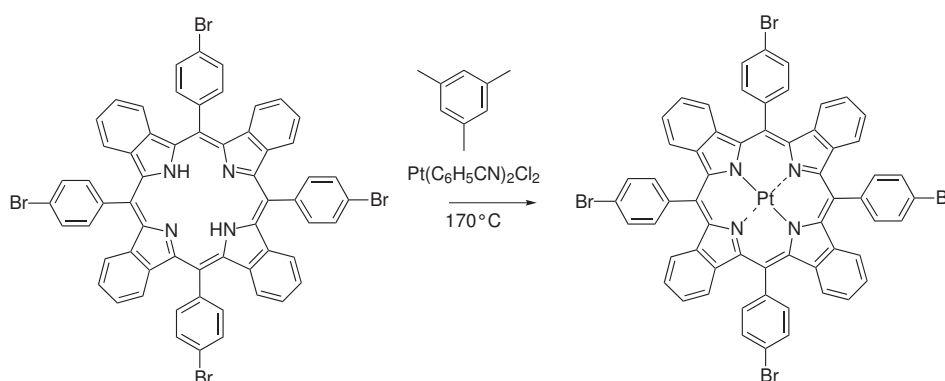


**Figure 4.6:** A reaction scheme for the platination of  $H_2TPTBPBr_4$



## 4.2.2 PtTPTBPBr

## Template Condensation

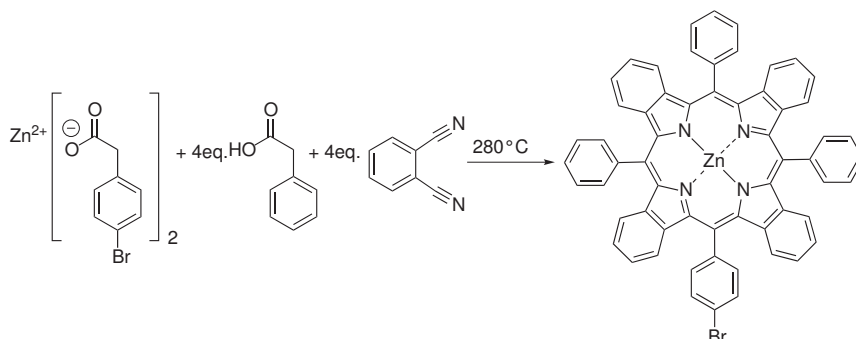


**Figure 4.7:** A reaction scheme for the template-directed synthesis of ZnTPTBPBr

One equivalent of "*Zn(4-BrPhAcO)<sub>2</sub>*" [493.46], four equivalents of *dicyanobenzene* [128.13] and eight equivalents of *PhAcOH* [136.15] were weighed, mixed and homogenised using a mortar. The solid mixture was split into equal portions of roughly 700 mg, placed into a 2.5 mL Supelco®vials and compressed. A suitable magnetic stirring bar was placed atop, the vials were de-oxygenated by gently blowing Argon into the vial for 2 min each. The vials were sealed with a metal screw cap, placed into a pre-heated aluminium heating block at 140 °C. The mixtures were heated to a temperature of 280 °C and left to react for 40 min while stirring. The vials were removed from the heating block and left to cool. Upon cooling the melt in each vial was dissolved in acetone.

## CLEAN-UP:

Absorption spectra were recorded and thin-layer chromatography was conducted using Alox-TLC-plates and a mixture of 60% *dichloromethane* and 40% *hexane* to assess product formation. The unified solutions of raw product were precipitated from an equal volume of ethanol with 10% saturated brine added. The suspension was centrifuged, the solution discarded. The precipitate was redissolved in *dichloromethane*. This process was repeated three times. After each step absorption spectra were recorded.

The precipitate was redissolved and dried onto aluminium oxide to facilitate column chromatography. The raw product dried onto aluminium oxide was placed atop a chromatography column, packed with aluminium oxide in *hexane* and covered with sea sand. The product was eluted after purple, red and yellow fractions by gradually increasing the polarity from *hexane* to a mixture of *dichloromethane* (90%) and *tetrahydrofuran* (10%). Absorption spectra were recorded to identify the fractions containing product. The product containing fractions were unified. The solvent was removed and the residual solvent dried in the oven at 70 °C. The solid was redissolved in *dichloromethane* and precipitated from a four-fold volume of *hexane*. The solid was filtered off and dried in the oven over night, yielding a dark-blue solid.

## CHARACTERISATION:

The product was characterised using MALDI-TOF-MS, thin layer chromatography and absorption spectra.

**De-metallation and Platination**

De-metallation, as well as platination are conducted using the same procedure as used in the synthesis of "*PtTBPTBPr<sub>4</sub>*".

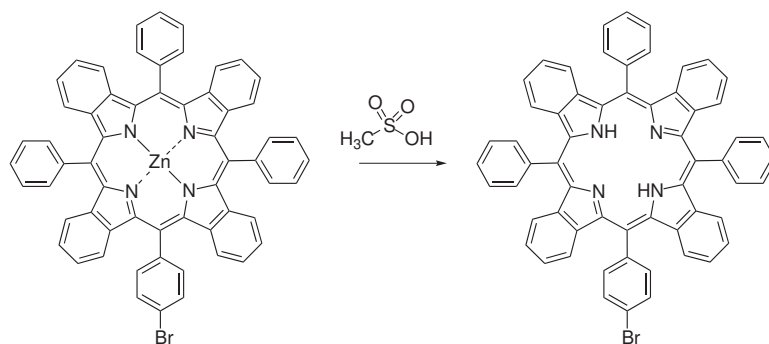


**Figure 4.8:** A reaction scheme for demetallation of ZnTPTBPr

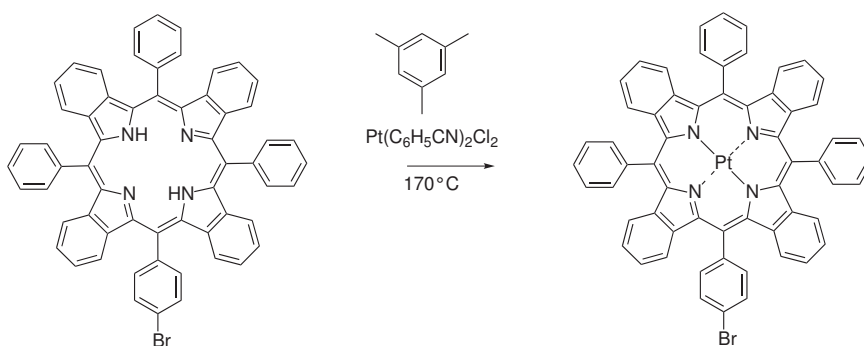


**Figure 4.9:** A reaction scheme for Platination of H<sub>2</sub>TPTBPr

## 4.3 Polymer Synthesis

Polystyrene is one of the most widely-used matrices in optical oxygen sensors based on benzo-porphyrin indicators. Consequently, polystyrene was chosen as model matrix in this thesis.

Styrene-vinylbenzeneboronic acid-copolymers can readily be prepared under solvent-free conditions using radical mass-polymerisation, employing solely the monomers and a suitable radical-initiator. A series of copolymers were prepared characterised by a content of boronic acid-residues ( $x \cdot 100\%$ ) varying between  $0.05 \text{ mol}\%$  and  $1 \text{ mol}\%$ .

### 4.3.1 Synthesis of Styrene-Vinylbenzeneboronic acid-Copolymers

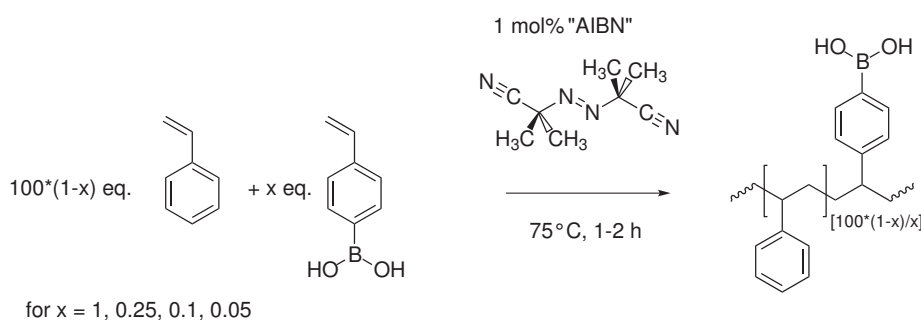


**Figure 4.10:** a reaction scheme for the synthesis of styrene-vinylbenzeneboronic acid-copolymers

The Styrene used in this synthesis was filtered through a column packed with aluminium oxide to remove the contained inhibitor (*4-Tert-butylcatechol*). In an appropriately-sized Schlenk-flask,  $x$  equivalents of *4-vinylbenzeneboronic acid* [147.97] were dissolved in  $1 - x$  equivalents of *styrene* [104.15]. The solution was stirred at room temperature under heavy flow of argon for 20 min to establish de-oxygenation.  $1 \text{ mol}\%$  of *2,2'-Azobis(2-methylpropanitrile)* ("*AIBN*") [164.21] was added under argon. The flask was sealed and the solution was allowed to react at  $75^\circ\text{C}$  for up to four hours while stirring. Upon complete solidification due to polymerisation, the polymer was allowed to cool.

#### CLEAN-UP:

The polymer was dissolved in *dichloromethane* to give a  $10 \text{ wt}\%$  solution. The solution was added drop-wise to a five-fold volume of methanol, resulting in the precipitation of a white, powder-like precipitate. The suspension was filtered through a white-band filter and redissolved in *dichloromethane* to give a solution containing  $10 \text{ wt}\%$  of polymer. This step of dissolving and precipitation was repeated three to five times. The polymer was dried in the oven at  $70^\circ\text{C}$  to yield a white, powder-like solid.

#### CHARACTERISATION:

The polymers were characterised by means of gel-permeation chromatography to assess the molecular weight-distribution, and analysed by means of elemental analysis to assess the content of boronic acid residues.

**Considerations regarding the subsequent use of the polymers**

A pseudo-molecular weight was calculated for each of the synthesised polymers in order to facilitate calculations to determine the required quantities of substrates in polymer modification reactions. Assuming *Styrene* and *4-vinylbenzenboronic acid* co-polymerise following the same kinetics, the actual content of boronic acid-residues in the polymer should reflect the quantities of substrates used in the polymerisation. Thus, a pseudo-molecular weight can be calculated, which reflects the mass of polymer which contains one mole of boronic acid-residues.

Pseudo-molecular weights were calculated based on equation 4.1. Table 4.1 contains the values calculated for the synthesised polymers.

$$MW_{\text{pseudo}} = \frac{(100 - x)}{x} \cdot MW_{\text{Styrene}} + MW_{4\text{-vinylbenzenboronic acid}} \quad (4.1)$$

$x$  - mol% of *4-Vinylbenzenboronic acid* relative to the total number of monomer units  
 $\frac{(100-x)}{x}$  - number of phenyl residues corresponding to one phenylboronic acid residue

**Table 4.1:** Composition and calculated pseudo-molecular weights of the polymers synthesised.

mol%	$\frac{(100-x)}{x}$	$MW_{\text{pseudo}} / [g \cdot mol^{-1}]$
4-vinylbenzenboronic acid		
1	99	10458.82
0.25	399	41703.82
0.1	999	104193.82
0.05	1999	208343.82

## 4.4 Suzuki Coupling

### 4.4.1 Polymer Modification

Calculations performed to determine the required quantities of substrates for the reactions performed in this sections were based on the pseudo-molecular weights calculated for each polymer as listed in table 4.1.

#### Coupling of PtTPTBBr<sub>4</sub>

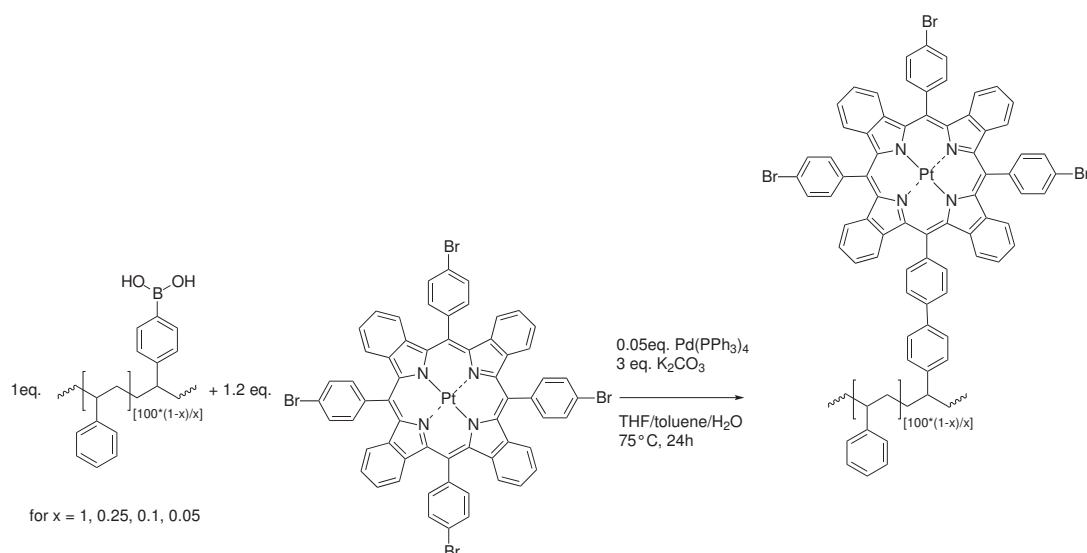


**Figure 4.11:** a reaction scheme for the Suzuki-coupling of PtTPTBBr<sub>4</sub> and polystyrenes carrying boronic-acid residues

#### SYNTHESIS

One equivalent of polymer-bound boronic acid residue [see table 4.1] and 1.2 equivalents of PtTPTBBr<sub>4</sub> [1323.62] were placed into a Schlenk-flask and dissolved in *tetrahydrofuran*. *toluene* and distilled water were added to give a solvent mixture of the composition two volume-parts *toluene*, two volume-parts and one volume-part water. Three equivalents of K<sub>2</sub>CO<sub>3</sub> were added. De-oxygenation was established by means of heavy stirring of the solution under strong argon flow. 0.05 mol% of *tetrakis(triphenylphosphine)palladium* (Pd(PPh<sub>3</sub>)<sub>4</sub>) were added under argon. The vessel was closed, heated to 70 °C and left to react for 24h while stirring. CLEAN-UP: The solution was added drop-wise to a five-fold volume of methanol, resulting in the precipitation of a green precipitate. The suspension was filtered through a white-band filter and redissolved in *dichloromethane* to give a solution containing 10 wt% of polymer. This step of dissolving and precipitation was repeated three to five times, until no more washing out of dye could be observed (proof of covalent immobilisation!). The polymer was dried in the oven at 70 °C to yield a green, powder-like solid.

#### CHARACTERISATION:

Yields were estimated based on absorption spectra, by applying Beer's Law. The sensor polymer was characterised by means of gel-permeation chromatography to assess the molecular weight-distribution. Additionally, the calibration curve and the quantum yield of a sensor film prepared from the polymer was determined.

## Coupling of PtTPTBPBr

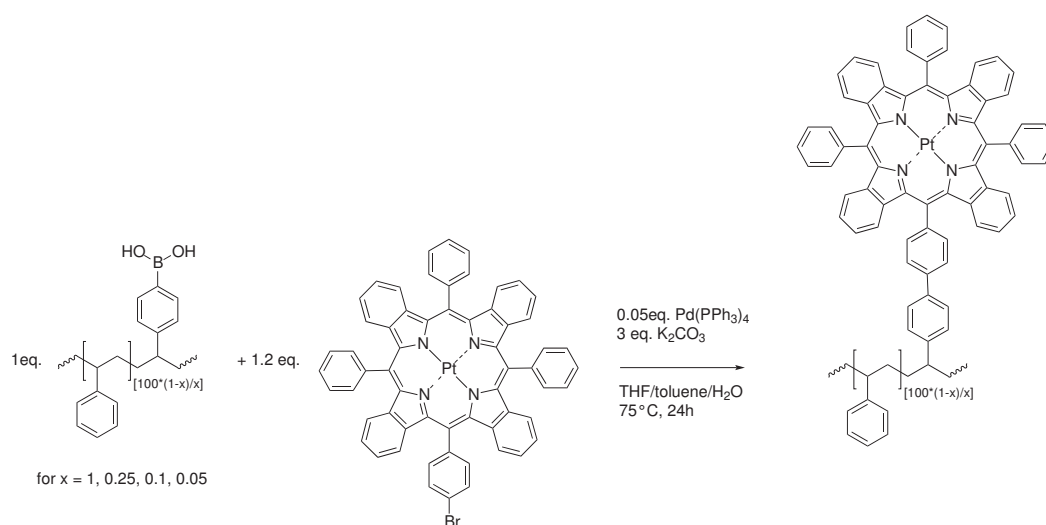


**Figure 4.12:** a reaction scheme for the Suzuki-coupling of PtTPTBPBr and polystyrenes carrying boronic-acid residues

## SYNTHESIS

One equivalent of polymer-bound boronic acid residue [104193.82] and 1.2 equivalents of *PtTPTBPBr* [1086.93] were placed into a Schlenk-flask and dissolved in tetrahydrofuran. *toluene* and distilled water were added to give a solvent mixture of the composition two volume-parts *toluene*, two volume-parts and one volume-part water. Three equivalents of  $K_2CO_3$  were added. De-oxygenation was established by means of heavy stirring of the solution under strong argon flow. 0.05 mol% of *tetrakis(triphenylphosphine)palladium* ( $Pd(PPh_3)_4$ ) were added under argon. The vessel was closed, heated to 70 °C and left to react for 24h while stirring. CLEAN-UP: The solution was added drop-wise to a five-fold volume of methanol, resulting in the precipitation of a green precipitate. The suspension was filtered through a white-band filter and redissolved in *dichloromethane* to give a solution containing 10 wt% of polymer. This step of dissolving and precipitation was repeated three to five times, until no more washing out of dye could be observed. The polymer was dried in the oven at 70 °C to yield a green, powder-like solid.

## CHARACTERISATION:

Yields were estimated based on absorption spectra, by applying Beer's Law. The sensor polymer was characterised by means of gel-permeation chromatography to assess the molecular weight-distribution. Additionally, the calibration curve and the quantum yield of a sensor film prepared from the polymer was determined.

### 4.4.2 Dye Modification

In an effort to prepare a readily polymerisable dye, functionalisation of the *PtTPTBPBr* with a styryl-group was attempted by means of Suzuki-coupling of *PtTPTBPBr* with *4-vinylbenzeneboronic acid*. In the attempted reaction, Heck-cross-coupling constitutes a possible side-reaction, which would result in a dye carrying a boronic acid-residue. Furthermore coupling of Heck-side-product and un-reacted *PtTPTBPBr* would lead to dimerisation of two porphyrin units.

Due to carrying a highly polar group, the side-product formed via Heck-reaction is expected to be removable from the product mixture by means of column chromatography. In order to reduce the possibility of the formation of porphyrin dimers, a high excess of *4-vinylbenzeneboronic acid* was used.

#### SYNTHESIS

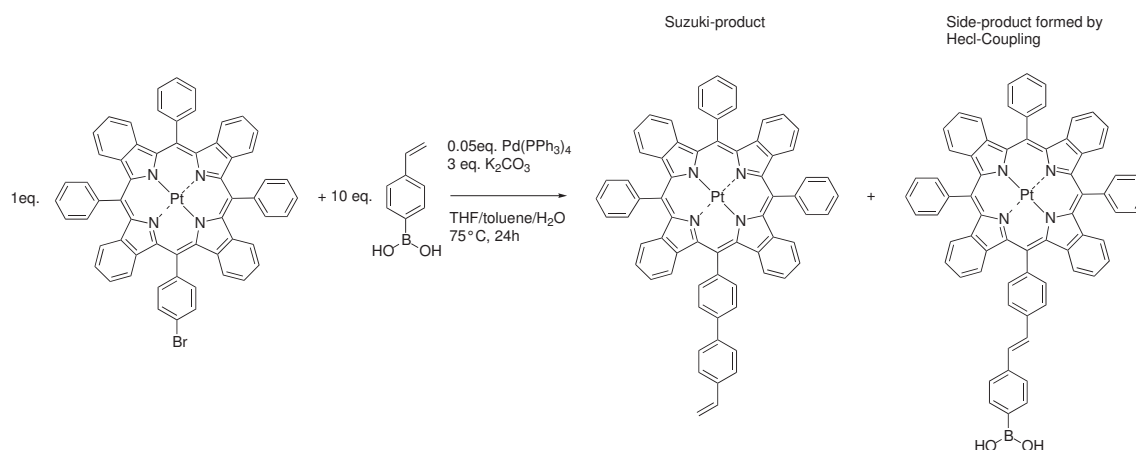


**Figure 4.13:** a reaction scheme for the Suzuki-coupling of *PtTPTBPBr* and *4-vinylbenzeneboronic acid*

One equivalent of *PtTPTBPBr* [1086.93] and ten equivalents of *4-vinylbenzeneboronic acid* [147.97] were placed into a small Schlenk-flask and dissolved in *tetrahydrofuran*. *toluene* and distilled water were added to give a solvent mixture of the composition two volume-parts *toluene*, two volume-parts and one volume-part water. Three equivalents of  $K_2CO_3$  were added. De-oxygenation was established by means of heavy stirring of the solution under strong argon flow. 0.05 mol% of *tetrakis(triphenylphosphine)palladium* ( $Pd(PPh_3)_4$ ) were added under argon. The vessel was closed, heated to 70 °C and left to react for 24h while stirring. Thin-layer chromatography, conducted after completion of the reaction, confirmed the expectations formulated above: On aluminium oxide as well as on silica gel solid phases, using a solvent mixture of two volume-parts *dichloromethane* and one volume-part *hexane*, a very weak polar spot (*side product formed by Heck-reaction*) was observed along with one strong non-polar spot (*desired styryl-functionalised PtTPTBPBr*)

#### CLEAN-UP

The products were precipitated from an equal volume of ethanol with 10% saturated brine added. The suspension was centrifuged, the solution discarded. The precipitate was redissolved and dried onto aluminium oxide to facilitate column chromatography. The raw product dried onto aluminium oxide was placed atop a chromatography column, packed with aluminium oxide in *hexane* and covered with sea sand. The product was eluted by gradually increasing the

polarity from *hexane* to a mixture of two volume-parts of *dichloromethane* and one volume-part of *hexane*. The side product was eluted using a mixture of four volume-parts of *dichloromethane* and one volume-part Methanol. The non-polar product was dried in the oven at 70 °C, yielding a green solid (95 % yield).

### Co-Polymerisation

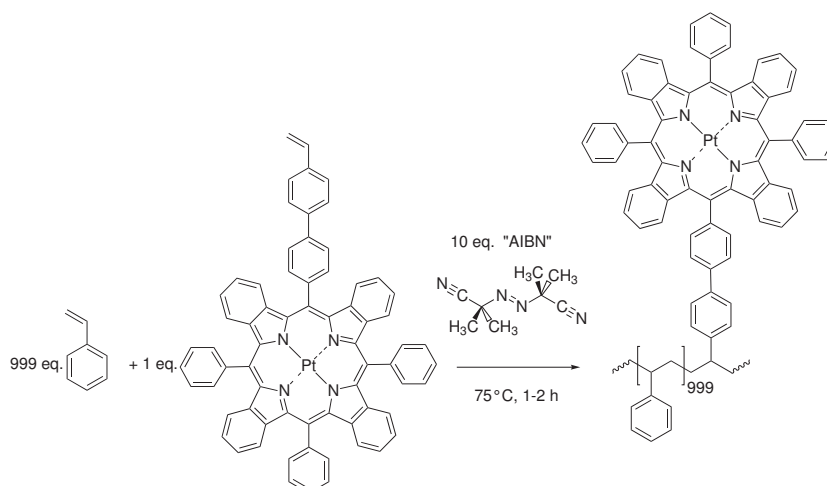


**Figure 4.14:** a reaction scheme for the co-polymerisation of styrene and styryl-functionalised PtTPTBP.

The Styrene used in this synthesis was filtered through a column packed with aluminium oxide, to remove the contained inhibitor (*4-tert-butylcatechol*). In a Schlenk-flask, one equivalent of the *styryl-functionalised PtTPTBP* [1110.17] were dissolved in 999 equivalents of *styrene* [104.15]. The solution was stirred at room temperature under heavy flow of argon for 20 min, to establish de-oxygenation. 1 mol% of 2,2'-azobis(2-methylpropionitrile) ("AIBN") [164.21] was added under argon. The flask was sealed and the solution was allowed to react at 75 °C for up to four hours while stirring. Upon complete solidification due to polymerisation, the polymer was allowed to cool.

#### CLEAN-UP:

The polymer was dissolved in *dichloromethane* to give a 10 wt% solution. The solution was added drop-wise to a five-fold volume of methanol, resulting in the formation of a green precipitate. The suspension was filtered through a white-band filter and redissolved in *dichloromethane* to give a solution containing 10 wt% of polymer. This step of dissolving and precipitation was repeated three to five times, until no more washing out of dye could be observed. The polymer was dried in the oven at 70 °C to yield a green, powder-like solid.

#### CHARACTERISATION:

The sensor polymer was characterised by means of gel-permeation chromatography to assess the molecular weight-distribution. An absorption spectrum was recorded. Additionally, the calibration curve and the quantum yield of a sensor film prepared from the polymer was determined.



---

## 5 Results and Discussion

### 5.1 Polymer Characterisation

#### 5.1.1 Boronic acid-residue-Loading

Boronic acid-residue-loading was determined by means of elemental analysis, as described in section 3.4.2. Data calculated from the obtained concentrations, as well as pseudo-molecular weights, calculated based on the experimentally-obtained values, are listed in table 5.1.

**Table 5.1:** Boronic acid-residue-loading of the polymers synthesised, as determined by elemental analysis.

$mol\%$ theo $Ph-B(OH)_2$	$MW_{pseudo, theo}$	$mol\%$ exp $Ph-B(OH)_2$	$MW_{pseudo, exp}$
1	10458.82	1.55	6763.17
0.25	41703.82	0.20	52118.82
0.1	104193.82	0.07	148829.53
0.05	208343.82	0.05	208343.82

The boronic acid-residue loading, which was experimentally obtained shall be henceforth given in order to accurately identify the polymers synthesised.

#### 5.1.2 Molecular Weight Distribution

The molecular weight distribution was assessed by means of gel-permeation chromatography, as described in section 3.4.1. Table 5.2 provides the data obtained for the polymers synthesised in this thesis. The polymers are identified by the mole-percentage determined by means of elemental analysis.

**Table 5.2:** Molecular Weight Distributions of Styrene-4-vinylbenzeneboronic acid-co-polymers

$mol\%$ $Ph-B(OH)_2$	$M_n [g \cdot mol^{-1}]$	$M_w [g \cdot mol^{-1}]$	$M_z [g \cdot mol^{-1}]$	PDI
1.55	25 500	46 680	74 180	1.831
0.20	58 120	244 070	828 230	4.199
0.07	99 710	404 020	1 218 120	4.052
0.05	59 920	181 580	494 700	3.030

The data indicates that large differences in the molecular-weight-distributions arose despite applying the same synthetic protocol in all polymer syntheses.

The *PDI* is a measure for the breadth of the molecular weight-distribution. Apart from the polymer "1.55" all polymers synthesised are characterised by broad MW-distributions.

No clear influence of the number of equivalents of *4-Vinylbenzeneboronic acid* used in the

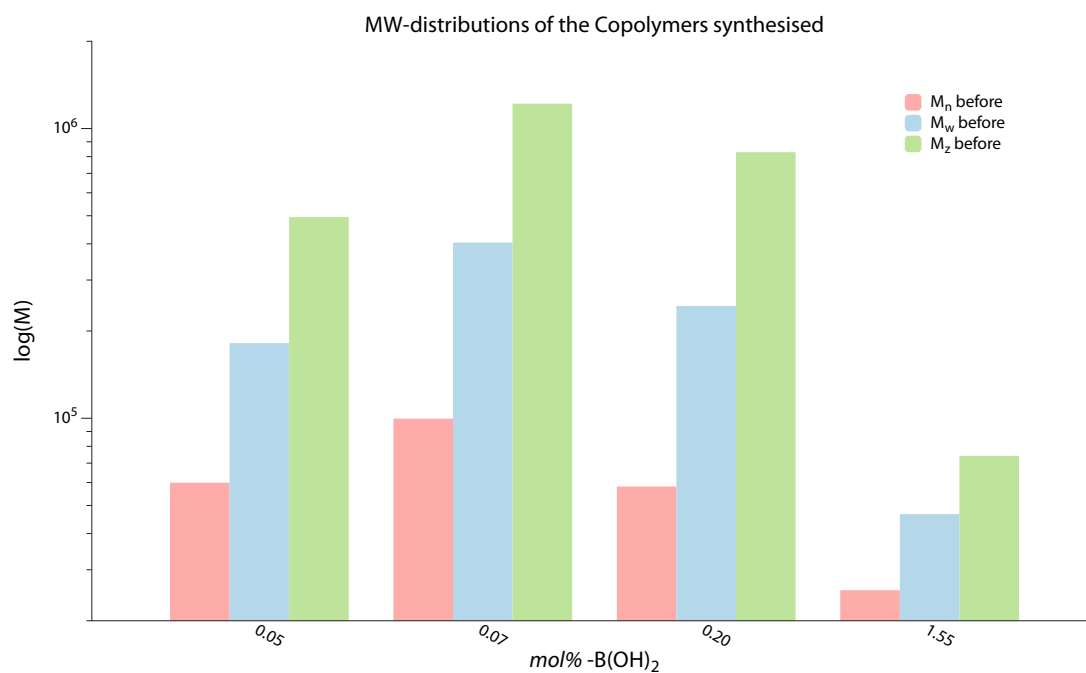


**Figure 5.1:** An Illustration of the MW-distributions determined for the synthesised polymers.

polymer-synthesis on the molecular weight distributions of the resulting polymers is indicated in the data, thus it has to be assumed that the differences arose due to varying synthetic conditions.

Syntheses of polymers containing a higher content of boronic acid residues were attempted using the same protocol, yet proved unsuccessful due to limited solubility of *4-vinylbenzeneboronic acid* under solvent-free mass-co-polymerisation conditions.

## 5.2 Dye Characterisation

### 5.2.1 Photophysical Properties

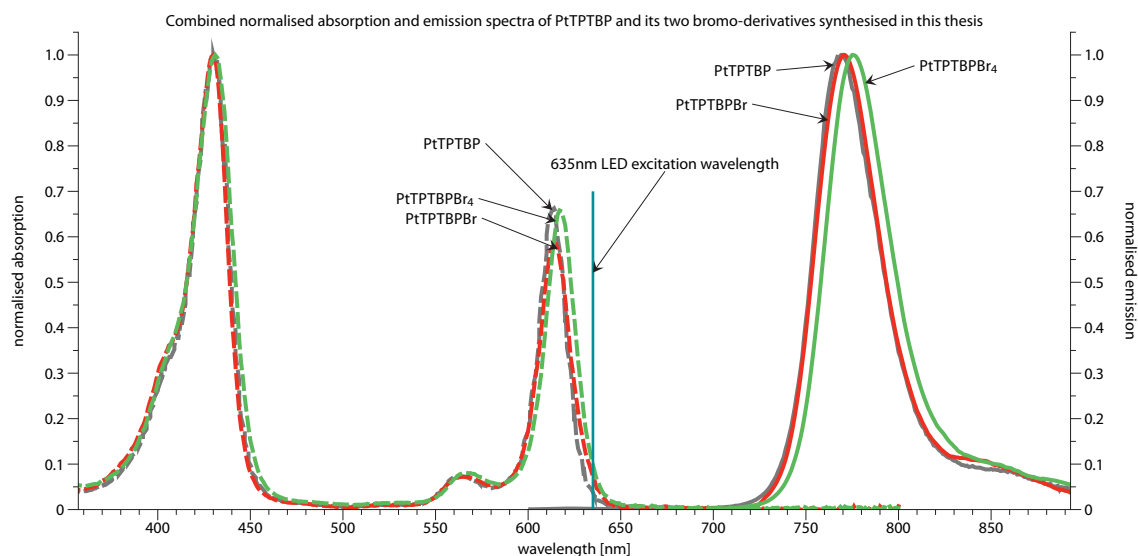


**Figure 5.2:** Combined normalised absorption and emission spectra of PtTPTBP, PtTPTBPBr and PtTPTBPBr<sub>4</sub> in Dichloromethane

The spectra show that the absorption in the *Soret-band* remains more or less unchanged by the introduction of one or four bromines.

The absorption in *Q-band* however, is changed: The introduction of bromines results in a bathochromic shift of 1 nm for *PtTPTBPBr* and almost 5 nm for *PtTPTBPBr<sub>4</sub>*. Moreover the extinction coefficient for absorption in the *Q-band* region slightly drops in the case of *PtTPTBPBr* but is comparable to *PtTPTBP* in the case of *PtTPTBPBr<sub>4</sub>*. Otherwise the spectra are similar in terms of shape.

*The absorption spectra were recorded in dichloromethane, emission spectra were recorded in toluene.*

**Table 5.3:** An overview of the photophysical properties of PtTPTBP, PtTPTBPBr and PtTPTBPBr<sub>4</sub>

Indicator	$\lambda_{\max}^{\text{abs}}$ [nm]	$\epsilon$ [M <sup>-1</sup> *cm <sup>-1</sup> ]	$10^{-3} \lambda_{\max}^{\text{em}}$ [nm]	$\phi$	$\tau_0$ [ $\mu$ s]	Ref.
PtTPTBP	430, 564, 614	205, 16, 136	770	0.51	47	[12], [16]
PtTPTBPBr	430, 566, 624	245, 20, 175	770	0.39	46	<i>this work</i>
PtTPTBPBr <sub>4</sub>	431, 569, 627	330, 24, 196	775	0.54	46	<i>this work</i>

*PtTPTBPBr* and *PtTPTBPBr<sub>4</sub>* were characterised by means of absorption and emission spectra, quantum yields as well as extinction coefficients were determined. Figure 5.2 gives a comparison of the normalised absorption and emission spectra of *PtTPTBPBr* and *PtTPTBPBr<sub>4</sub>*, as well as those of *PtTPTBP* as a reference point.

The absorption spectra, measured in Dichloromethane, show that the absorption in the *Soret-band* remains more or less unchanged by the introduction of one or four bromides.

The absorption in the *Q-band*, however, is changed. The introduction of bromides results in a bathochromic shift of 1 nm for *PtTPTBPBr* and almost 5 nm for *PtTPTBPBr<sub>4</sub>*. Moreover, the extinction coefficient for absorption in the Q-band region slightly drops in the case of *PtTPTBPBr* but is comparable to *PtTPTBP* in the case of *PtTPTBPBr<sub>4</sub>*. The spectra do not, however, differ with regard to their shape.

As in the case of the substances' absorption spectra, the emission bands of the bromo-substituted benzoporphyrins slightly shift to regions of longer wavelength.

Quantum yields were determined by reference method using *PtTPTBP* as a reference. Values for phosphorescence-lifetime were obtained in the course of the quantum-yield experiment and obtained as described in section 3.3.

*PtTPTBPBr* shows a significantly smaller quantum yield than the two other dyes listed above. This fact may be attributable to quenchers being present in the sample as a consequence of insufficient purification. *PtTPTBPBr<sub>4</sub>* shows a small increase in quantum yield, which may be attributable to increased population of the triplet state as a consequence of the bromide's influence on spin-orbit coupling. However, the increase is small and in the error margin of the experiment (10%). Table 5.3 contains aggregated photo-physical data obtained for the dyes synthesised in this thesis as well as data for *PtTPTBP* as reference values.

### 5.2.2 Chemical Analysis

In the case of *PtTPTBPBr<sub>4</sub>*, MALDI-TOF-MS was performed after successful platination of the ligand synthesised, and directly after template-directed synthesis, in the case of *PtTPTBPBr* to identify the desired product early in the synthesis.

Table 5.4 gives a summary of the MS(MALDI)-results obtained for *PtTPTBPBr<sub>4</sub>* and table 5.5 summarises the data obtained for *ZnTPTBPBr*.

The MS(MALDI)-data obtained for *PtTPTBPBr<sub>4</sub>* indicates a product mixture of *PtTPTBPBr<sub>4</sub>*,

**Table 5.4: MALDI-MS: *PtTPTBPBr<sub>4</sub>*** - A comparison of calculated and experimentally found ions matrix-amplified laser-desorption ionisation

Type of ion	$m/z$ calculated	$m/z$ experimental
$M^+$	1329.90, 1322.90	1323.89, 1321.90
$[M-Br+H]^+$	1243.99, 1245.99	1243.98, 1245.98

**Table 5.5: MALDI-MS: *ZnTPTBPBr*** - A comparison of calculated and experimentally found ions matrix-amplified laser-desorption ionisation

Type of ion	$m/z$ calculated	$m/z$ experimental
$M^+$	956.12	956.12
$[M-Br+H]^+$	875.99	875.98

*PtTPTBPBr<sub>3</sub>*, however the *PtTPTBPBr<sub>4</sub>* product appears to be the main component of the

mixture.

The MS(MALDI)-data obtained for *ZnTPTBPBr* indicates a product mixture of *ZnTPTBPBr*, and *ZnTPTBP*. The mixture can be considered in-separable by means of column-chromatography, yet *ZnTPTBPBr* appears to be the main product and *ZnTPTBP*, which carries no bromides, can be considered as inert under the Suzuki-coupling conditions employed.

## 5.3 Covalent Coupling

### 5.3.1 The Effect of Suzuki Coupling on the Polymer's Molecular Weight Distribution

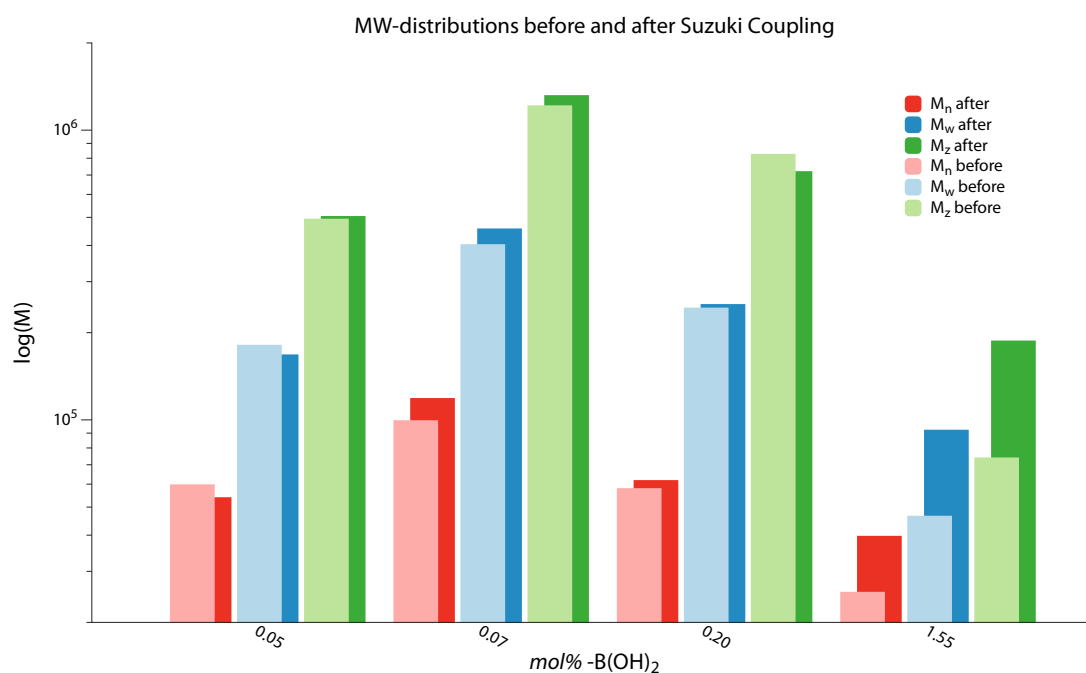


**Figure 5.3:** An Illustration of the change in MW-Distribution due to Suzuki-Coupling

**Table 5.6:** Molecular Weight Distributions of Styrene-4-Vinylbenzeneboronic acid-Co-polymers

$mol\% Ph-B(OH)_2$	$M_n^* [g \cdot mol^{-1}]$	$M_w^* [g \cdot mol^{-1}]$	$M_z^* [g \cdot mol^{-1}]$	PDI*
1.55	39790	92470	187850	2.324
0.20	61960	251010	721800	4.051
0.07	118950	457810	1320760	3.849
0.05	54080	168230	505320	3.111

In the approach using Suzuki-coupling to immobilise  $PtTPTBPr_4$  in polystyrene carrying boronic acid-residues, the question of potential cross-linking due to the presence of four aryl-bromides in the dye, which are able to undergo Suzuki-coupling, was to be assessed, despite having been considered in the calculation of the necessary amounts of substrates by using dye in large excess.

An apparent loss of solubility due to cross-linking by means of Suzuki-coupling was not observed in any of the samples prepared.

Molecular weight-distributions were determined before and after coupling by means of gel-permeation-chromatography and the obtained values were compared. The data is summarised in figure 5.3 and table 5.6.

Analysis of the data shows no significant increase in any of the key parameters ( $M_n$ ,  $M_w$ ,

$M_z$ , PDI), as would have been expected if cross-linking had occurred. Consequently, the use of  $PtTPTBPBr_4$  in large excess sufficiently tackles the possible problem of cross-linking.

### 5.3.2 Coupling efficiency

Coupling efficiency and indicator content after covalent modification were assessed by comparing the experimental data obtained for boronic acid-residue-loading and data obtained by determining the dye concentration in solutions containing a defined amount of modified polymer. The coupling efficiency was determined as the quotient of the experimental and theoretical values for dye-loading in *wt%*.

**Table 5.7:** Dye-loading in the sensor polymers and coupling efficiency

$mol\%_{\text{exp}}$ <i>Ph-B(OH)<sub>2</sub></i>	Dye	$wt\%_{\text{theo}}$ <i>dye</i>	$wt\%_{\text{exp}}$ <i>dye</i>	coupling efficiency (%)
1.55	PtTPTBPBr <sub>4</sub>	19.61	<b>5.65</b>	29
0.20	PtTPTBPBr <sub>4</sub>	2.57	<b>1.48</b>	58
0.07	PtTPTBPBr <sub>4</sub>	0.87	<b>0.52</b>	59
0.05	PtTPTBPBr <sub>4</sub>	0.65	<b>0.27</b>	42
0.07	PtTPTBPBr	0.62	<b>0.41</b>	66
<i>co-polymerised</i>	PtTPTBPBr	1	<b>1</b>	95

### 5.3.3 Comparison and Discussion of the Synthetic Approaches

When comparing the data obtained for polymer-modification by means of Suzuki-coupling with the yield of the step which involved the modification of the dye with a styrene-monomer, the latter appears to be the far more reasonable approach:

- **Yield**

The modification of PtTPTBPBr with *Vinylbenzeneboronic acid* yields the desired *Styrene-modified PtTPTBP* in 95 % yield, whereas attempts to immobilise the dye in a boronic acid-functionalised polymer by means of Suzuki-coupling are typically characterised by yields (coupling efficiency) ranging between 40 % and 60 %. These, in terms of Suzuki-coupling, rather low yields may be attributed to the more complex system involved in the coupling of dyes and functionalised polymers, which entail concentrated solutions in terms of polymer-concentration, but diluted solutions in terms of reactant- and catalyst concentration. Furthermore, the sterical environment of polymer-bound boronic acid-residues may have a negative influence on the yield of Suzuki-coupling reactions by impeding the necessary co-ordination and isomerisation step in the catalytic cycle.

- **Ease of Use and Controllability**

The strategies based on covalent coupling after polymerisation entail elemental analysis in order to determine the boronic acid-residue loading of a synthesised polymer as well as complicated calculations and constant re-assessment of the obtained values. Furthermore, they are characterised by a low degree of flexibility with regards to the dye loading and its controllability, since the dye loading is principally determined by the amount

of *4-vinylbenzeneboronic acid* used in polymerisation, but may be subject to influences which cause it to deviate from the target value, such as lower-than-expected boronic acid-residue-loading caused during polymerisation and low yields in the Suzuki-coupling step.

In the approach based on dye-modification, however, these problems are alleviated to a certain extent. The small amounts of by-product produced in the high-yielding Suzuki-coupling step can easily be separated by column-chromatography. This allows for defined amounts of polymerisable dye to be used in the synthesis. Moreover, the strategy provides a certain degree of flexibility with respect to the desired dye-loading of the sensor polymer, which is determined in the last step of its synthesis, i.e. polymerisation. As seen in the synthesis of boronic acid-functionalised polystyrene, however, dye loading of polystyrene-based sensor-polymers prepared by mass-co-polymerisation of a styrene-modified dye and Styrene under solvent-free conditions will be limited by the dye's solubility in Styrene.

- **Flexibility**

With regards to the possibility to easily transfer the procedures developed herein to a system based on different dyes or different polymers, the strategy based on the modification of the dye with an adequate monomer promises to offer more flexibility.

A variety of polymers are synthesised based on radical-mass-co-polymerisation. A covalent immobilisation of the indicator dye in these polymers could, in principle, be realised using the *Styrene-modified PtTPTBP*, which was synthesised in the course of this thesis. Theoretically, the strategic approach developed, would also enable the use of a variety of dyes carrying aryl-bromide-functionalities, as well as the synthesis of a variety of co-polymers, provided the availability of adequate aryl-boronic acid-carrying monomers.



## 5.4 Sensor Characterisation

### 5.4.1 Sensor films - Photo-physical Characterisation

The sensor films prepared from the sensor polymers synthesised as outlined in section 3.2.1 were characterised by means of absorption and emission spectra. Quantum yields were determined as described in section 3.3.3.

#### The Dyes in Different Media

Figure 5.4 and figure 5.5 illustrate the absorption- and emission -behaviour of the *PtTPTBPr* and *PtTPTBPr<sub>4</sub>* in solution, covalently bound to a polymer and in the sensor film, i.e. in bulk polymer medium.

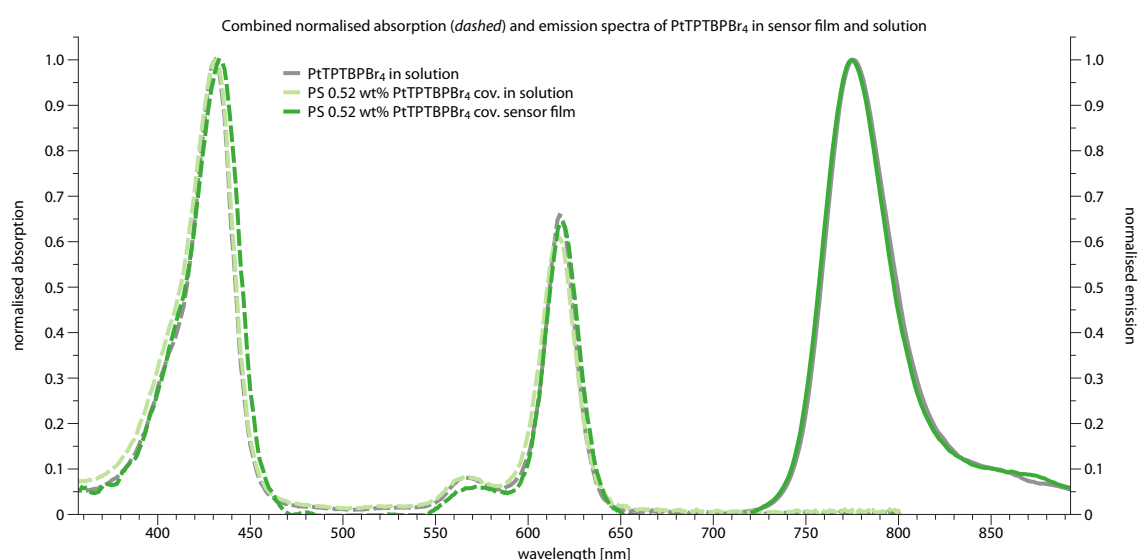


**Figure 5.4:** Combined absorption and emission spectra of *PtTPTBPr<sub>4</sub>* in different media, illustrating the photophysical behaviour of the dye in solution, covalently bound to a polymer (dissolved) and covalently bound to a polymer (bulk polymer).

The difference in medium results in a weak bathochromic shift with respect to the dye in solution, which is very weak for the dissolved sensor polymer and a little bit more pronounced in the case of bulk polymer medium. The slight shift may in parts also be attributable to the substitution of a bromine atom with an aryl-residue.

In both cases, employing *PtTPTBPr* and *PtTPTBPr<sub>4</sub>*, a slight bathochromic shift is observed, with respect to the dye dissolved in Dichloromethane. The shift is very weak in the samples of dissolved sensor polymer and a little bit stronger in the samples of bulk polymer. The bathochromic shift may be attributable to the more rigid environment of the dye, which hinders rotation of the phenyl residue, as well as to the substitution of a bromine atom with one of polystyrene's phenyl residues.

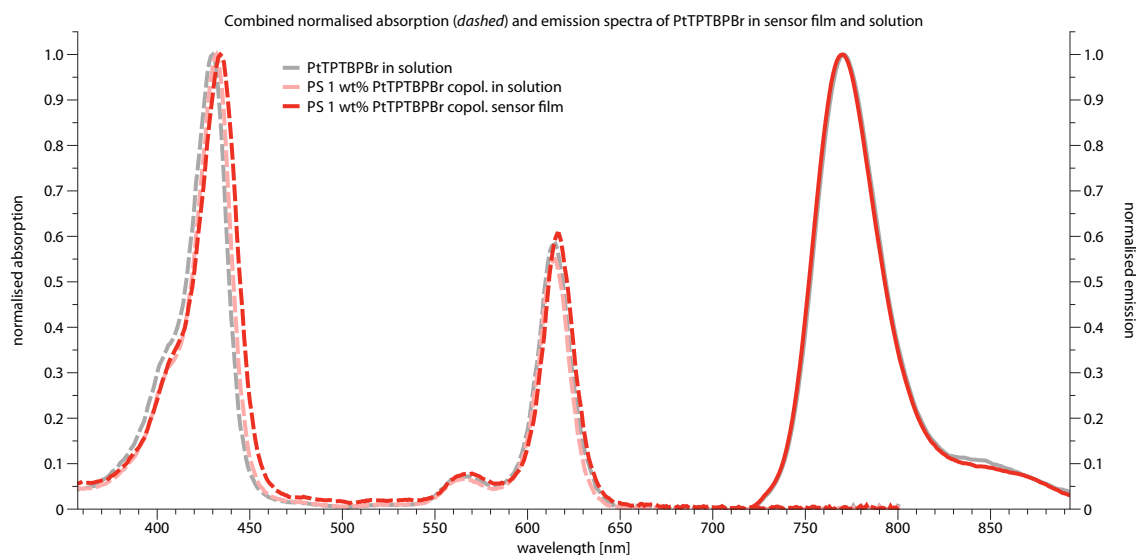


**Figure 5.5:** Combined absorption and emission spectra of PtTPTBPBr in different media, illustrating the photophysical behaviour of the dye in solution, covalently bound to a polymer (dissolved) and covalently bound to a polymer (bulk polymer).

The difference in medium results in a weak bathochromic shift with respect to the dye in solution, which is very weak for the dissolved sensor polymer and stronger in the case of bulk polymer medium. The slight shift may in parts also be attributable to the substitution of a bromine atom with an aryl-residue. Compared to PtTPTBPBr<sub>4</sub>, the bathochromic shift here is stronger.

### Sensor Films - Quantum Yields and the Influence of Dye Loading

Figures 5.6 and 5.7 depict combined absorption and emission spectra of the sensor films prepared based on the sensor polymers synthesised in this thesis. Films of 1 wt% of PtTPTBPBr, 1 wt% and 3 wt% of PtTPTBPBr<sub>4</sub> were prepared by physically entrapping the dyes in the polymers and used as references.

The absorption spectrum of the sensor polymer containing 5.65 wt% of PtTPTBPBr<sub>4</sub> was measured, however absorption at both the Soret- and the Q-band exceeded 3, thus it was omitted from the spectrum.

Table 5.8 lists the quantum yields as determined for the prepared sensor films. The quantum yields determined for the references of both PtTPTBPBr and PtTPTBPBr<sub>4</sub> of comparable dye content (1 wt%) physically-entrapped in the polymer matrix are comparable in magnitude. Increasing the dye content, as in the reference containing 3 wt% of PtTPTBPBr<sub>4</sub>, leads to a reduced quantum yield.

The effect of decreasing quantum yield with increasing dye content is very well reflected in the data obtained for films of varying wt% of PtTPTBPBr<sub>4</sub> covalently immobilised in polystyrene, although quantum yields obtained for covalently immobilised dye were found to be generally slightly lower than those found for the physically-entrapped dyes. The quantum yield found for the sensor film of covalently immobilised PtTPTBPBr (Suzuki) generally fits this picture, being

of comparable magnitude to the quantum yield of the PtTPTBBr<sub>4</sub>-sample of corresponding dye content.

An explanation to this behaviour could be that residual potassium bromide, which is produced as a by-product in Suzuki-coupling, got entrapped in the polymer upon precipitation, and could not be entirely removed from the sensor polymer. Bromide-anions act as effective excited state quenchers. A high concentration of bromides could thus sufficiently reduce the observed quantum yield in the sensor polymers produced by means of polymer modification through Suzuki-coupling. In the case of the co-polymerised dye, the by-products formed during Suzuki-coupling can be expected to be effectively removed by means of column chromatography. The observed decrease of quantum yield with increasing dye-content can be attributed to a variety of photo-physical phenomena involving the interaction of dye-molecules, such as self-quenching, whose probability increases with increasing dye concentration. The quantum yield determined for the sensor film based on co-polymerised Styrene-modified PtTPTBP, however, turned out to be even slightly higher than the quantum yield of the physically-entrapped dye.

**Table 5.8:** Quantum yields determined for the sensor films

<i>wt%</i> Dye/Polymer	Dye	method of immobilisation	Quantum Yield [% ]
1	PtTPTBBr <sub>4</sub>	<i>phys. entrapped</i>	34.50
1	PtTPTBPBr	<i>phys. entrappedd</i>	34.67
3	PtTPTBBr <sub>4</sub>	<i>phys. entrapped</i>	27.05
0.27	PtTPTBBr <sub>4</sub>	<i>covalent (Suzuki)</i>	35.19
0.52	PtTPTBBr <sub>4</sub>	<i>covalent (Suzuki)</i>	30.13
2.57	PtTPTBBr <sub>4</sub>	<i>covalent (Suzuki)</i>	28.56
5.56	PtTPTBBr <sub>4</sub>	<i>covalent (Suzuki)</i>	19.19
0.41	PtTPTBPBr	<i>covalent (Suzuki)</i>	30.41
1	PtTPTBBr <sub>4</sub>	<i>co-polymerised</i>	35.32

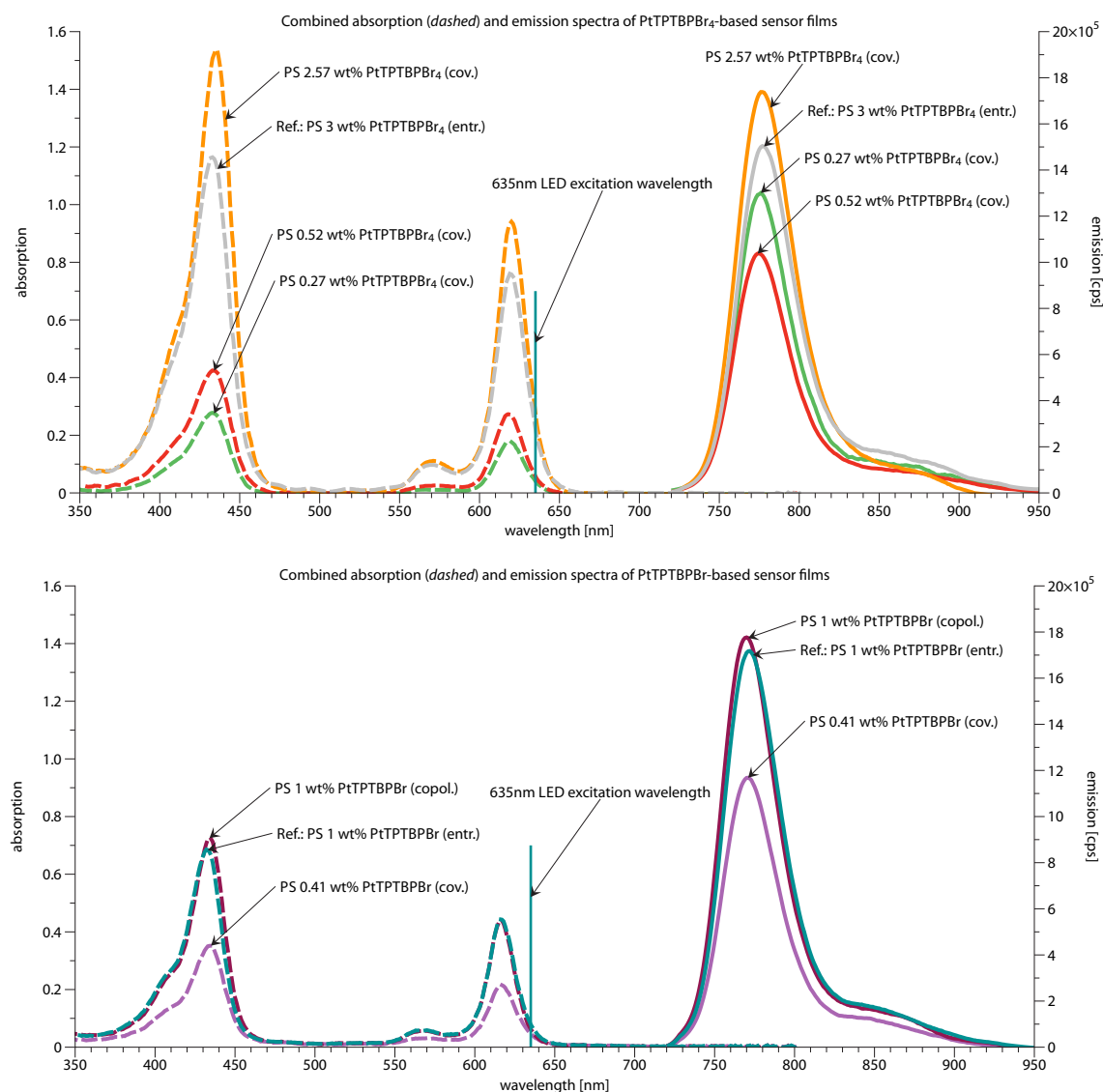


**Figure 5.6: Combined absorption and emission spectra: PtTPTBPBr<sub>4</sub>- and PtTPTBPBr-based sensor films.** These spectra illustrate the effect of the dye loading on the sensor films' absorption and emission characteristics. Due to comparable film thickness, the absorption spectra behave as it would be expected following Beer's-law, and thus absorption linearly increases with dye content. The emission intensity of the sensor films, however, does not increase in such a manner - a fact which is reflected in the quantum yields determined. - A close comparison of spectral properties of PtTPTBPBr- and PtTPTBPBr<sub>4</sub>-based films is depicted in fig 5.7

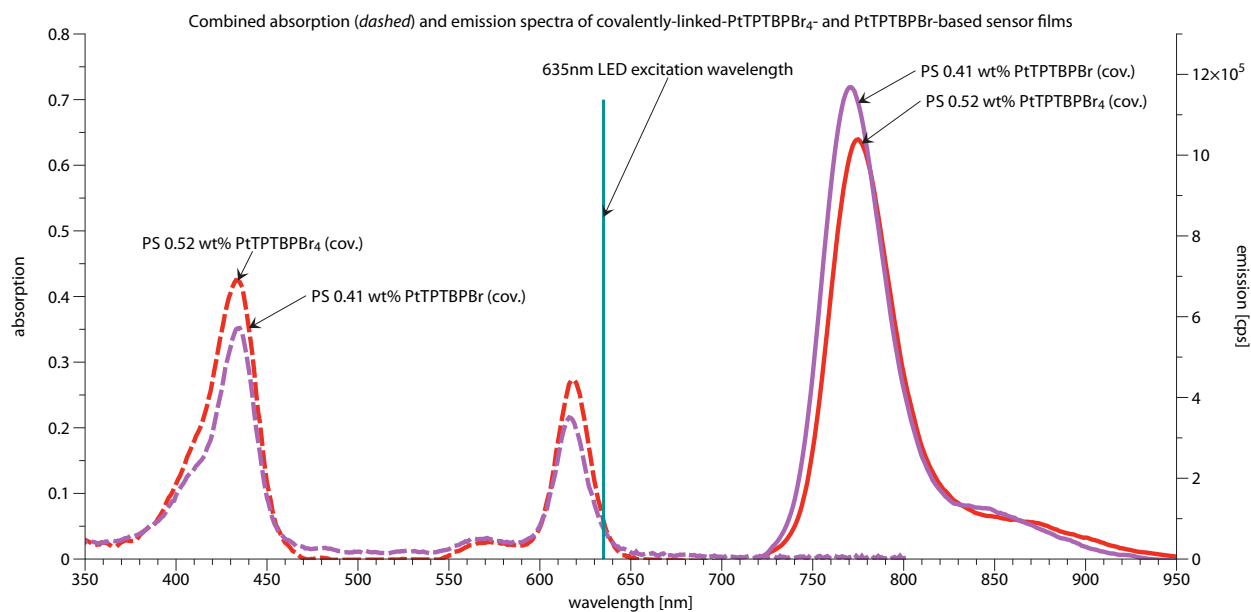


**Figure 5.7: Combined absorption and emission spectra: A close comparison of PtTPTBPBr- and PtTPTBPBr<sub>4</sub>-based sensors** The above spectra provide a close comparison of the spectral properties of PtTPTBPBr- and PtTPTBPBr<sub>4</sub>-based sensor films of comparable (molar) dye loading. The PtTPTBPBr<sub>4</sub>-based film shows slightly bathochromic shifted Q-band absorption, as well as emission band, compared to the PtTPTBPBr-based sensor film. The latter, however, albeit showing weaker absorption, is characterised by higher emission intensity.

### 5.4.2 Calibration Curves

Calibration curves were obtained as described in section 3.3.4. Figure 5.8 and figure 5.9 show  $\tau$ -based, as well as luminescence-intensity-based Stern-Volmer-plots (SV-plot) of the data obtained for the sensor polymers synthesised, grouped in a manner as to facilitate the discussion of various effects observed.

The  $\tau$ -based SV-plots were fitted using the the Two-Site-Model [3] (see section 2.1.12), luminescence intensity-based SV-plots were fitted using the simplified Two-Site-Model, which gave better correlation coefficients in the light of the higher linearity of these plots. The correlation coefficients for all fits performed exceeded 0.999. The fitting parameters obtained are listed in table 5.10 and table 5.9.

**Table 5.9:** Fitting parameters -  $\tau$ -based SV-plots

$wt\%$ Dye/Poly.	Dye	Immobilisation	$\tau_0$	$f$	$K_{SV1}$ (hPa <sup>-1</sup> )	$K_{SV2}$ (hPa <sup>-1</sup> )
1	PtTPTBPr <sub>4</sub>	<i>phys. entrapped</i>	48.83	0.5641	0.0303	0.0057
1	PtTPTBPr	<i>phys. entrapped</i>	47.01	0.6452	0.0327	0.0053
3	PtTPTBPr <sub>4</sub>	<i>phys. entrapped</i>	44.43	0.5029	0.0289	0.0062
0.27	PtTPTBPr <sub>4</sub>	<i>covalent (Suzuki)</i>	50.79	0.6857	0.0280	0.0046
0.52	PtTPTBPr <sub>4</sub>	<i>covalent (Suzuki)</i>	48.96	0.6417	0.0303	0.0054
2.57	PtTPTBPr <sub>4</sub>	<i>covalent (Suzuki)</i>	47.27	0.5247	0.0343	0.0073
5.56	PtTPTBPr <sub>4</sub>	<i>covalent (Suzuki)</i>	37.98	0.1339	0.0746	0.0126
0.41	PtTPTBPr	<i>covalent (Suzuki)</i>	47.06	0.3406	0.0696	0.0118
1	PtTPTBPr <sub>4</sub>	<i>co-polymerised</i>	47.29	0.2610	0.0795	0.0125

**Table 5.10:** Fitting parameters -  $I$ -based SV-plots

$wt\%$ Dye/Polymer	Dye	Immobilisation	$f$	$K_{SV1}$ (hPa <sup>-1</sup> )
1	PtTPTBPr <sub>4</sub>	<i>phys. entrapped</i>	0.9820	0.0164
1	PtTPTBPr	<i>phys. entrapped</i>	0.9899	0.0194
3	PtTPTBPr <sub>4</sub>	<i>phys. entrapped</i>	0.9829	0.0146
0.27	PtTPTBPr <sub>4</sub>	<i>covalent (Suzuki)</i>	0.9839	0.0183
0.52	PtTPTBPr <sub>4</sub>	<i>covalent (Suzuki)</i>	0.9809	0.0184
2.57	PtTPTBPr <sub>4</sub>	<i>covalent (Suzuki)</i>	0.9892	0.0176
5.56	PtTPTBPr <sub>4</sub>	<i>covalent (Suzuki)</i>	1.0000	0.0152
0.41	PtTPTBPr	<i>covalent (Suzuki)</i>	0.9892	0.0211
1	PtTPTBPr <sub>4</sub>	<i>co-polymerised</i>	0.9930	0.0195

#### Covalently immobilised dye vs. physically-entrapped dye

Covalent immobilisation affects the slope of the Stern-Volmer-plot ( $K_{SV}$ ). Sensor polymers employing the covalently immobilised indicator are characterised by steeper calibration curves.

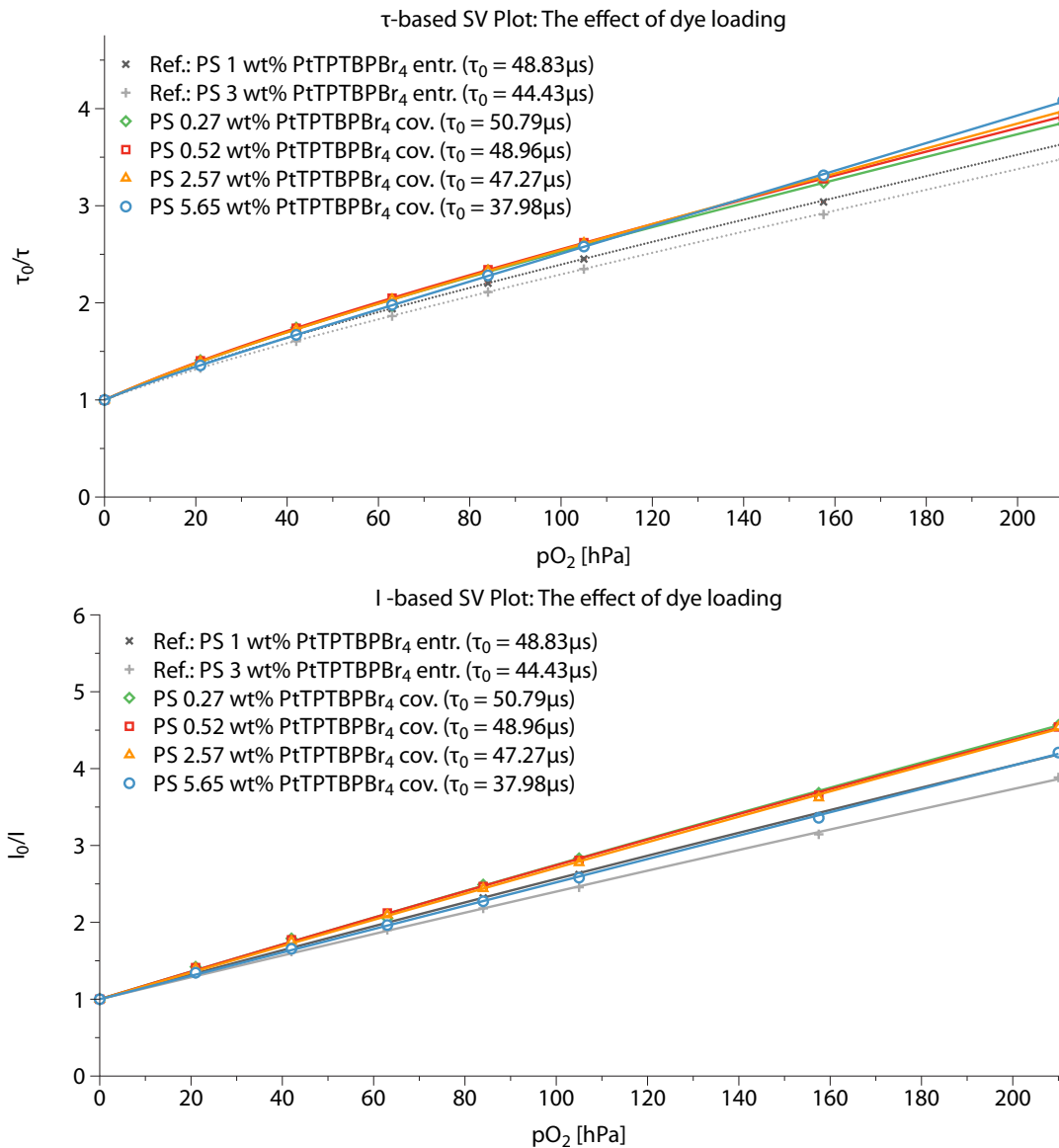


**Figure 5.8: SV-Plot: The effect of dye loading** - Calibration curves of sensor foils based on PtTPTBBr<sub>4</sub> covalently immobilised or physically-entrapped in a polystyrene matrix. All sensor films prepared from PtTPTBBr<sub>4</sub> appear to be better quenchable than the reference films of physically-entrapped dye. Loading, here given as the *wt%* of covalently immobilised PtTPTBBr<sub>4</sub> affects the flexion of the curves in the  $\tau$ -based SV-plot. The degree of flexion decreases with increasing *wt%* of covalently immobilised dye. The slopes of the curves in the I-based SV-plots are comparable in magnitude. The blue curve corresponding to 5.65 *wt%* PtTPTBBr<sub>4</sub> covalently immobilised in polystyrene, however, shows a significantly smaller slope and is comparable to the reference sample of 1 *wt%* of PtTPTBBr<sub>4</sub> physically-entrapped in polystyrene.

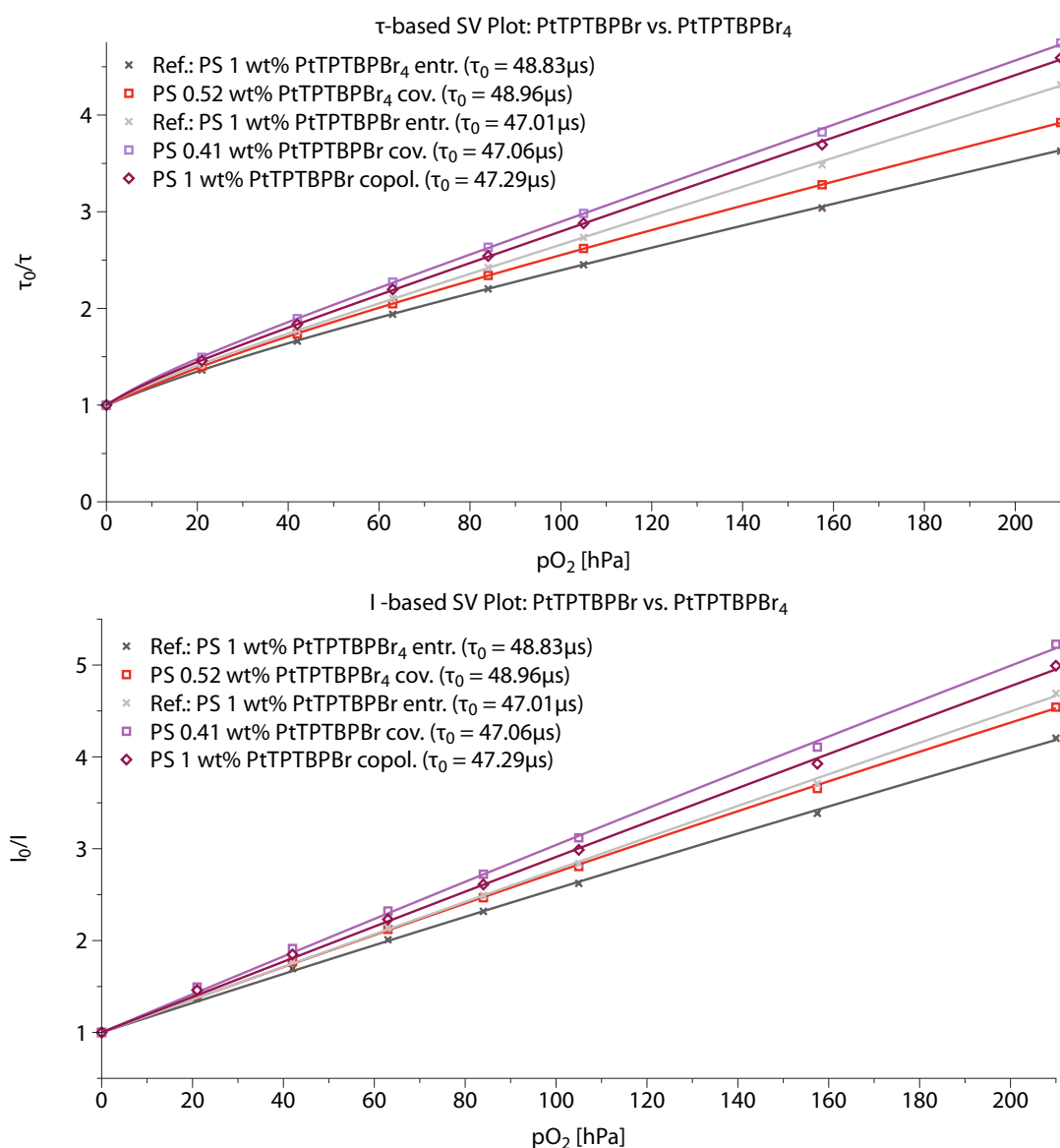


**Figure 5.9: SV-Plot: PtTPTBPBr vs. PtTPTBPBr<sub>4</sub>** - Calibration curves of sensor foils based on PtTPTBPBr<sub>4</sub> covalently immobilised or physically-entrapped in a polystyrene matrix.

The comparison of SV-plots of data corresponding to PtTPTBPBr and PtTPTBPBr<sub>4</sub> shows that sensor films based on PtTPTBPBr are generally better quenchable than corresponding sensor films based on PtTPTBPBr<sub>4</sub>.

Furthermore, a higher degree of linearity ( $f$ ) was observed in the case of sensor polymers employing the covalently immobilised indicator.

Both effects are likely to originate from altered properties of the sensor matrix. Along this line of reasoning, the indicator dye may be thought of as having a positive influence on the polymer



properties by contributing to a more homogeneous environment, thus reducing the effects of micro-heterogeneities, which cause Stern-Volmer-plots to deviate from ideal behaviour.

#### **The influence of covalent dye-loading**

The lifetime was observed to decrease with increasing dye content, regardless of the nature of immobilisation. As already discussed in the section on quantum yields, this phenomenon may be attributable to interactions between the indicator molecules, such as self-quenching. Furthermore, increased dye loading leads to a reduced slope of the calibration curve, thus reducing the sensor's sensitivity. A high degree of indicator dye loading, however, has a beneficial effect on the form of the Stern-Volmer-plots obtained for the sensor films. The higher the dye content, the more linear the obtained calibration curve. Again, this phenomenon may be attributable to the influence of the indicator dye on the orientation of the polymer strands, as briefly discussed above.

#### **Comparison between PtTPTBPBr and PtTPTBPBr<sub>4</sub>**

Based on the data obtained when comparing sensor polymers based on the two different dyes, polymers based on PtTPTBP can be considered as better quenchable than the corresponding systems based on PtTPTBPBr<sub>4</sub>, despite the slightly lower luminescence lifetimes observed in the systems based on PtTPTBPBr.

## 5.4.3 Sensor Response

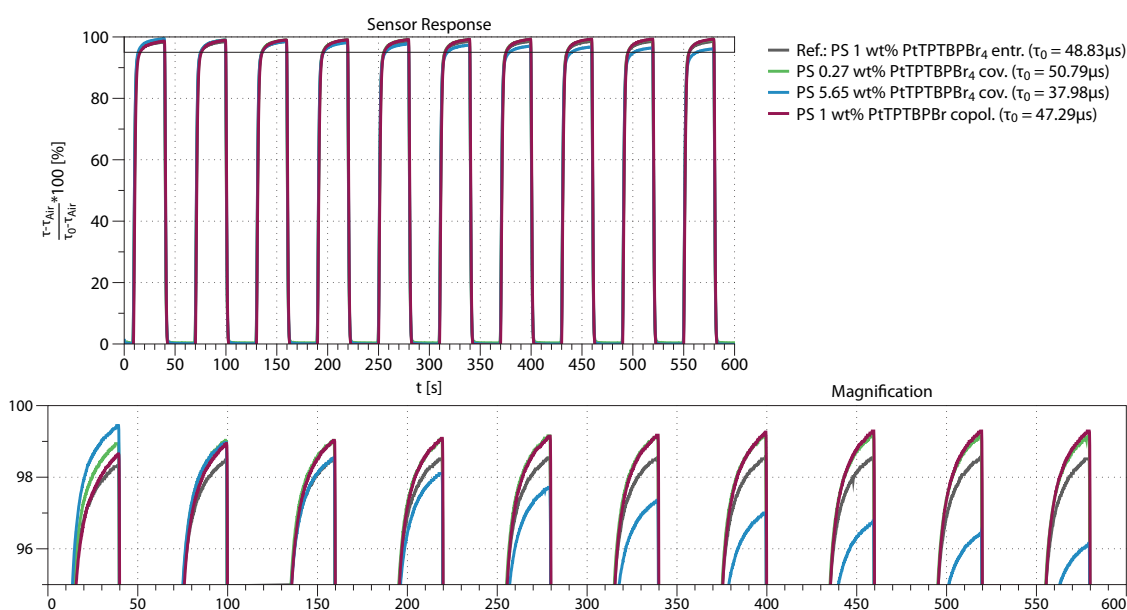


**Figure 5.10: Sensor Response - Luminescence lifetime normalised between  $\tau_0$  and  $\tau_{\text{air}}$  as a function of time**

100 % correspond to the value for  $\tau_{\text{air}}$ , which was determined for each material in the course of the calibration experiments, whereas 0 % correspond to  $\tau_0$ . The loss of response observable for the sample based on 5.56 wt% PtTPTBPr<sub>4</sub> is likely to be the manifestation of rapid photobleaching of the sample. All other sensors are characterised by a very fast response.

The response of the sensor to changing concentrations of oxygen were assessed as outlined in section 3.3.4. All materials investigated show a very fast response to changes in oxygen concentrations, reaching between 99 % and 97 % of the final  $\tau$  when switching from nitrogen to air saturation. When changing from air saturation to nitrogen, the response was generally immediate. It is interesting to note that the response was observed to be faster with lower indicator loading. The sample containing 5.56 wt% of PtTPTBPr<sub>4</sub> covalently immobilised initially showed a very fast response, which may be attributable to the bulky indicator's influence on the polymer's secondary structure. With increasing number of cycles, however, the lifetime measured after 30 s under air decreased, which is likely to be due to photobleaching. Thus, the response of the sensor does not change, however, the large amount of singlet oxygen produced in the quenching process reacts with the dye and the polymer leading to changes in their structure and ultimately reduces the observed luminescence lifetime.

## 5.4.4 Photostability

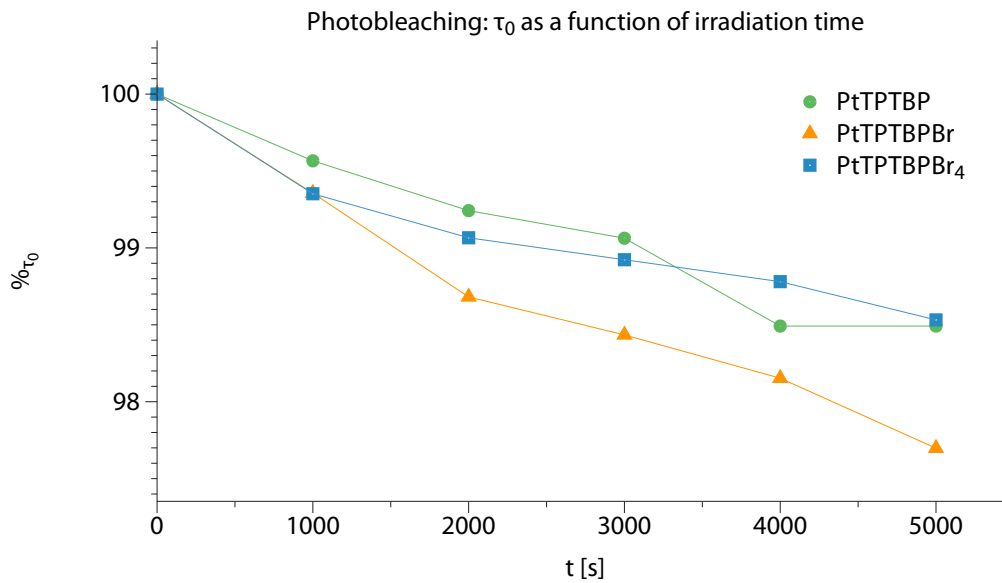


**Figure 5.11: Photostability - Decrease of  $\tau_0$  in % of its initial value**

Photostability was assessed by exposing the sensor fibres prepared by physically entrapping the dyes in polystyrene to prolonged irradiation generated by an LED set at high intensity. All three dyes show a small decrease in luminescence lifetime under nitrogen. The change is strongest in the case of PtTPTBPBr.

Photostability was assessed based on the experiment outlined in section 3.3.5. The decrease in luminescence lifetime was monitored over prolonged irradiation time under air. Cocktails were prepared based on indicator dyes physically-entrapped in polystyrene. Luminescence lifetime under nitrogen ( $\tau_0$ ) is the parameter most heavily affected by processes involved in photobleaching. All three dyes show a small decrease of  $\tau_0$  over time. The decrease is most pronounced for PtTPTBPBr, whereas the decrease for PtTPTBP and PtTPTBPBr<sub>4</sub> is comparable in magnitude. The changes observed under the extreme conditions employed to bring about an observable change in luminescence lifetime are comparably small and qualify all three dyes to be employed in applications, which generally use lower LED-intensities. An impurity contained in the sample of PtTPTBPBr is likely to be the cause of the slightly altered properties observed in this experiment.



---

## 6 Outlook and Conclusions

In this thesis, two covalent immobilisation approaches for an optical oxygen sensor system based on PtTPTBTP and polystyrene have been developed and investigated. Both approaches rely on the introduction of bromides into the *meso*-position of the porphyrin structure and subsequent functionalisation employing Suzuki-coupling.

In one approach, the dye is grafted to a boronic-acid-residue carrying polystyrene polymer, in the other approach the dye is further modified with a 4-Vinylbenzeneboronic acid, which results in the introduction of a vinyl group, which opens the possibility of co-polymerisation. From a practical point of view, the latter approach may be deemed favourable, since it is more easily controllable and offers a higher degree of versatility.

The sensor polymers prepared using both approaches were characterised with regard to their potential application as optical oxygen sensors. The covalent immobilisation not only resolves problems connected to leaching of the indicator and indicator aggregation, it also results in slightly improved sensor characteristics such as higher quenchability as well as a more linear Stern-Volmer-plots.

A high content of covalently immobilised indicator was observed to result in almost ideal Stern-Volmer-plots, but deteriorated sensor performance in many other aspects such as quantum yield and sensitivity. The improved linearity is likely to be connected with the steric impact imposed by bulky indicator dye on the polymer's secondary structure, whereas the observed deteriorations in sensor performance are likely to have a photophysical cause. Introducing rigid and bulky substituents, which do not alter the sensor's photophysical properties, may provide a way to further increase the linearity of the sensor system's Stern-Volmer-plot without compromising quantum yield and sensitivity.

The immobilisation strategies developed in this thesis open new and interesting possibilities regarding the design of optical oxygen sensors and derivative systems. Bio-conjugation using Thiol-ene-click-chemistry, the preparation of cross-linked nanoparticles and the preparation of metal-organic-frameworks based on the developed strategies will be the focus of future work.

---

## 7 References

- [1] JR Partington. "The Discovery of Oxygen". In: *Journal of Chemical Education* 39.3 (1962), p. 123.
- [2] Bernard Valeur. *Molecular Fluorescence: Principles and Applications*. 1st ed. Wiley-VCH, Oct. 2001.
- [3] ER Carraway, JN Demas, BA DeGraff, and JR Bacon. "Photophysics and photochemistry of oxygen sensors based on luminescent transition-metal complexes". In: *Anal. Chem* 63.4 (1991), pp. 337–342.
- [4] Colette McDonagh, Conor S Burke, and Brian D MacCraith. "Optical chemical sensors". In: *Chemical Reviews* 108.2 (Jan. 2008), pp. 400–422.
- [5] Sergey M Borisov and Otto S Wolfbeis. "Optical biosensors." In: *Chemical Reviews* 108.2 (Feb. 2008), pp. 423–461.
- [6] Y Amao. "Probes and polymers for optical sensing of oxygen". In: *Microchimica Acta* 143.1 (2003), pp. 1–12.
- [7] Stefan Nagl and Otto S Wolfbeis. "Optical multiple chemical sensing: status and current challenges." In: *Analyst* 132.6 (June 2007), pp. 507–511.
- [8] Sergey M Borisov and Ingo Klimant. "Luminescent nanobeads for optical sensing and imaging of dissolved oxygen". In: *Microchimica Acta* 164.1-2 (May 2008), pp. 7–15.
- [9] Günter Mistlberger, Klaus Koren, Sergey M Borisov, and Ingo Klimant. "Magnetically remote-controlled optical sensor spheres for monitoring oxygen or pH." In: *Anal. Chem* 82.5 (Mar. 2010), pp. 2124–2128.
- [10] Dmitri B Papkovsky and Tomás C O riordan. "Emerging Applications of Phosphorescent Metalloporphyrins". In: *Journal of Fluorescence* 15.4 (July 2005), pp. 569–584.
- [11] S.A. Vinogradov and D.F. Wilson. "Metalloporphyrins. New phosphorescent probes for oxygen measurements". In: *J. Chem. Soc., Perkin Trans. 2* 1 (1995), pp. 103–111.
- [12] SM Borisov, G Nuss, W Haas, R Saf, M. Schmuck, and I Klimant. "New NIR-emitting complexes of platinum (II) and palladium (II) with fluorinated benzoporphyrins". In: *Journal Of Photochemistry And Photobiology A-Chemistry* 201.2-3 (2009), pp. 128–135.
- [13] S M Borisov, G Nuss, and I Klimant. "Red light-excitable oxygen sensing materials based on platinum(II) and palladium(II) benzoporphyrins." In: *Anal. Chem* 80.24 (Dec. 2008), pp. 9435–9442.
- [14] Sergey M Borisov and Ingo Klimant. "Ultrabright oxygen optodes based on cyclometalated iridium(III) coumarin complexes." In: *Anal. Chem* 79.19 (Oct. 2007), pp. 7501–7509.
- [15] A.K. Bansal, W Holzer, A Penzkofer, and T. Tsuboi. "Absorption and emission spectroscopic characterization of platinum-octaethyl-porphyrin (PtOEP)". In: *Chemical physics* 330.1 (2006), pp. 118–129.

- 
- [16] Carsten Borek et al. "Highly efficient, near-infrared electrophosphorescence from a Pt-metalloporphyrin complex." In: *Angewandte Chemie (International ed. in English)* 46.7 (2007), pp. 1109–1112.
- [17] J.E. Rogers, K.A. Nguyen, D.C. Hufnagle, D.G. McLean, W. Su, K.M. Gossett, A.R. Burke, S.A. Vinogradov, R. Pachter, and P.A. Fleitz. "Observation and Interpretation of Annulated Porphyrins: Studies on the Photophysical Properties of m *eso*-Tetraphenylmetalloporphyrins". In: *The Journal of Physical Chemistry A* 107.51 (2003), pp. 11331–11339.
- [18] Otto S Wolfbeis. "Materials for fluorescence-based optical chemical sensors". In: *Journal of Materials Chemistry* 15.27-28 (Jan. 2005), p. 2657.
- [19] C.A.G.N. Montalbetti and V. Falque. "Amide bond formation and peptide coupling". In: *Tetrahedron* 61.46 (2005), pp. 10827–10852.
- [20] HC Kolb, MG Finn, and KB Sharpless. "Click chemistry: diverse chemical function from a few good reactions". In: *Angewandte Chemie International Edition* 40.11 (2001), pp. 2004–2021.
- [21] U Mansfeld, C Pietsch, R Hoogenboom, C.R. Becer, and U.S. Schubert. "Clickable initiators, monomers and polymers in controlled radical polymerizations—a prospective combination in polymer science". In: *Polymer Chemistry* 1.10 (2010), pp. 1560–1598.
- [22] Akira SUZUKI. "Cross-coupling reactions of organoboranes: an easy way to construct C-C bonds (Nobel Lecture)." In: *Angewandte Chemie (International ed. in English)* 50.30 (July 2011), pp. 6722–6737.
- [23] Akira SUZUKI. "Organoborane coupling reactions (Suzuki coupling)". In: *Proceedings of the Japan Academy, Series B* 80.8 (2004), pp. 359–371.
- [24] JK Stille. "Mechanisms of oxidative addition of organic halides to Group 8 transition-metal complexes - Accounts of Chemical Research (ACS Publications)". In: *Accounts of Chemical Research* (1977).
- [25] AL Casado. "On the Configuration Resulting from Oxidative Addition of RX to Pd(PPh<sub>3</sub>)<sub>4</sub> and the Mechanism of the cis-to-trans Isomerization of [PdRX(PPh<sub>3</sub>)<sub>2</sub>] Complexes (R = Aryl, X = Halide)† - Organometallics (ACS Publications)". In: *Organometallics* (1998).
- [26] Karl Matos and John A Soderquist. "Alkylboranes in the Suzuki-Miyaura Coupling: Stereochemical and Mechanistic Studies." In: *Journal Of Organic Chemistry* 63.3 (Feb. 1998), pp. 461–470.
- [27] Norio Miyaura and Akira SUZUKI. "Palladium-Catalyzed Cross-Coupling Reactions of Organoboron Compounds". In: *Chemical Reviews* 95.7 (Nov. 1995), pp. 2457–2483.
- [28] Gary A Molander and Betina Biolatto. "Palladium-catalyzed Suzuki-Miyaura cross-coupling reactions of potassium aryl- and heteroaryltrifluoroborates." In: *Journal Of Organic Chemistry* 68.11 (May 2003), pp. 4302–4314.
- [29] AF Littke, CY Dai, and GC Fu. "Versatile catalysts for the Suzuki cross-coupling of arylboronic acids with aryl and vinyl halides and triflates under mild conditions". In: *Journal Of The American Chemical Society* 122.17 (2000), pp. 4020–4028.
- [30] JP Wolfe, RA Singer, BH Yang, and SL Buchwald. "Highly active palladium catalysts for Suzuki coupling reactions". In: *Journal Of The American Chemical Society* 121.41 (1999), pp. 9550–9561.

- [31] K Yamada and A Suzuki. “A new stereospecific cross-coupling by the palladium-catalyzed reaction of 1-alkenylboranes with 1-alkenyl or 1-alkynyl halides”. In: *Tetrahedron letters* (1979).
- [32] N Miyaura and T Yano. “The palladium-catalyzed cross-coupling reaction of 1-alkenylboranes with allylic or benzylic bromides. Convenient syntheses of 1,4-alkadienes and allybenzenes from alkynes via hydroboration”. In: *Tetrahedron letters* (1980).
- [33] L.O. Pålsson and A.P. Monkman. “Measurements of solid-state photoluminescence quantum yields of films using a fluorimeter”. In: *Advanced Materials* 14.10 (2002), p. 757.
- [34] Jonathan S Lindsey, Irwin C Schreiman, Henry C Hsu, Patrick C Kearney, and Anne M Marguerettaz. “Rothmund and Adler-Longo reactions revisited: synthesis of tetraphenylporphyrins under equilibrium conditions”. In: *Journal Of Organic Chemistry* 52.5 (Mar. 1987), pp. 827–836.



---

## 8 List of Figures

2.1	Jablonski Diagram - Overview . . . . .	2
2.2	Jablonski Diagram - Absorption . . . . .	2
2.3	A schematic illustration of the Franck-Condon Principle . . . . .	3
2.4	Jablonski Diagram - Internal Conversion . . . . .	4
2.5	Jablonski Diagram - Inter-System Crossing . . . . .	4
2.6	Jablonski Diagram - Fluorescence . . . . .	5
2.7	Jablonski Diagram - Phosphorescence . . . . .	5
2.8	Jablonski Diagram - Delayed Fluorescence . . . . .	6
2.9	Static vs. Dynamic Quenching . . . . .	8
2.10	A general Scheme of Chemical Sensors . . . . .	10
2.11	Transduction in optical chemical sensors . . . . .	11
2.12	Transduction in optical oxygen sensors . . . . .	13
2.13	Examples of common oxygen indicators . . . . .	14
2.14	Thiophosgen-based coupling . . . . .	17
2.15	EDC/NHS-Conjugation . . . . .	18
2.16	Immobilisation based on vicinal diols . . . . .	18
2.17	Click Chemistry - Overview . . . . .	19
2.18	Overview of the most common Pd(0) catalysed cross-coupling reactions. . . . .	21
2.19	Suzuki-Coupling - The Catalytic Cycle . . . . .	22
2.20	Suzuki-Coupling - Organoboranes . . . . .	23
2.21	Suzuki-Coupling - Ligands . . . . .	24
3.1	Optical Fibres . . . . .	26
3.2	A plot illustrating phaseshift in frequency domain measurements . . . . .	29
4.1	Template Directed Synthesis of ZnTPTBP . . . . .	35
4.2	Modified Template Directed Synthesis of ZnTPTBP . . . . .	35
4.3	A schematic illustration of the steps and species involved in porphyrin synthesis . . . . .	36
4.4	Template Directed Synthesis of ZnTPTBPBr <sub>4</sub> . . . . .	37
4.5	Demetallation of ZnTPTBPBr <sub>4</sub> . . . . .	37
4.6	Platination of H <sub>2</sub> TPTBPBr <sub>4</sub> . . . . .	38
4.7	Template Directed Synthesis of ZnTPTBPBr . . . . .	39
4.8	Demetallation of ZnTPTBPBr . . . . .	40
4.9	Platination of H <sub>2</sub> TPTBPBr . . . . .	40
4.10	Synthesis of styrene-vinylbenzeneboronic acid-copolymers . . . . .	41
4.11	Suzuki-coupling of PtTPTBPBr <sub>4</sub> and polystyrenes carrying boronic-acid residues . . . . .	43
4.12	Suzuki-coupling of PtTPTBPBr and polystyrenes carrying boronic-acid residues . . . . .	44
4.13	Suzuki-coupling of PtTPTBPBr and vinylbenzeneboronic acid . . . . .	45
4.14	Co-Polymerisation of styrene and styryl-functionalised PtTPTBP . . . . .	46
5.1	Illustration of MW-Distributions - Polymers . . . . .	48

5.2	Combined normalised absorption and emission spectra - PtTPTBP, PtTPTBPBr, PtTPTBPBr <sub>4</sub> . . . . .	49
5.3	The change in MW-Distribution due to Suzuki-Coupling . . . . .	52
5.4	Combined absorption and emission spectra of PtTPTBPBr <sub>4</sub> in different media . . . . .	55
5.5	Combined absorption and emission spectra of PtTPTBPBr in different media . . . . .	56
5.6	Combined Absorption and emission spectra: PtTPTBPBr <sub>4</sub> - and PtTPTBPBr-based sensor films . . . . .	58
5.7	Combined Absorption and emission spectra: A comparison of PtTPTBPBr- and PtTPTBPBr <sub>4</sub> -based sensors . . . . .	59
5.8	SV-Plot: The effect of dye loading . . . . .	61
5.9	SV-Plot: PtTPTBPBr vs. PtTPTBPBr <sub>4</sub> . . . . .	62
5.10	Sensor Response . . . . .	64
5.11	Photostability . . . . .	65

---

## 9 List of Tables

2.1	Common luminescence-based oxygen indicators . . . . .	14
3.1	Chemicals Used . . . . .	25
4.1	Boronic acid-modified Polymers - Compositions and Molecular Weights . . . . .	42
5.1	Boronic acid-Residue-Loading of the Polymers Synthesised . . . . .	47
5.2	Molecular Weight Distribution - Styrene-4-vinylbenzeneboronic acid-co-polymers	47
5.3	Photophysical properties - PtTPTBP, PtTPTBPBr, PtTPTBPBr <sub>4</sub> . . . . .	49
5.4	MALDI-MS: <i>PtTPTBPBr</i> <sub>4</sub> . . . . .	50
5.5	MALDI-MS: <i>ZnTPTBPBr</i> . . . . .	50
5.6	Molecular Weight Distribution- Styrene-4-Vinylbenzeneboronic acid-Co-polymers	52
5.7	Dye-loading in the sensor polymers and coupling efficiency . . . . .	53
5.8	Quantum yields determined in the sensor films . . . . .	57
5.9	Fitting parameters - $\tau$ -based SV-plots . . . . .	60
5.10	Fitting parameters - <i>I</i> -based SV-plots . . . . .	60
10.1	Standard Laboratory Equipment . . . . .	75



---

## 10 Appendix

**Table 10.1:** A list of standard laboratory equipment used.

Type	Specification
<i>Balance</i>	Scaltec SBC32
<i>Balance</i>	Denver Instruments SI234
<i>Analytical Balance</i>	Denver Instruments SI234
<i>Ultrasonic Bath</i>	Elma Transsonic Digital S
<i>Rotary Evaporator</i>	ILMVAC ROdist/RObath
<i>Rotary Evaporator</i>	Heidolph Laborota 4000/WB
<i>Vacuum Pump</i>	ILMVAC membrane pump
<i>Vacuum Pump</i>	ILMVAC rotary vane pump

## 10.1 Failed Experiments

### 10.1.1 PtTPTBP-NH<sub>2</sub>

In an effort to obtain an indicator carrying amino-groups, which are suitable for a variety of covalent-linking approaches, a strategy towards the synthesis of a *PtTPTBP-NH<sub>2</sub>-derivative* was developed.

#### Synthesis of the "amide-substrate" 4-(4-Chlorobenzoylamido)aminophenylacetic acid

A reaction which was expected to be highly selective was chosen to prepare a 4-amidophenylacetic acid substrate. The amide-functionality would protect the amino-group from undergoing unspecific reaction during template-directed synthesis and would bring about a difference in polarity well-pronounced enough to enable separation of the desired product from undesired by-products.

One equivalent of *4-aminophenylacetic acid* [151.16] were dissolved in 10mL *tetrahydrofuran*. One equivalent of *triethylamine* was added. One equivalent of *4-Chlorobenzoic chloride* was dissolved in *tetrahydrofuran* and added dropwise to the solution containing *4-aminophenylacetic acid*, resulting in the formation of a brown solution. The product was precipitated from water and filtered. The slightly brown coloured solid was redissolved in Tetrahydrofuran. The washing step by means of precipitation was repeated thrice, yielding a fine white powder in 72 % yield.

#### Template Condensation

One equivalent of "*Zn(4-PhAcO)<sub>2</sub>*" [335.58], four equivalents of "*Dicyanobenzene*" [128.13] and eight equivalents of "*4-(4-chlorobenzoylamido)aminophenylacetic acid*" [289.71] were weighed, mixed and homogenised using a mortar. The solid mixture was split into equal portions of roughly 700 mg, placed into a 2.5 mL Supelco® vials and compressed. A suitable magnetic stirring bar was placed atop, the vials were de-oxygenated by gently blowing Argon into the vial for 2 min each. The vials were sealed with a metal screw cap, placed into a pre-heated aluminium heating block at 140 °C. The mixtures were heated to a temperature of 280 °C and left to react for 40 min while stirring. The vials were removed from the heating block and left to cool. Upon cooling the melt in each vial was dissolved in Acetone.

#### CLEAN-UP:

Absorption spectra were recorded and thin-layer chromatography was conducted using silica gel- and aluminium oxide- TLC-plates and a mixture of 60% *dichloromethane* and 40% *hexane* to assess product formation.

The unified solutions of raw product were precipitated from an equal volume of Ethanol with 10% saturated brine added. The suspension was centrifuged, the solution discarded. The precipitate was redissolved in Dichloromethane. This process was repeated three times. After each step absorption spectra were recorded.

The a small-scale column chromatography-test showed that the product does not move at all using aluminium oxide as a solid phase, even under the most polar elution conditions. Hence a clean-up-method based on silica gel was developed.

The precipitate was dissolved in a mixture of two parts *dichloromethane* and 3 parts *toluene*

transferred onto a silica gel column packed using the same solvent mixture. The product was eluted by gradually increasing solvent polarity.

In the course of the column chromatography, a colour change of the upper parts of the collected fractions, which were in contact with ambient air was noticed. The colour of the solutions changed from green to deep red.

A sample from the most concentrated product-containing solution was taken and transferred into two cuvettes. One cuvette was sealed with a septum and de-oxygenated by bubbling argon through the solution for 20 min, the other cuvette was left open to the air. Both cuvettes were kept in the dark for the duration of the de-oxygenation. Both samples did not show photo-bleaching, which was assessed by measuring absorption spectra before and after the 20 min in the dark. Both cuvettes were then placed into the sunlight and rapid irreversible photo-bleaching could be observed in the sample exposed to air. Due to this rapid photo-bleaching the dye was deemed to be unsuitable for use in optical oxygen sensors and the experiment was aborted.